REPUBLIQUE ALGERIENNE DEMOCRATIQUE ET POPULAIRE

MINISTERE DE L'ENSEIGNEMENT SUPERIEURE ET DE LA RECHERCHE SCIENTIFIQUE

UNIVERSITE Dr YAHIA FARES DE MEDEA



FACUILTE DE TECHNOLOGIE

DEPARTEMENT DE GENIE MECANIQUE

MEMOIRE DE FIN D'ETUDE DE MASTER

NUMERICAL STUDY OF THE EFFECT OF RIB SHAPE ON THE LAMINAR HEAT TRANSFER AND NANOFLUID FLOW IN MICROCHANNELS

FILIERE: GENIE MECANIQUE

OPTION : ENERGÉTIQUE

PRESENTER PAR :

MADANI Zineddine

PROPOSER ET DIRIGER PAR :

Dr. REBHI Redha

ANNEE UNIVERSITAIRE: 2020-2021

Thanks

I express MY deep gratitude to {ALLAH} the Almighty who gave me the necessary energy for the realization of this project.
Before presenting this study i would like to present my thanks and respect to my promoter Redha Rebhi, for his precious help and advice.
And to all those i have contributed from far or near to the realization of this project.

Dedications

I dedicate this modest work to those who are the most expensive in the world:

- To my parents:

For their sacrifices, their encouragement and their concerns.

- To my dear brother & sister
- To all my frinds specially Hichem & Hajji
- Without forgetting all my family from near and far and those who know "zinou".

Abstract:

This is a numerical study by ANSYS WORKBRENCH software of water and water-Ag nanofluid in rib shaped rectangular microchannel under constant heat flux. This study shows the influence of rectangular, triangular, elliptical and trapezoidal ribs on laminar heat transfer using Finite volume method and assuming that the height and width of the ribs are fixed, to study Different rib forms. Model of laminar flow choosed is (Re=1, 10, 50, and 100) and nanofluid volume fraction Scores of 0%, 2% and 4%. The results show that the increase in Reynolds number leads to friction coefficient increases In contrast temperature and fluid velocity decreases. Among all the rib forms investigated. the triangular rib shape have the best thermal performance evaluation also friction coefficient shows that the trapezoidal rib is recommended to use a high Reynolds number.

Keywords: ANSYS WORKBRENCH; Nanofluid; Microchannel; Ribs; Finite volume method; Heat transfer; Laminar flow.

ملخص:

هذه دراسة رقمية أجريت بواسطة برنامج ANSYS WORKBRENCH لاثنين من الموائع الماء و مائع نانوي مكون من الماء و الفضة في قناة مجهرية مستطيلة الشكل تحت تدفق حراري ثابت. توضح هذه الدراسة تأثير الأضلاع المستطيلة والمثلثة والدائرية وشبه المنحرفة على انتقال الحرارة الصفحي باستخدام طريقة الحجوم المحدودة وبافتراض أن ارتفاع وعرض الأضلاع ثابتان لدراسة أشكال الأضلاع المختلفة. تم اختيار نموذج التدفق الصفحي (رقم رينولدز = 1 و 10 و 50 و 100) وكسر حجم الموائع النانوية درجات 0%, 2%, 4% أظهرت النتائج أن الزيادة في رقم رينولدز تؤدي إلى ارتفاع معامل الاحتكاك اما في المقابل تناقص درجة الحرارة و سرعة الموائع. من بين جميع أشكال الاضلاع التي تم فحصها. شكل الضلع المثلثي لديه أفضل تقييم للأداء الحراري كما يوضح معامل الاحتكاك أن الضلع الشبه المنحرف يوصى به في حالة استخدام ارقام رينولدز عالية.

الكلمات المفتاحية: ANSYS WORKBRENCH , المائع النانوي, قناة مجهرية, الاضلاع, طريقة الحجوم المحدودة, انتقال الحرارة, التدفق الصفحي

Résumé:

Dans cette étude, une simulation numérique par le logiciel ANSYS WORKBRENCH de l'eau et du nanofluide eau-Ag dans un microcanal rectangulaire en forme de nervure sous flux de chaleur constant. Cette étude montre l'influence des nervures rectangulaires, triangulaires, elliptiques et trapézoïdales sur le transfert de chaleur laminaire en utilisant la méthode des volumes finis et en supposant que la hauteur et la largeur des nervures sont fixes, pour étudier différentes formes de nervures. Le modèle de flux laminaire choisi est (Re=1, 10, 50 et 100) et des scores de fraction volumique de nanofluide de 0%, 2% et 4%. Les résultats montrent que l'augmentation du nombre de Reynolds entraîne une augmentation du coefficient de frottement. En revanche, la température et la vitesse du fluide diminue. Parmi toutes les formes de côtes étudiées. la forme de la nervure triangulaire a la meilleure évaluation des performances thermiques et le coefficient de frottement montre que la nervure trapézoïdale est recommandée pour utiliser un nombre de Reynolds élevé.

Mots-clés: ANSYS WORKBRENCH ; Nanofluide ; Microcanal ; Nervure; Méthode des volumes finis ; Transfert de chaleur; Écoulement laminaire.

Nomenclature:

A Area, m^2
f Friction factor
C_p Heat capacity, J/kg K
D Microchannel height, μm
H Ribbed height, m
k Thermal conductivity coefficient, W/m K
K Inlet microchannel length, m
L microchannel length, m
m ribbed length, m
Nu Nusselt number
P Fluid pressure, Pa
p Ribbed pitch, m
Pe Peclet number
Pr Prandtl number
Re Reynolds number
T Temperature, K
U, V Dimensionless velocity components in x, y directions
X, Y Cartesian dimensionless coordinates
u, v velocity components in x, y directions, m/s
u_c Inlet velocity in x directions, m/s
u_s Brownian motion velocity, m/s
w Outlet microchannel length, m

Greek symbols:

α Thermal diffusivity,m^2/s
φ Nanoparticles volume fraction
κ_b Boltzmann constant, J/K
μ Dynamic viscosity, Pa s
θ Dimensionless temperature
ρ Density, kg/m^3
υ Kinematics viscosity,m^2/s

Super and Sub scripts:

C Cold
Eff Effective
F Base fluid (distilled water)
H Hot
Ave Average
Nf Nanofluid
S Solid nanoparticles

Introduction:

Ever-growing consumption of energy and fossil fuels for living conditions and well-being improvement has become inevitable. That's while, this consumption is an influential factor on production of greenhouse gases and air pollutant emissions as well as the destruction of natural resources in many countries. Nowadays, taking efficient heat transfer methods and industrial processes has prevented the destruction of environment. By development of technology in various industries, reducing size of heat exchangers and ultimately increasing energy and fuel efficiency has become vital. Cooling is considered in many industries as the most important challenge in energy saving. The first stumbling block in this way is the weak heat transfer properties of common industrial fluids. Cooling systems are among the most paramount concerns of industries such as microelectronics, nanoelectromechanical, aerospace and automotive industry. The need for implementing modern and new methods of heat transfer in microscale industries like microelectronics is entailed by advances in microscale industries. The use of metal and non-metal powdery

Fluids currently used in industrial installations and thermal flow systems are very often modified with different types of additives in order to make them achieve the best possible thermodynamic parameters, and thus to improve heat transfer conditions. In 1995, researchers from the Argonne. National Laboratory proposed for the first time the practical use of copper nanoparticles dispersed in water the fluid which is most commonly used in all sorts of heat exchangers in order to improve the thermal conductivity. However, the origin of nanotechnology and nanoscience definition/concept reaches back to 1959, when an American Nobel laureate Richard Feynman proposed a new theory of quantum electrodynamics. Norio Taniguchi, who presented the basic concept of ‘nano-technology‘ in 1974 during the International Conference on Production Engineering in Japan is also thought to be a pioneer of nanotechnology as a science.

To this day, this discipline is growing and is used in many sectors of the economy, thermotechnology (mini channels extended surfaces as fins, phase change materials PCMs and soon), solar technology, electronics, as well as in chemical industry, agriculture, and even medicine.

Even regarding the potential upside of nanofluids in heat transfer, using the suspensions with suspending particles (metal or non-metalpolymer) in millimeter and even micrometer sizes will lead to problems including corrosion of passages by the particles, blocking of channel, corrosion of piping network, reduction in momentum transfer and a greater pressure loss. Instability problems should also be taken into account while suspending these particles especially regarding the fact that these particles tend to sediment in the suspension. A great deal of studies focused on nanofluids utilization on various surfaces as well as geometries most of which have been aiming to study the heat transfer behavior and fluid flow on rough surfaces.

In this study, the effect of using rectangular, triangular, trapezoidal and elliptical ribs has been simulated in a two-dimensional rectangular microchannel with constant heat flux boundary condition. In order to improve the heat transfer in the studied microchannel.

All shapes in this study have been simulated using ANSYS WORKBRENCH commercial package. The results of the present study can be implemented to design more efficient microchannels for cooling electronic parts.

I.1: Introduction:

The engineering area frequently referred to as thermal science includes thermodynamics and heat transfer. The role of heat transfer is to supplement thermodynamic analyses, which consider only systems in equilibrium, with additional laws that allow prediction of time rates of energy transfer. These supplemental laws are based upon the three fundamental modes of heat transfer, namely conduction, convection, and radiation.

I.1.1: CONDUCTION

A temperature gradient within a homogeneous substance results in an energy transfer rate within the medium which can be calculated by

$$q = -kA\frac{\partial T}{\partial n} \tag{1.1}$$

Where aT/dn is the temperature gradient in the direction normal to the area A**.** The thermal conductivity k is an experimental constant for the medium involved, and it may depend upon other properties, such as temperature and pressure, as discussed in Section **1.4.** The units of **k** are $W/m.K$ orBtu/h. ft."F. (For units systems, see Section second law of thermodynamics: thermal energy transfer

The minus sign in Fourier's law, is required by the resulting from a thermal gradient must be from a warmer to a colder region.

If the temperature profile within the medium is linear (Fig. 1-1), it is permissible toreplace the temperature **Fig. I-1** gradient (partial derivative) with

$$\frac{\Delta T}{\Delta x} = \frac{T_2 - T_1}{x_2 - x_1} \tag{1.2}$$

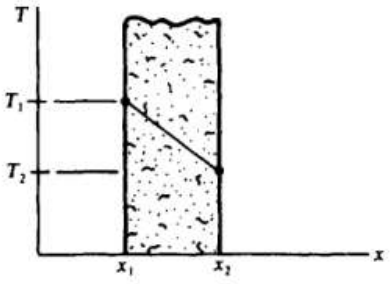


Figure I.1: Heat conduction through a wall.

Such linearity always exists in a homogeneous medium of fixed **k** during steady state heat transfer.

Steady state transfer occurs whenever the temperature at every point within the body, including the surfaces, is independent of time. If the temperature changes with time, energy is either being stored in or removed from the body. This storage rate is

$$q_{stored} = mc_p \frac{\partial T}{\partial t} \qquad (1.3)$$

Where the mass m is the product of volume ***V*** and density ***p.***

I.1.2: CONVECTION

Whenever a solid body is exposed to a moving fluid having a temperature different from that of the body, energy is carried or convected from or to the body by the fluid.

If the upstream temperature of the fluid is T, and the surface temperature of the solid is T,, the heat transfer per unit time is given by

$$q = hA(T_S - T_x) \qquad (1.4)$$

Which is known as Newton's law of cooling.This equation defines the convective heat transfer coefficient h as the constant of proportionality relating the heat transfer per unit time and unit area to the overall temperature difference. The units of h are W/m2-K or Btu/h.ft2. "E It is important to keep in mind that the fundamental energy exchange at a solid-fluid boundary is by conduction, and that this energy is then convected away by the fluid flow. By comparison of (1.1) and (1.4), we obtain, for y = n.

$$hA(T_s - T_x) = -kA(\frac{\partial T}{\partial y})_s \qquad (1.5)$$

Where the subscript on the temperature gradient indicates evaluation in the fluid at the surface.

I.1.3: RADIATION

The third mode of heat transmission is due to electromagnetic wave propagation, which can occur in a total vacuum as well as in a medium. Experimental evidence indicates that radiant heat transfer is proportional to the fourth power of the absolute temperature, whereas conduction and convection are proportional to a linear temperature difference. The fundamental ***Stefan-Boltzmann law*** is

$$q = \sigma A T^4 \qquad (1.6)$$

Where T is the absolute temperature. The constant σ is independent of surface, medium and temperature; its value is $5.6697\ X\ 10^{-8} W/m^4.K^4$ or$0.1714\ X\ 10^{-8}\ Btu/h.ft^2.R^4$.

The ideal emitter, or **blackbody,** is one which gives off radiant energy according to all other surfaces emit somewhat less than this amount, and the thermal emission from many surfaces **(gray bodies)** can be well represented by

$$q = \varepsilon\sigma AT^4 \tag{1.7}$$

Where ***E,*** the ***emissivity*** of the surface, ranges from zero to one.[1]

I.2: ENGINEERING HEAT TRANSFER

Heat Transfert Problems are of critical importance in almost all areas of engineering and technology, especially in the field of mechanical engineering. Over several decades, engineers and scientists have been working on solving these problems by designing and optimizing components and systems needed for transferring, handling, and storing thermal energy. Heat can be transferred via different mechanisms, like conduction and convection. Heat condition is the process of transferring heat from a high temperature region to a low temperature region within a body via molecular motion. Heat convection occurs by macroscopic fluid motion, e.g., when a fluid is flowing along a surface and has a different temperature than the solid surface. In this chapter, some practical nonlinear conduction–convection heat transfer problems will be discussed. Differential or partial differential equations that govern the physical process will be introduced and solved via different analytical approac.

I.2.1: Anatomy of Heat Transfer Problems

Heat transfer is a consequence of variations in the scalar field of temperature. Therefore we, consider a heat transfer problem solved if we know the temperature distribution, T = T(r, t), where, in the general case, T is a function of 3 space dimensions, $r = x\hat{i} + y\hat{j} + z\hat{k}$, and time, t. Often, a problem will depend on only a subset of these independent coordinates, but there can be many other contributors, e.g. fluid motion, V, and energy generation, $\dot{q}$. That is to say, the temperature problem is often more intimidating in terms of its dependencies:

$$T = T(r, t, V, \dot{q}, \dots) \tag{1.8}$$

Presuming the distribution of T can actually be derived by suitable methods, the heat transfer follows as a direct consequence of its gradient, ∇T, whether it be via conduction (according to Fourier's Law or other appropriate phenomenological relationships) or convection, where the so called "no–slip" boundary condition of velocity (Panton, 1984) will be presumed to apply for our purposes, so that the temperature gradient at the boundary implies a convection coefficient.

Although heat transfer comprises a large fraction of the material presented here, we will give greater schrift to T, both because it is the more basic entity and because it generally poses the primary technical problem. The latter ranges from the moderately difficult (i.e. those problems" of a mostly "academic nature that may be physically improbable, or even wholly contrived) to the almost impossible (most "real–world" problems). The processes of deriving T are what we will pay special devotion to, including assessments of when a problem can be solved exactly and when suitable approximation methods must be employed.[3]

I.2.2: Conduction Heat Transfer

We will start by examining conduction heat transfer. We must first determine how to relate the heat transfer to other properties (either mechanical, thermal, or geometrical). The answer to this is rooted in experiment, but it can be motivated by considering heat flow along a "bar" between two heat reservoirs atT_A, T_B as shown in Figure I.2. It is plausible that the heat transfer rate $\dot{Q}$ is a function of the temperature of the two reservoirs, the bar geometry and the bar properties. (Are there other factors that should be considered? If so, what?). This can be expressed as

$$\dot{Q} = f_1(T_A, T_B, \text{ bar geometrie . bar properties }) \qquad (1.9)$$

It also seems reasonable to postulate that $\dot{Q}$ should depend on the temperature difference $T_A - T_B$ If $T_A - T_B$is zero, then the heat transfer should also be zero. The temperature dependence can therefore be expressed as

$$\dot{Q} = f_2[(T_A - T_B), T_A, \text{ bar geometrie . bar properties}] \qquad (1.10)$$

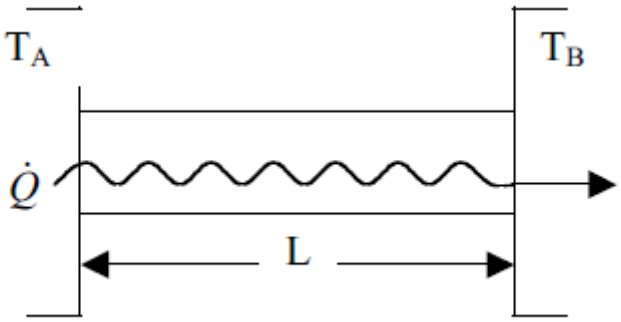


Figure I.2: Heat transfer along a bar

An argument for the general form of f_2 can be made from physical considerations. One requirement, as said, is $f_2 = 0$ if $T_A = T_B$ using a MacLaurin series expansion, as follows:

$$f(\Delta T) = f(0) + \left.\frac{\partial f}{\partial(\Delta T)}\right|_0 \Delta T + \ldots \tag{1.11}$$

If we define $\Delta T = TA - TB$ and $f = f2$, we find that (for small $TA - TB$),

$$f_2(T_A - T_B) = \dot{Q} = f_2(0) + \left.\frac{\partial f_2}{\partial(T_A - T_B)}\right|_{T_A - T_B = 0} (T_A - T_B) + \ldots \tag{1.12}$$

We know that $f_2(0) = 0$ .The derivative evaluated at $T_A = T_B$ (thermal equilibrium) is a measurable property of the bar. In addition, we know that $Q > 0$ if $T_A > T_B$ or $\frac{\partial f_2}{\partial(T_A - T_B)} > 0$

It also seems reasonable that if we had two bars of the same area, we would have twice the heat transfer, so that we can postulate that $\dot{Q}$ is proportional to the area. Finally, although the argument is by no means rigorous, experience leads us to believe that as L increases $\dot{Q}$ should get smaller. All of these lead to the generalization (made by Fourier in 1807) that, for the bar, the derivative in equation (1.12) has the form

$$\left.\frac{\partial f_2}{\partial(T_A - T_B)}\right|_{T_A - T_B = 0} = \frac{kA}{L}. \tag{1.13}$$

In equation (1.13), k is a proportionality factor that is a function of the material and the temperature; A is the cross sectional area and L is the length of the bar. In the limit for any temperature difference ΔT across a length Δx as both$L$, $T_A - T_B \to 0$, we can say.

$$\dot{Q} = kA\frac{(T_A - T_B)}{L} = -kA\frac{(T_B - T_A)}{L} = -kA\frac{dT}{dx} \qquad (1.14)$$

A more useful quantity to work with is the heat transfer per unit area, defined as

$$\frac{\dot{Q}}{A} = \dot{q} \qquad (1.15)$$

The quantity q& is called the heat flux and its units are Watts/m2. The expression in (1.14) can be written in terms of heat flux as

$$\dot{q} = -k\frac{dT}{dx} \qquad (1.16)$$

Equation (1.16) is the one-dimensional form of Fourier's law of heat conduction. The proportionality constant k is called the thermal conductivity. Its units are$W / m - K$. Thermal conductivity is a well tabulated property for a large number of materials. Some values for familiar materials are given in Table 1; others can be found in the references. The thermal conductivity is a function of temperature and the values shown in Table 1 are for room temperature.

Table I.1: Thermal conductivity at room temperature for some metals and non-metals

Metals	Ag	Cu	Al	Fe	Steel
k [W/m-K]	420	390	200	70	50

Non-metals	H_20	Air	Engine oil	H_2	Brick	Wood	Cork
k [W/m-K]	0.6	0.026	0.15	0.18	0.4-0.5	0.2	0.04

I.2.1.1: Steady-State One-Dimensional Conduction:

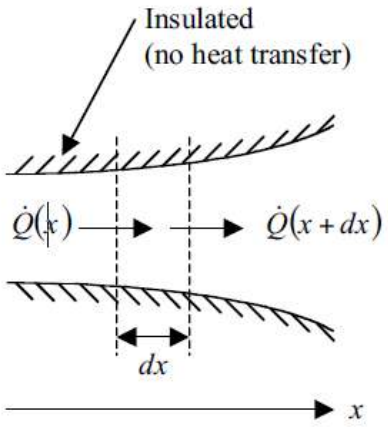


Figure I.3: One-dimensional heat conduction

For one-dimensional heat conduction (temperature depending on one variable only), we can devise a basic description of the process. The first law in control volume form (steady flow energy equation) with no shaft work and no mass flow reduces to the statement that $\Sigma\dot{Q}$ for all surfaces = 0 (no heat transfer on top or bottom of figure I.3). From equation (1.16), the heat transfer rate in at the left (at *x*) is

$$\dot{Q}(x) = -k\left(A\frac{dT}{dx}\right)_x \tag{1.17}$$

The heat transfer rate on the right is

$$\dot{Q}(x+dx) = \dot{Q}(x) + \left.\frac{d\dot{Q}}{dx}\right|_x dx + \cdots \tag{1.18}$$

Using the conditions on the overall heat flow and the expressions in (1.17) and (1.18)

$$\dot{Q}(x) - \left(\dot{Q}(x) + \frac{d\dot{Q}}{dx}(x)dx + \cdots\right) = 0 \tag{1.19}$$

I.2.1.2: Thermal Resistance Circuits:

There is an electrical analogy with conduction heat transfer that can be exploited in problem solving. The analog of $\dot{Q}$ is current, and the analog of the temperature difference, $T1 - T2$, is voltage difference. From this perspective the slab is a pure resistance to heat transfer and we can define

$$\dot{Q} = \frac{T_1 - T_2}{R} \tag{1.20}$$

Where $R = L/kA$, the thermal resistance. The thermal resistance *R* increases as *L* increases, as *A* decreases, and as *k* decreases. The concept of a thermal resistance circuit allows ready analysis of problems such as a composite slab (composite planar heat transfer surface). In the composite slab shown in Figure I.4**.**the heat flux is constant with x. The resistances are in series and sum to$R = R_1 + R_2$. If TL is the temperature at the left, and T_R is the temperature at the right, the heat transfer rate is given

$$\dot{Q} = \frac{T_L - T_R}{R} = \frac{T_L - T_R}{R_1 + R_2} \tag{1.21}$$

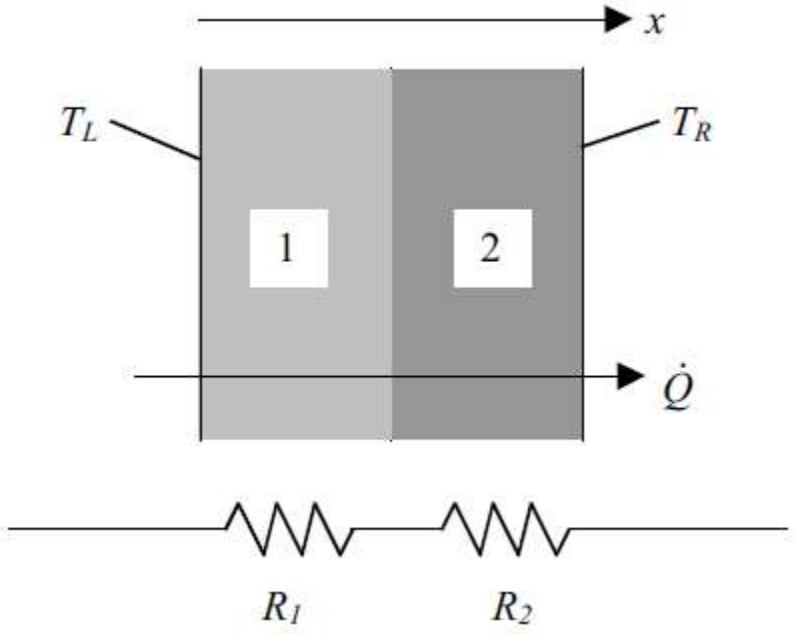


Figure I.4: Heat transfer across a composite slab (series thermal resistance)

I.2.1.3: Steady Quasi-One-Dimensional Heat Flow in Non-Planar Geometry:

The quasi one-dimensional equation that has been developed can also be applied to non planar geometries. An important case is a cylindrical shell, a geometry often encountered in situations where fluids are pumped and heat is transferred. The configuration is shown in Figure I.5

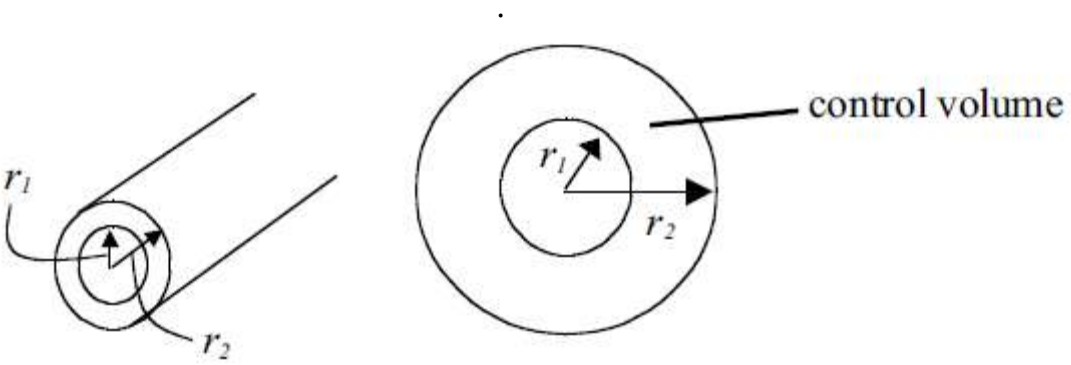


Figure I.5: Cylindrical shell geometry notation

I.2.3: Convective Heat Transfer

The second type of heat transfer to be examined is convection, where a key problem is determining the boundary conditions at a surface exposed to a flowing fluid. An example is the wall temperature in a turbine blade because turbine temperatures are critical as far as creep (and thus blade) life. A view of the problem is given in Figure 1.6, which shows a cross-sectional view of a turbine blade. There are three different

types of cooling indicated, all meant to ensure that the metal is kept at a temperature much lower than that of the combustor exit flow in which the turbine blade operates. In this case, the turbine wall temperature is not known and must be found as part of the solution to the problem.

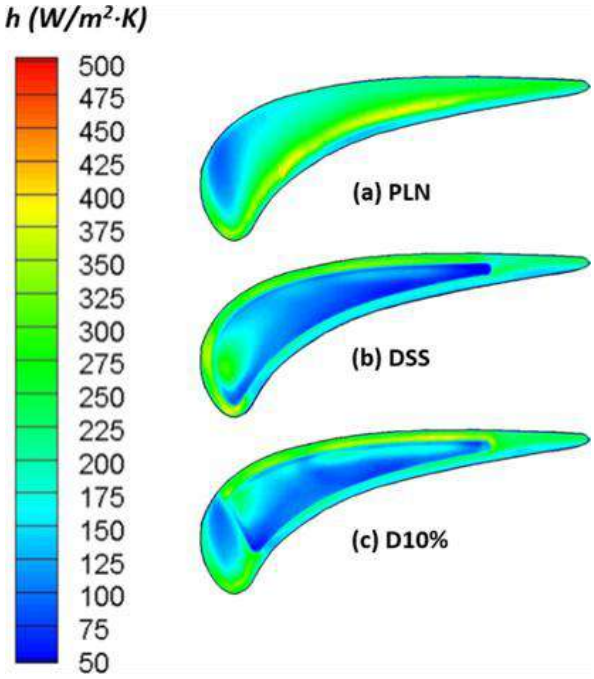


Figure I.6: Turbine blade heat transfer configuration.

To find the turbine wall temperature, we need to analyze convective heat transfer, which means we need to examine some features of the fluid motion near a surface. The conditions near a surface are illustrated schematically in Figure 1.7.

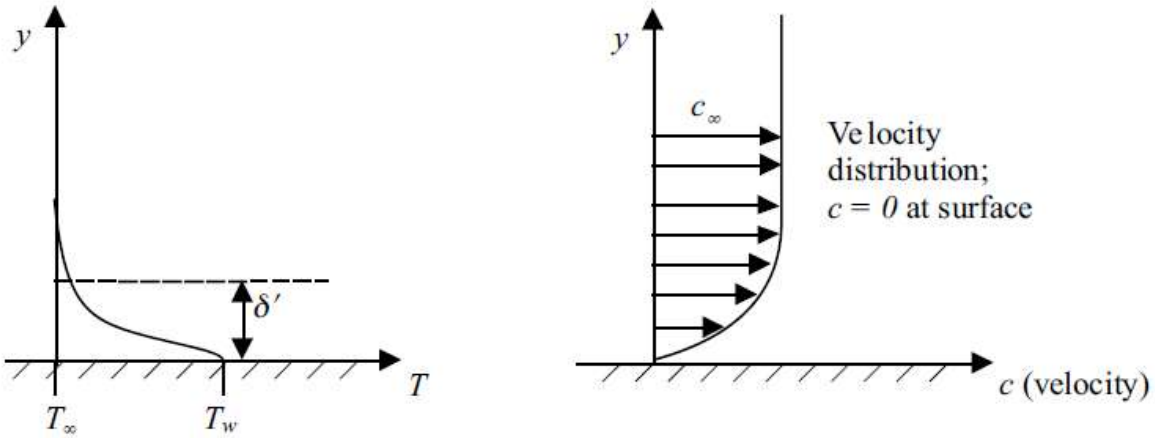


Figure I.7: Temperature and velocity distributions near a surface.

In a region of thickness δ′, there is a thin "film" of slowly moving fluid through which most of the temperature difference occurs. Outside this layer, *T* is roughly uniform (this defines δ′). The heat flux can thus be expressed as

$$\dot{q}=\frac{\dot{Q}}{A}=\frac{k(T_w-T_\infty)}{d'} \tag{1.22}$$

It cannot be emphasized enough that this is a very crude picture. The general concept, however, is correct, in that close to the wall, there is a thin layer in which heat is transferred basically by conduction. Outside of this region is high mixing. The difficulty is that the thickness of the layer is not a fluid property. It depends on velocity (Reynolds number), structure of the wall surface, pressure gradient and Mach number. Generally δ' is not known and needs to be found and it is customary to calculate the heat transfer using $[kfluid\ /\ \delta']$. this quantity has the symbol *h* and is known as the convective heat transfer coefficient. The units of h are$W/m2K$. The convective heat transfer coefficient is defined by

$$\dot{q}=\frac{\dot{Q}}{A}=h(T_w-T\infty) \tag{1.23}$$

Equation (1.23) is often called *Newton's Law of Cooling*. For many situations of practical interest, the quantity *h* is still known mainly through experiments.

I.2.3.1: Combined Conduction and Convection:

We can now analyze problems in which both conduction and convection occur, starting with a wall cooled by flowing fluid on each side. As discussed, a description of the convective heat transfer can be given explicitly as

$$\frac{\dot{Q}}{A}=\dot{q}=h(T_w-T_\infty) \tag{1.24}$$

This could represent a model of a turbine blade with internal cooling. Figure I.8 shows the configuration

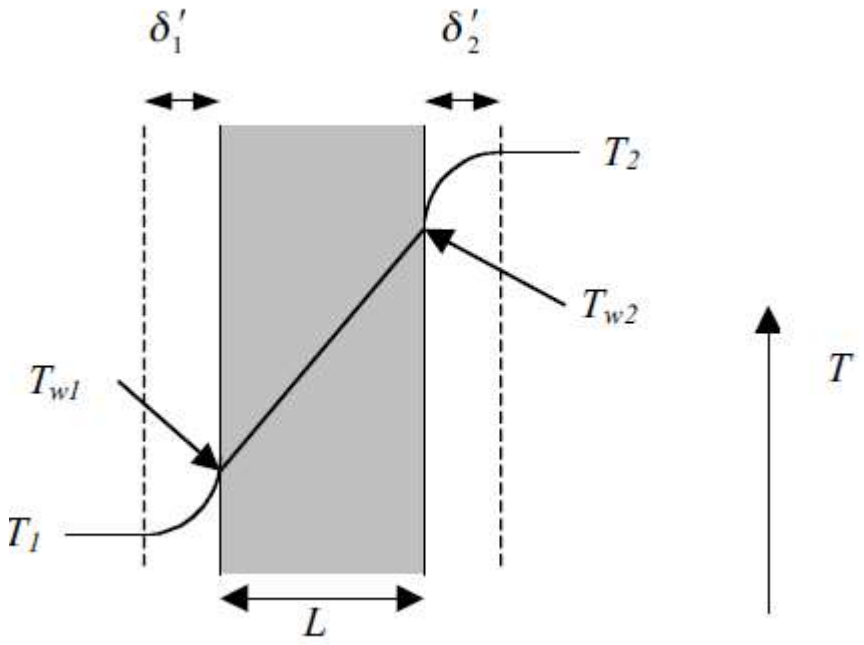


Figure I.8: Wall with convective heat transfer

The heat transfer in fluid 1 is given by

$$\frac{\dot{Q}}{A} = \dot{q} = h_1(T_{W1} - T_1) \tag{1.25}$$

Which is the heat transfer per unit area to the fluid. The heat transfer in fluid (2) is similarly given by

$$\frac{\dot{Q}}{A} = h_2(T_2 - T_{w2}) \tag{1.26}$$

Across the wall, we have

$$\frac{\dot{Q}}{A} = \frac{k}{L}(T_{w2} - T_{w1}) \tag{1.27}$$

The quantity $\dot{Q}/A$ is the same in all of these expressions. Putting them all together to write the known overall temperature drop yields a relation between heat transfer and overall temperature drop$T_2 - T_1$:

$$T_2 - T_I = (T_2 - T_{w2}) + (T_{w2} - T_{wI}) + (T_{wI} - T_I) = \frac{\dot{Q}}{A}\left[\frac{1}{h_1} + \frac{L}{k} + \frac{1}{h_2}\right] \tag{1.28}$$

We can define a thermal resistance, *R*, as before, such that

$$\dot{Q} = \frac{(T_2 - T_1)}{R} \tag{1.29}$$

Where *R* is given by

$$R = \frac{1}{h_1 A} + \frac{L}{Ak} + \frac{1}{h_2 A} \tag{1.30}$$

Equation (1.30) is the thermal resistance for a solid wall with convection heat transfer on each side.

I.2.4: Temperature Distributions in the Presence of Heat Sources

There are a number of situations in which there are sources of heat in the domain of interest. Examples are:

1) Electrical heaters where electrical energy is converted resistively into heat
2) Nuclear power supplies
3) Propellants where chemical energy is the source

These situations can be analyzed by looking at a model problem of a slab with heat sources $\alpha\ (W/m3)$ distributed throughout. We take the outside walls to be at temperatureT_w, and we will determine the maximum internal temperature.

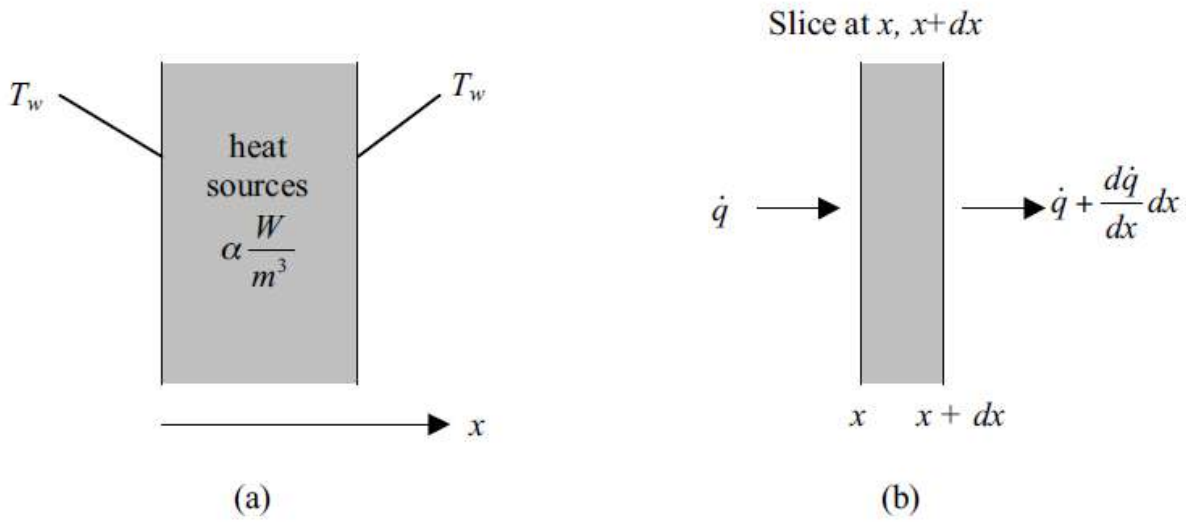


Figure I.9: Slab with heat sources (a) overall configuration, (b) elementary slice

With reference to Figure I.9(b), a steady-state energy balance yields an equation for the heat flux, $\dot{q}$

$$q + adx - \left(q + \frac{dq}{dx} dx \right) = 0 \tag{1.31}$$

Or:

$$\frac{d\dot{q}}{dx} = \alpha. \tag{1.32}$$

There is a change in heat flux with x due to the presence of the heat sources. The equation for the temperature is

$$\frac{d^2T}{dx^2} + \alpha / k = 0 \tag{1.33}$$

Equation (1.33) can be integrated once,

$$\frac{dT}{dx} = -\frac{\alpha}{k} x + a \tag{1.34}$$

And again to give

$$T = -\frac{\alpha}{2k} x^2 + ax + b \tag{1.35}$$

Where a and b are constants of integration. The boundary conditions imposed are $T\,(0) = T\,(L) = T_w$ Substituting these into Equation (1.35) gives $b = T_w$ and $a = \frac{\alpha L}{2k}$

The temperature distribution is thus

$$T = -\frac{\alpha x^2}{2k} + \frac{\alpha}{2k} Lx + T_W \tag{1.36}$$

Writing (1.36) in a normalized, non-dimensional fashion gives a form that exhibits in a more useful manner the way in which the different parameters enter the problem:

$$\frac{T - T_W}{\alpha L^2 / k} = \frac{1}{2}\left(\frac{x}{L} - \frac{x^2}{L^2} \right) \tag{1.37}$$

This distribution is sketched in Figure I.10. It is symmetric about the mid-plane at $x = \frac{L}{2}$ with half the energy due to the sources exiting the slab on each side.

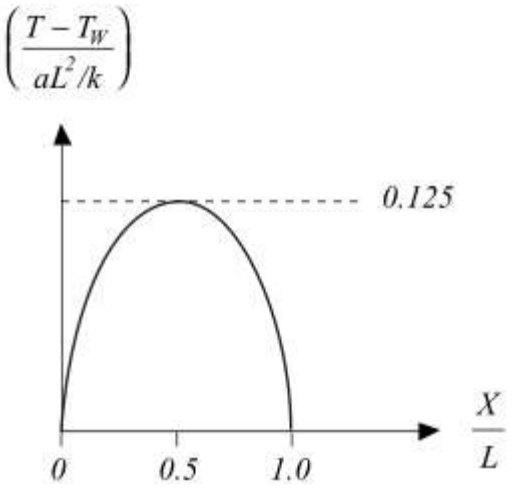


Figure I.10: Temperature distribution for slab with distributed heat sources

The heat flux at the side of the slab, x = 0, can be found by differentiating the temperature distribution and evaluating at x = 0: $-k\left.\frac{dT}{dx}\right|_{x=0} = -k\frac{\alpha L^2}{2K}\left(\frac{1}{L}\right) = -\alpha L/2$

This is half of the total heat generated within the slab. The magnitude of the heat flux is the same at x = L, although the direction is opposite.

A related problem would be one in which there were heat flux (rather than temperature) boundary conditions at x = 0 and x = L, so that T_w is not known. We again determine the maximum temperature. At x = 0 and L, the heat flux and temperature are continuous so

$$-k\frac{dT}{dx} = h\left(T - T_\infty\right) \text{ at } x = 0, L. \tag{1.38}$$

Referring to the temperature distribution of Equation (1.30) gives for the two terms in Equation (1.38),

$$k\frac{dT}{dx} = k\left(-\frac{\alpha x}{k} + a\right) = (-\alpha x + ka) \tag{1.39}$$

$$h\left(T - T_\infty\right) = h\left(-\frac{\alpha x^2}{k} + \alpha x + b - T_\infty\right) \tag{1.40}$$

Evaluating (1.40) at x = 0 and L allows determination of the two constants a and b. This is left as an exercise for the reader

I.2.5: Heat Transfer from a Fin

Fins are used in a large number of applications to increase the heat transfer from surfaces.

Typically, the fin material has a high thermal conductivity. The fin is exposed to a flowing fluid, which cools or heats it, with the high thermal conductivity allowing increased heat being conducted from the wall through the fin. The design of cooling fins is encountered in many situations and we thus examine heat transfer in a fin as a way of defining some criteria for design.

A model configuration is shown in Figure I.11. The fin is of length$L$. The other parameters of the problem are indicated. The fluid has velocity $c_\infty$and temperature T_∞

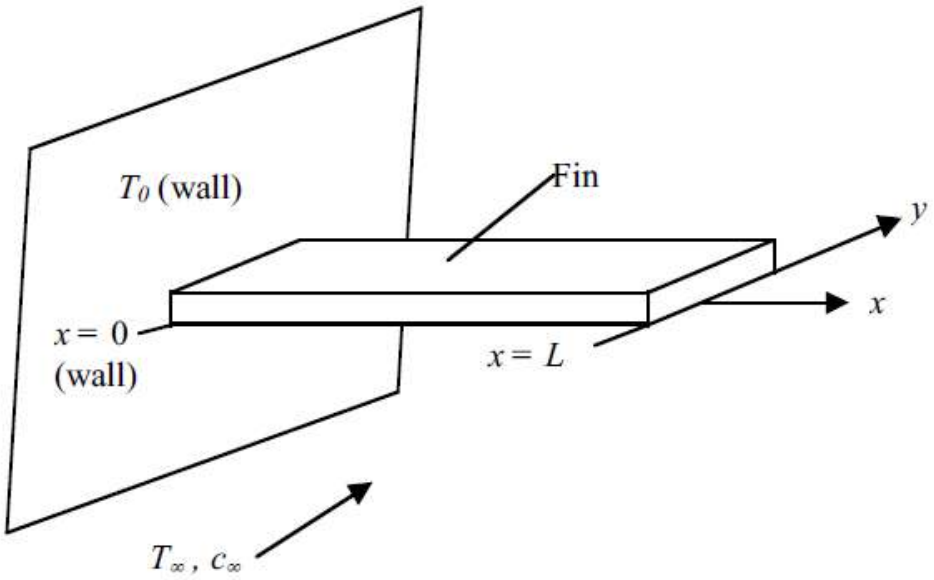


Figure I.11: Geometry of heat transfer fin

We assume (using the Reynolds analogy or other approach) that the heat transfer coefficient for the fin is known and has the value h. The end of the fin can have a different heat transfer coefficient, which we can call hL.

The approach taken will be quasi-one-dimensional, in that the temperature in the fin will be assumed to be a function of x only. This may seem a drastic simplification, and it needs some explanation. With a fin cross-section equal to A and a perimeter P, the characteristic dimension in the transverse direction is A / P (For a circular fin, for example, A / P = r / 2). The regime of interest will be taken

To be that for which the Biot number is much less than unity, $Bi = \frac{h(A/P)}{k} << 1$ which is a realistic approximation in practice.

The physical content of this approximation can be seen from the following. Heat transfer per unit area out of the fin to the fluid is roughly of magnitude ~h(Tw - $T\infty$) per unit area. The heat transfer per unit area *within the* fin in the transverse direction is (again in the same approximate terms)

$k\frac{(T_1 - T_W)}{A/P}$, where T_1 is an internal temperature. These two quantities must be of the same magnitude. If $h\frac{A/P}{k} << 1$,then $\frac{T_1 - T_W}{T_W - T_\infty} << 1$ In other words, if *Bi << 1* there is a much larger capability for heat transfer per unit area across the fin than there is between the fin and the fluid, and thus little variation in temperature inside the fin in the transverse direction. To emphasize the point, consider the limiting case of zero heat transfer to the fluid i.e., an insulated fin. Under these conditions, the temperature within the fin would be uniform and equal to the wall temperature.

I.2.6: Heat Exchangers

The general function of a heat exchanger is to transfer heat from one fluid to another. The basic component of a heat exchanger can be viewed as a tube with one fluid running through it and another fluid flowing by on the outside. There are thus three heat transfer operations that need to be described:

1) Convective heat transfer from fluid to the inner wall of the tube
2) Conductive heat transfer through the tube wall
3) Convective heat transfer from the outer tube wall to the outside fluid

Heat exchangers are typically classified according to flow arrangement and type of construction. The simplest heat exchanger is one for which the hot and cold fluids move in the same or opposite directions in a concentric tube (or double-pipe) construction. In the parallel flow arrangement of Figure I.12a, the hot and cold fluids enter at the same end, flow in the same direction, and leave at the same end. In the counterflow arrangement of Figure I.12b, the fluids enter at opposite ends, flow in opposite directions, and leave at opposite ends.

Alternatively, the fluids may be in cross flow (perpendicular to each other), as shown by the finned and unfinned tubular heat exchangers of Figure I.13. The two

configurations differ according to whether the fluid moving over the tubes is unmixed or mixed. In Figure I.13a, the fluid is said to be unmixed because the fins prevent motion in a direction (y) that is transverse to the main flow direction (x). In this case the fluid temperature varies with x and y. In contrast, for the unfinned tube bundle of Figure I.13b, fluid motion, hence mixing, in the transverse direction is possible, and temperature variations are primarily in the main-flow direction. Since the tube flow is unmixed,

Both fluids are unmixed in the finned exchanger, while one fluid is mixed and the other unmixed in the unfinned exchanger.

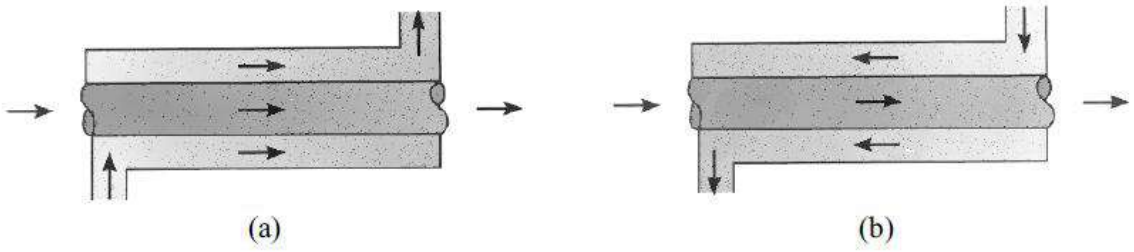


Figure I.12: Concentric tubes heat exchangers. (a) Parallel flow. (b) Counterflow

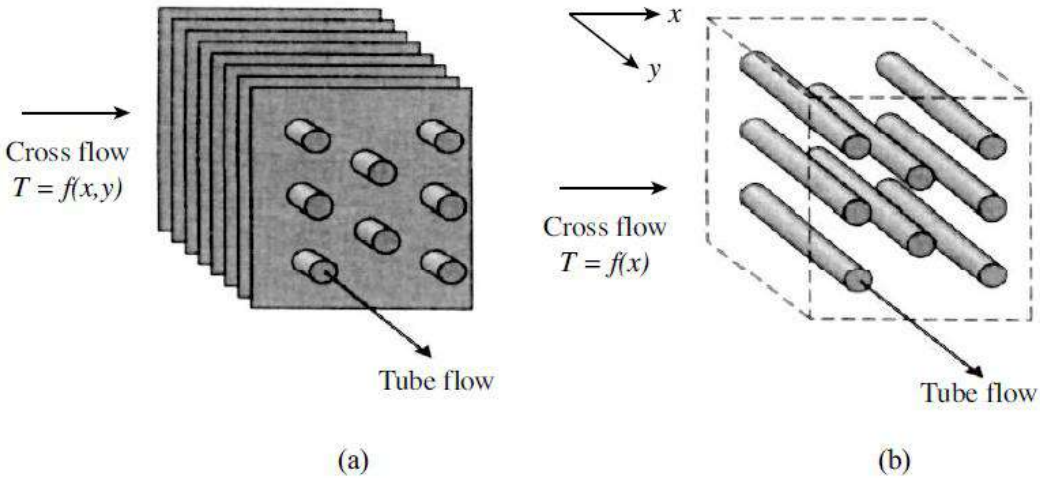


Figure I.13: Cross-flow heat exchangers. (a) Finned with both fluids unmixed. (b) Unfinned with one fluid mixed and the other unmixed

To develop the methodology for heat exchanger analysis and design, we look at the problem of heat transfer from a fluid inside a tube to another fluid outside.

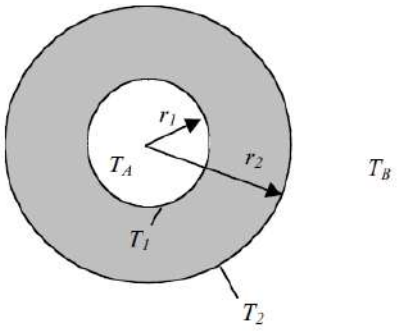


Figure I.14: Geometry for heat transfer between two fluids

We examined this problem before and we found that the heat transfer rate per unit length is given by

$$\dot{Q} = \frac{2\pi k\left(T_A - T_B\right)}{\frac{k}{r_1 h_1} + \ln\frac{r_2}{r_1} + \frac{k}{r_2 h_2}} \tag{1.41}$$

It is useful to define an overall heat transfer coefficient *h0* per unit length as

$$\dot{Q} = 2\pi r_2 h_0\left(T_A - T_B\right) \tag{1.42}$$

From (1.41) and (1.42) the overall heat transfer coefficient, h_0, is

$$\frac{1}{h_0} = \frac{r_2}{r_1 h_1} + \frac{r_2}{k}\ln\frac{r_2}{r_1} + \frac{1}{h_2} \tag{1.43}$$

I.2.7: Radiation Heat Transfer (Heat transfer by thermal radiation)

All bodies radiate energy in the form of photons moving in a random direction, with random phase and frequency. When radiated photons reach another surface, they may either be absorbed, reflected or transmitted. The behavior of a surface with radiation incident upon it can be described by the following quantities:

α = absorptance - fraction of incident radiation absorbed

ρ = reflectance - fraction of incident radiation reflected

τ = transmittance – fraction of incident radiation transmitted

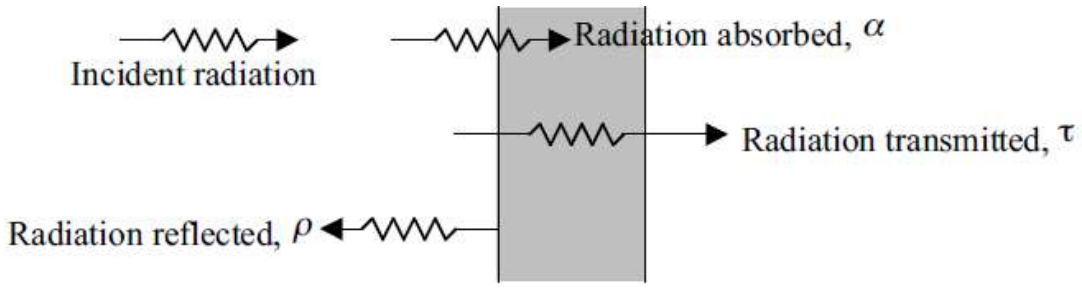


Figure I.15: Radiation Surface Properties

From energy considerations the three coefficients must sum to unity

$$\alpha + \rho + \tau = 1 \tag{1.44}$$

Reflective energy may be either diffuse or specular (mirror-like). Diffuse reflections are independent of the incident radiation angle. For specular reflections, the reflection angle equals the angle of incidence.

I.2.7.1: Ideal Radiators:

An ideal thermal radiator is called a "black body". It has several properties:

1) It has $\alpha = 1$, and absorbs all radiation incident on it.
2) The energy radiated per unit area is $E_B = \sigma T^4$where σ is the Stefan-Boltzmann constant,

$$\alpha = 5.67 \times 10^{-8} \frac{W}{m^2 K^4} \tag{1.45}$$

The units of E_b are therefore $\frac{W}{m^2}$

The energy of a black body,E_b, is distributed over a range of wavelengths of radiation. We can define $e_\lambda = \frac{dE_b}{d\lambda} \approx \frac{\Delta E_b}{\Delta\lambda}$, the energy radiated per unit area for a range of wavelengths of width $\Delta\lambda$ .The behavior of $e_\lambda$is given in Figure I.16

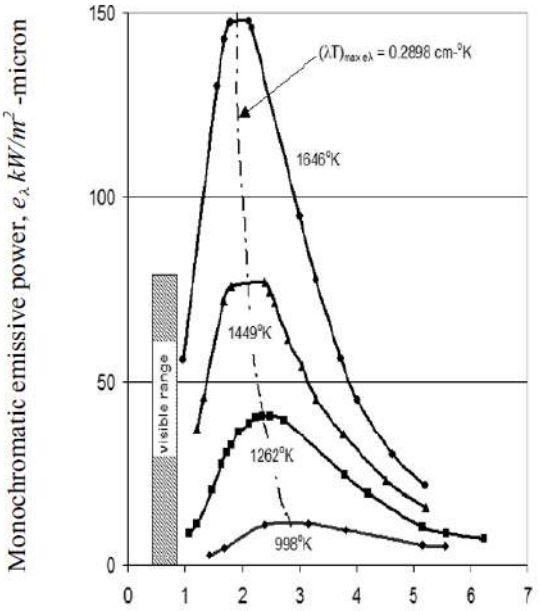


Figure I.16: Emissive power of a black body at several temperatures - predicted and observed

$(\lambda T)_{e\lambda_{max}} = 0.2898$ **cm K [adapted from: *A Heat Transfer Textbook* by Lienhard, J.]**

The distribution of eλ varies with temperature. The quantity λ*T* at the condition where *e*λ is a maximum is given by $(\lambda T)_{e\lambda_{\max}} = 0.2898$ cm k. As *T* increases, the wavelength for maximum energy emission shifts to shorter values. The frequency of the radiation, *f*, is given by $f = c/\lambda$ so high energy means short wavelengths and high frequency.

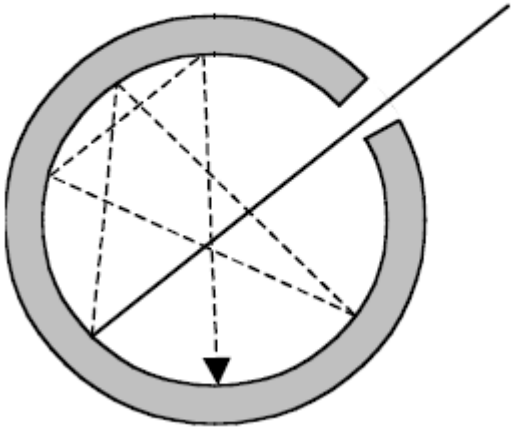


Figure I.17: A cavity with a small hole (approximates a black body)

A physical realization of a black body is a cavity with a small hole. There are many reflections and absorptions. Very few entering photons (light rays) will get out. The inside of the cavity has radiation which is homogeneous and isotropic (the same in any direction, uniform everywhere).

Suppose we put a small black body inside the cavity as seen in Figure I.18. The cavity and the black body are both at the same temperature.

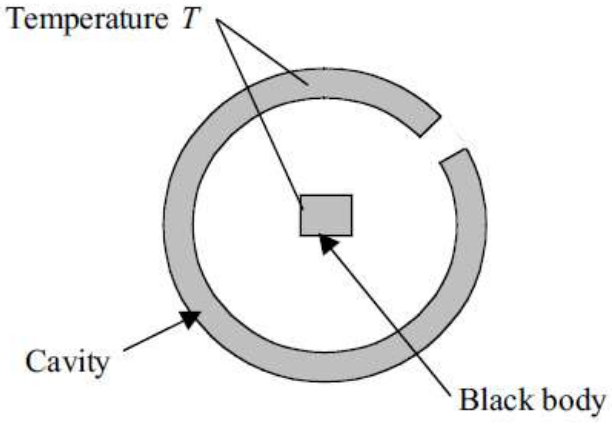


Figure I.18: A small black body inside a cavity

The radiant energy absorbed by the black body per second and per m^2 is $\alpha_B H$, where H is the irradiance, the radiant energy falling on any surface inside the cavity. The radiant energy emitted by the black body is E_B. Since $\alpha_B = 1$ for a black body $H = E_B$. The irradiance within a cavity whose walls are at temperature T is therefore equal to the radiant emittance of a black body at the same temperature and irradiance is a function of temperature only.

I.2.7.2: Kirchhoff's Law and "Real Bodies":

Real bodies radiate less effectively than black bodies. The measurement of this is the emittance, ε, defined by

Emittance: $\varepsilon = \dfrac{E \leftarrow \text{radiation from real body at } T}{E_b \leftarrow \text{radiation from black body at } T}$

Values of emittance vary greatly for different materials. They are near unity for rough surfaces such as ceramics or oxidized metals, and roughly 0.02 for polished metals or silvered reflectors. A table of emittances for different substances is given at the end of this section, taken from the book by Lienhard.

The level of the emittance can be related to the absorptance using the following arguments. Suppose we have a small non-black body in the cavity. The power absorbed per unit area is equal to αH. The power emitted is equal to E. An energy balance gives $E = E_b \varepsilon = \alpha H = \alpha E_b$ .. Thus

$$\frac{E}{E_b} = \alpha = \varepsilon \qquad (1.46)$$

Equation (1.46), the relation α = ε, is known as Kirchhoff's Law. It implies that good radiators are good absorbers. It was derived for the case when $T_{body} = T_{surroundings}$ (cavity) and is not strictly true for all circumstances when the temperature of the body and the cavity are different, but it is true if $\alpha_\lambda = \alpha, \varepsilon_\lambda = \varepsilon$ so the absorptance and emittance are not functions of λ . This situation describes a "gray body". Also, since $\alpha_\lambda, \varepsilon_\lambda$ are properties of the surface, $\alpha_\lambda = \varepsilon_\lambda$

I.3: Conclusion:

Thermodynamics is the study of heat transfer and the changes related to it. Conduction is nothing but the heat transfer from the hotter part to the colder one. Convection is the heat transfer by up and down motion of the fluid. Radiation occurs when heat travels through empty space.

In the simplest of terms, the discipline of heat transfer is concerned with only two things: temperature and the flow of heat. Temperature represents the amount of thermal energy available, whereas heat flow represents the movement of thermal energy from place to place.

Adsorption cooling or heating is the most promising technology that will alleviate high dependency of energy use by adopting the conventional vapor compression systems. Nevertheless, the uptake of adsorption systems is still at the laboratory scale due to few drawbacks of low heat transfers in the adsorbent bed. The most common enhancement method that this reviewed revealed is embedding the adsorbent material in the heat exchanger fins. Indeed, this approach is considered as the most efficient compared to coating the adsorbent onto to the heat exchanger fins. Technically, most of the researchers have chosen on insertion of metal inside the adsorbent bed or adsorber. This method may increase the thermal conductivity of the adsorbent bed which are relatively lower than metal.

II.1 Introduction:

Over the past decade, micromachining technology has been used to develop a number of microfluidic systems in silicon, glass, quartz, and plastics. Microchannels and chambers are essential components of any such system. Inaddition to connecting different devices, microchannels are alsoused for reactant delivery, as bio/chemical reaction chambers, in physical particle separation , in inkjet print heads, or as heat exchangers for cooling computer chips .Currently, fluid flows in microchannels and micromachined fluid systems (e.g., pumps and valves) are analyzed using theNavier-Stokes equations . However, a number of publications have shown that (a) flows on the microscale are different from that on the macroscale and that (b) the Navier-Stokes equations alone are incapable of modeling the occurring phenomena. Thus, in order to design and fabricate such microdevices effectively, the fluid flow on the microscale must be better understood. Several effects, which are normally neglected when considering macroscale flow, may be significant on the microscale. The first of these microscale phenomena are the two- and three-dimensional transport effects. As characteristic lengths are reduced to the same order of magnitude as the hydrodynamic boundary layer thickness, momentum transfer in directions other than the streamwise direction can increase

Significantly. Another observed microscale effect is that of temperature variations in the transport fluid that can cause a significant variation in fluid properties (e.g., apparent fluid viscosity) throughout a microsystem, invalidating the oftenused assumption of constant properties. Other effects that may play a more significant role on the microscale include viscosity variation near the solid surface, slip flow at the boundary, and micropolar fluid effects.

Fluid dynamics in general is an empirical science that relies heavily on experimentation to determine the effects of changes in flow parameters. Unfortunately, until recently the ability to fabricate channels for microfluidic testing has been limited. With the advent of micromachining, a completely new realm of techniques for precise fabrication of microscale

Channels have emerged. The ability to precision fabricate channels, though, has not yet resolved the question regarding microfluidic effects. Whether the difficulty related to data collection and analysis of this type is related to the difficulty in making

measurements at dimensions of this size or other factors, the questions regarding scale effects in microchannel

Fluid flow has not yet been answered satisfactory. Consequently, much work remains to be completed in this area so that a complete understanding of fluid dynamics in small channels can be realized.[9]



II.2: Flow characteristics :

In fluid mechanics, some flows are quite turbulent, while others are smooth and regular. The regular movement of flow which is specified by smooth flow lines is called laminar flow. The motion of high viscous fluids at low speeds is generally laminar. On the other hand, a high degree of irregular fluid motion at high speeds is defined as turbulent. Since the transition from laminar flow the turbulent flow does not occur suddenly, between these flow regimes there is another type of fluid characteristic which is called transient.[10]

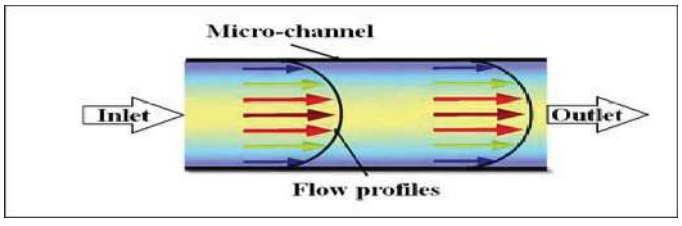


Figure II.1: Laminar flow vertical profile

II.3: Reynolds Number & Laminar Flow Patterning in Microchannels :

Using laminar flow pattern is a novel method in microchannels that allows two or more fluids (e.g. samples, analytes, biological fluids, solutions, etc.) to move side by side in a channel without interference. This terminology is applied in microfluidic

systems as a result of their microscale dimensions and correspondingly low Reynolds number flow.

Osborne Reynolds, the British scientist, found that all flow regimes depend on surface roughness, geometries, the flow velocity, and the type of material in addition to other factors.

After detailed experiments, he defined a non dimensional number which is called Reynolds number as the ratio of inertial forces to viscous forces in a significant flow configuration:

$$Re = (\rho \times u \times L)/\mu = (u \times L)/\nu \qquad (2.1)$$

Where:

ρ is the density of the fluid

u is the velocity of the fluid

; L is the typical length scale

μ is the dynamic viscosity of the fluid

ν is the kinematic viscosity of the fluid

If the Reynolds number is larger than about 2300, it corresponds to turbulent flow at which inertial forces are dominant. The region in which Reynolds number is smaller than about 1000, it is called laminar flow regime. When the microchannels are considered, small dimensions of these channels generally just let to obtain much less than 1000 Re.

It is possible to make Reynolds number clear by animating proof of concept: A man is running through the hallway in order to pass the corner. Suppose that another man is calling him from the opposite direction at that moment. Naturally, it is predicted that the running man will not change his direction suddenly because his momentum is high. Then, let's define the viscosity as the desire to stick to the wall. In the end, as the running man is pulled by the wall, Re decreases, or viscosity increases, he will turn the corner as much as possible.

This is the simplified representation of the Reynolds number. If the Reynolds number is low, you will run almost adherent to the wall (laminar flow); but if Re is high, you will break away from the corner, then you will be dispersed (turbulent flow).

Now, imagine a microchannel. In relation to this microchannel, the numerator of the Reynolds formula is very small due to low dimensions of the channel which is scaled from nano to millimeter, while the denominator usually states constantly for most fluids that relevant to Newtonian fluids. At that point, velocity is the only consideration which is capable to manipulate the flow whether turbulent or not.

Generally, a high-velocity profile of fluid inside the microfluidic systems cannot be achieved. It means that in any microchannel, flow is completely laminar and the emergence of turbulence is nearly impossible. More importantly, the laminar flow regime allows the straight parallel line of fluid to flow next to each other without mixing in microchannels except diffusion. Because the laminar flow is represented as straight parallel lines which are also called profile of the flow. These lines move directly into the microchannels without any warping away from its route.[10]

II.4: Examples in Microfluidics Utilizing Laminar Flow :

Micro fuel cells are being considered as an alternative power source at microscale range. The two flows (which are oxidant and fuel streams) are distinguished in a single microchannel. Laminar flow allows a controllable diffusion region for oxidant and fuel streams in micro-fuel cells.

Microfluidics is also used for the diagnostic device in chemical processes e.g. measurement of diffusion coefficients. In these devices (T-cells), two streams are introduced from the input. Then, the flows are run by laminar flow; it means that transportation only occurs via diffusion. This feature helps to find diffusion coefficients of materials

Laminar flow is mostly utilized in lab-on-a-chip devices. It exploits of easily generated laminar flows to move fluids and to deliver them for patterning. Patterning ability of growth medium is the unique feature which provides to modeling delicate structures of mammalian cells [10]

What requirements must be fulfilled for microfluidics to become a major new technology? Will it live up to the hopes experienced at its conception? As a field, the problems it faces are those faced by most fields as they develop. The fact that microfluidics has not yet lived up to its early advertising is not a surprise, and the reasons for the rate at which it has developed are both characteristic of new technologies, and suggestive of areas in which to focus work in the future.

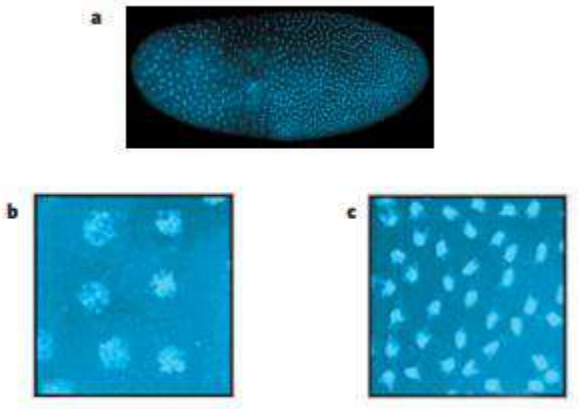


Figure II.2: A new platform for cellular and developmental biology

Laminar flow in microchannels, together with the biocompatibility of PDMS, enable new methods of studying cellular and developmental biology. One system examines the effect of temperature on the development of a fruitfly embryo55. The embryo (the large oval in a) is immobilized in the middle of a microchannel. Aqueous streams of two different temperatures flow over the halves of the embryo (b shows the cold half, c the warm half); the differences in the embryo are reflected in the density of cells (marked by the light-blue nuclei). The embryo is ~500 μm wide.

II.5: General issues in introducing new technologies:

The original hope for microfluidics, and that which still motivates many of us working in the field, is that it will be a practical technology one widely used in a number of different types of application. I am confident that, ultimately, it will be, but there are several problems that it in common with other new technologies must first solve. Above all, it must become successful commercially, rather than remain a field based on proof of concept demonstrations and academic papers. The impact of microfluidic systems as with other tools such as lasers, NMR (nuclear magnetic resonance) spectroscopy and scanning probe microscopes will only become

apparent when everyone is using them. Microfluidics must be able to solve problems for users who are not experts in fluid physics or nanolithography, such as clinicians, cell biologists, police officers or public health officials. For these applications, corporations must take on the task of making appropriate systems widely and inexpensively available.

As with all technology in transition from university laboratories to industry, the question of 'Who owns what?' The problem of intellectual property is one that must be resolved. For technology with very high value, such as biopharmaceuticals and information-processing systems, issues of intellectual property can usually be resolved by compromising on royalties, up-front payments or equity. However, some of the most interesting applications of microfluidics are those that would demand large volumes but low prices for example, in public heath monitoring, environmental monitoring, and for use in the medical systems of developing economies. In these areas, the historical differences in the valuations placed by universities and industry on university-based technology can become a serious issue: if the university places the value of an invention too high, it is simply not worthwhile to develop a commercial technology from it.

There is also the issue of the so called 'first-user premium'. In the introduction of a new technology, the first commercial user of that technology pays a disproportionate share of the costs of its development, and accepts a disproportionate share of the risk for that development. If the application of such a development is a very appealing if it is of potentially high value (the 'killer application', or 'killer app') these costs and risks are more acceptable. The high-value killer app for microfluidics has not yet emerged, although markets in research biology are certainly developing

II.6: Large-volume microanalytical tools:

Among the most interesting and important of the potential applications of microfluidic systems are those toward which it was originally targeted: biomedical and related applications requiring small amounts of sample, routine operation by untrained personnel, and low cost Figure II.3

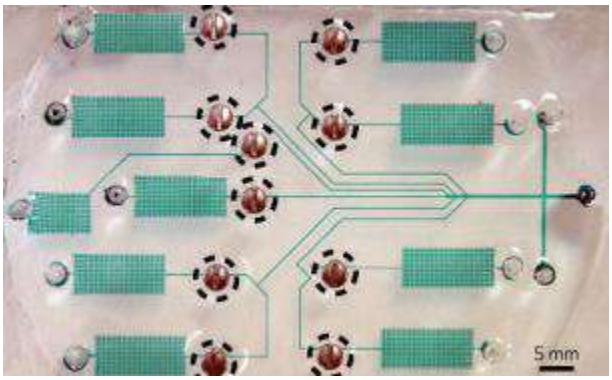


Figure II.3: A simple, inexpensive microfluidic diagnostic device

Components of microfluidic devices can be designed to be inexpensive and easy to operate. This device7 performs sandwich immunoassays tests that are used widely in medicine and biological research. The screws in this system (marked with dashed circles) act as simple manually operated valves. Green-dyed water marks the channels. Low-cost, portable, easy-to-operate microfluidic devices such as this one may find applications in resource-poor environments.

There is an appealing commonality in a number of these applications, and the volumes of appropriate analyses could, in principle, be very large (hundreds of millions of tests per year). This group of applications would include healthcare delivery and monitoring in developing economies, home healthcare and use in doctors' offices in developed economies, uses in homeland security and counterterrorism, use by first responders (police, paramedics and fire departments), applications in veterinary medicine, and incorporation into environmental and foodsafety monitoring. Diagnostic systems for developing economies will require low-cost, adaptable microfluidic technology for its success; this rapidly developing field is described in this issue by Yager et al. (see page 412).

These applications suffer from the problem of chicken and egg: the volume of use will only be large if the cost of the analysis is low and the state of development of the assay is high; and the cost will only be low if the volume is large.

II.7: New science and technology:

The development of microfluidics has just begun. A number of factors suggest that there are many early-stage applications of microsystems containing fluids, including the exploration of fluidic optics and cells, the development of new types of organic

synthesis in small channel systems, the continuing development of technologies based on large arrays of detectors and on high-throughput screening, the fabrication of microrobotic systems using hydraulic systems based on microfluidics, other fluidic versions of MEMS, and work on biomimetic systems with microfluidic components. The extension of microfluidic systems into nanofluidics in which the dimensions of the channels and the thickness of the layer of structured fluid at the walls of the device become comparable will make possible the exploration of the properties of near-surface water, and of ion and electrolyte transport at this interface. The biocompatibility of PDMS suggests that it might ultimately be possible to embed microfluidic devices in vivo for certain types of biomedically relevant analysis. Single-cell and single-molecule analysis require technologies that can work with small volumes of sample, which might allow the testing of fundamental assumptions of cell biology and molecular chemistry and biology.

II.8: Design and manufacturing systems for microfluidic devices:

An important aspect of the commercial development of microfluidics crucial to many of these applications is the development of the technology for manufacturing microfluidic devices. Ultimately, there will probably be several such technologies, but in the early stages the definition of a single set of materials and processes needed to convert laboratory demonstrations into working commercial devices is an important step. Should devices be developed in Mylar, or PDMS, or polycarbonate? What will be the specifications for user interfaces? How important will very large volume technologies, such as roll to roll processing, be? And what about technologies for sealing and packaging?[11]

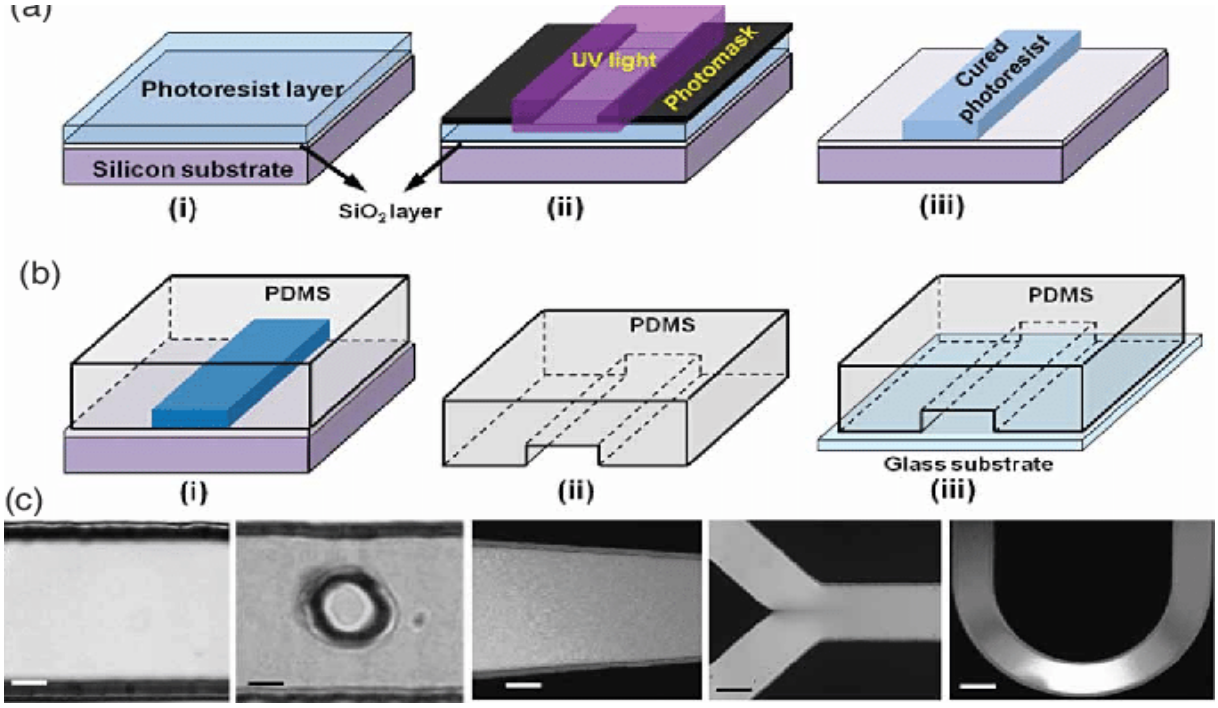


Figure II.4: Fabrication of microfluidic devices

II.9: using nanofluids in thermal transfer:

Since Nobel Prize wimer Richard Feynrnan presented the concept of micromachines in 1959, miniaturization has been a major trend in modern science and technology. Almost 40 years later, another Nobel Prize winner, H. Rohrer, presented the chances and challenges of the nano-age‖ (Rohrer, 1996). The steady miniaturization trend has dropped from the millimeter scale of the early 1950s to the present-day atomic scale (Sohn, 1998). The concept and development of nanofluids is directly related to trends in miniaturization and nanotechnology.

II.9.1: THE CONCEPT OF NANOFLUIDS:

In the development of energy efficient heat transfer equipment, the thermal conductivity of the heat transfer fluid plays a vital role. However, traditional heat transfer fluids such as water, oil, and ethylene glycol mixtures are inherently poor heat transfer fluids. With increasing global competition industries have a strong need to develop advanced heat transfer fluids with significantly higher thermal conductivities than are presently available.

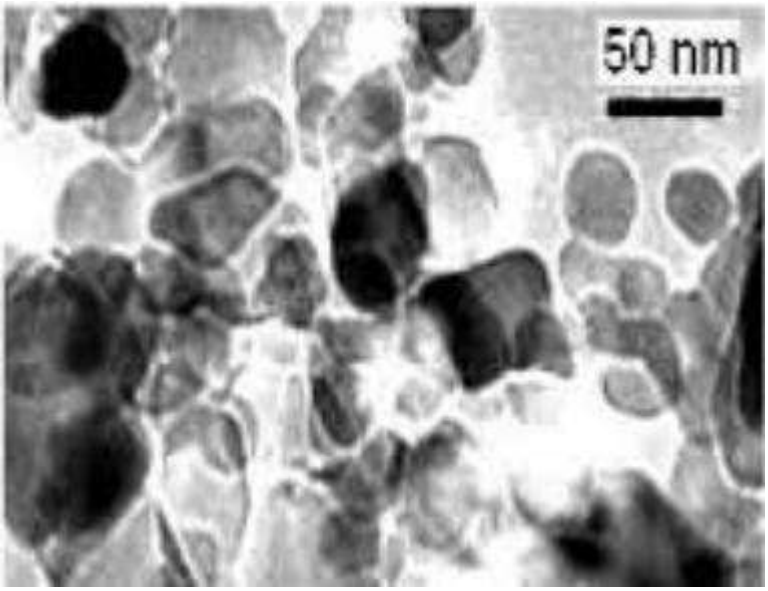


Figure II.5: Schematic view of Nanofluid

Despite considerable previous research and development efforts on heat transfer enhancement major improvements in cooling capabilities have been constrained because of the low thermal conductivity of conventional heat transfer fluids. However, it is well known that at room temperature, metals in solid form have orders of magnitude higher thermal conductivities than those of fluids (Touloukian et al., 1970). For example, the thermal conductivity of copper at room temperature is about 700 times greater than that of water and about 3000 times greater than that of engine oil. The thermal conductivity of metallic liquids is much greater than that of nano metallic liquids. Therefore, the thermal conductivities of fluids that contain suspended solid metallic particles could be expected to be significantly higher than those of conventional heat transfer fluids. In fact, numerous theoretical and experimental studies of the effective thermal conductivity of dispersions that contain solid particles have been conducted since Maxwell's theoretical work was published more than 100 years ago (Maxwell, 1873). However, all of the studies on thermal conductivity of suspensions have been confined to millimeter or micrometer sized particles. The major problem with suspensions containing millimeter or micrometer sized particles is the rapid settling of these particles. Furthermore, such particles are too large for micro systems

Modern nanotechnology provides great opportunities to process and produce materials with average crystallite sizes below 50 nm. Recognizing an opportunity to apply this emerging nanotechnology to established thermal energy engineering, the author proposed in 1993 that nanometer sized metallic particles could be suspended in

industrial heat transfer fluids such as water, ethylene glycol, or engine oil to produce a new class of engineered fluids with high thermal conductivity. Nanofluids are this new class of heat transfer fluids and are engineered by suspending nanometer sized particles in conventional heat transfer fluids. The average size of particles used in nanofluids is below 50 nm. The author coined the term nanofluids for this new class of heat transfer fluids (Choi, 1995).

It should be noted that in today science and technology, ''size does matter."`Maxwell's concept of enhancing the thermal conductivity of fluids by dispersing solid particles is old, but what is new and innovative with the concept of nanofluids is the idea of using the nanometer-sized particles that have become available to investigators only recently.[12]

II.9.2: PROPERTIES OF NANOFLUIDS:

The concept of adding small solid particles into a base fluid to increase the thermal conductivity of the suspension has been practiced for a long time. The Properties of nanofluids are Viscosity, Specific heat, Thermal Conductivity and Stability. These properties play a very important role in preparation of Nanofluids. The Properties are below:

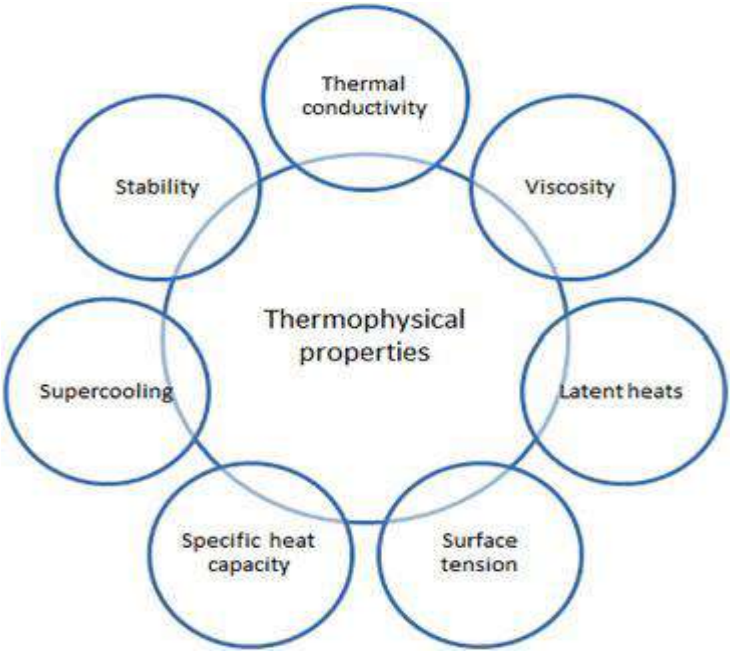


Figure II.6: thermophysical properties of nanofluid

II.9.3: Stability of Nanofluids:

Nanofluids have an undesirable propensity which influences their capability to exchange heat because of their inclination to coagulation. Subsequently, investigation on steadiness is an unavoidable issue that can change the thermophysical properties of nanofluids for application furthermore essential to dissect the compelling variables to the dependability of such suspensions. Underneath said is a brief talk on the strength development routines and dependability upgrade forms alongside a brief about the steadiness instruments identified with nanofluids.

II.9.4: Nanofluid Synthesis:

Planning of nanofluids is the first stride to the exploratory investigations of nanofluids. The best possible use of the capability of nanofluids relies on upon the planning of nanofluids. There are two principle routines to set up a nanofluid: The single step planning procedure and the two stage arrangement process

II.9.4.1: Single-step synthesis process:

The single-step readiness procedure demonstrates the blend of nanofluids in one-stage. A few single-step systems have been touched base for Nanofluid readiness. Akoh et al. investigated and built up a solitary step direct dissipation technique. In this technique the vaporized metal is dense and after that scattered by deionised water to deliver nanofluids. Leverage of blend by one-stage strategy is that Nanoparticles agglomeration is minimized. Be that as it may, prime issue is that just low vapour weight liquids are good with such a procedure. One-stage arrangement process (chemical procedure) of nanofluids is given in the Figure II.7



Figure II.7: One-step preparation process of Nano-fluids

II.9.4.2: Two-step preparation process:

Two-stage arrangement procedure is broadly utilized as a part of the union of nanofluids by blending base liquids with industrially accessible Nano powders got from diverse

mechanical, physical and substance procedures, for example, processing, crushing, and vapour stage techniques. An ultrasonic vibrator or higher shear blending gadget is for the most part used to blend Nano Powders with host liquids. Incessant utilization of Ultra Sonication blending is obliged to lessen molecule agglomeration. A few writers proposed that two-stage procedure is exceptionally suitable for get ready nanofluids containing oxide Nanoparticles than those containing metallic Nano-particles. Steadiness is a major issue that intrinsically identified with this operation as the powders effectively combine because of solid vanderwal forces among Nanoparticles. Regardless of such weaknesses this procedure is still prominent as the most financial procedure for nanofluids generation. The most widely recognized two -step strategy is indicated in Figure II.8

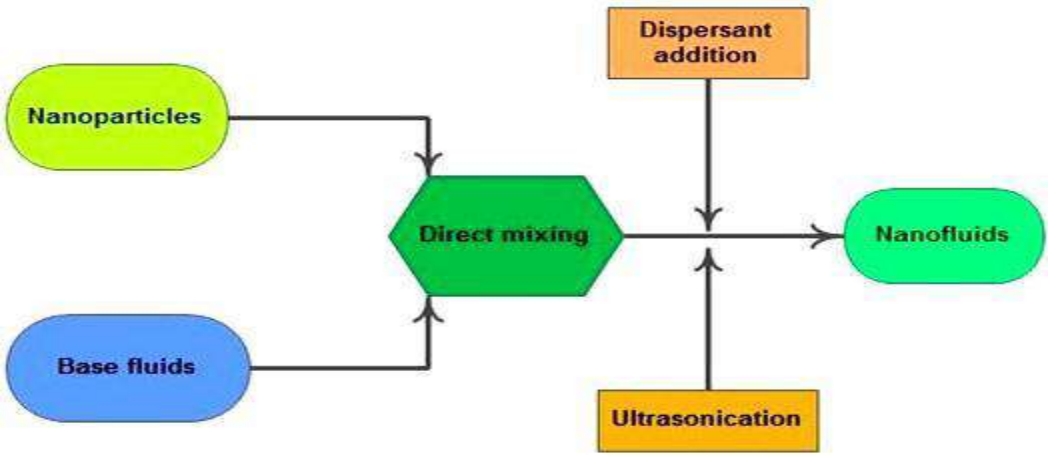


Figure II.8: Two step preparation process of Nanofluids

II.9.5: Advantages of Nanofluids:

Nanofluids cause drastic change in the properties of the base fluid so, the following benefits are expected to get on.

- Due to nano size particles, pressure drop is minimum.
- Higher thermal conductivity of nanoparticles will increase the heat transfer rate.
- Successful employment of nanofluid will lead to lighter and smaller heat exchanger.
- Heat transfer rate increases due to large surface area of the nanoparticles in the base fluid.

- Nanofluids are most suitable for rapid heating and cooling systems.
- Due to nano size particles, fluid is considered as integral fluid.
- Good mixture nanofluids will give better heat transfer.
- Microchannel cooling without clogging. Nanofluids are not only a better medium for heat transfer in general but they are also ideal for microchannel applications where high heat loads are needed.
- Cost and energy saving. Successful employment of nanofluids will result in significant energy and cost savings because heat exchange systems can be made smaller and lighter.[13]

II.9.6: APPLICATIONS OF NANOFLUIDS:

Nanofluids can be used in broad range of engineering applications due to their improved heat transfer and energy efficiency in a variety of thermal systems



II.9.6.1: Heat Transfer Intesification:

Since the origination of the nanofluid concept about a decade ago, the potentials of nanofluids in heat transfer applications have attracted more and more attention. Up to now, there are some review papers which present overviews of various aspects of nanofluids, including preparation and characterization, techniques for the measurements of thermal conductivity, theory and model, thermophysical properties, and convective heat transfer.

II.9.6.2: Electronic Applications:

Due to higher density of chips, design of electronic components with more compact makes heat dissipation more difficult. Advanced electronic devices face thermal management challenges from the high level of heat generation and the reduction of available surface area for heat removal. So, the reliable thermal management system is vital for the smooth operation of the advanced electronic devices. In general, there are two approaches to improve the heat removal for electronic equipment. One is to find an optimum geometry of cooling devices; another is to increase the heat transfer capacity. Nanofluids with higher thermal conductivities are predicated convective heat transfer coefficients compared to those of base fluids. Recent researches illustrated that nanofluids could increase the heat transfer coefficient by increasing the thermal conductivity of a coolant. Jang and Choi designed a new cooler, combined microchannel heat sink with nanofluids.

Higher cooling performance was obtained when compared to the device using pure water as working medium. Nanofluids reduced both the thermal resistance and the temperature difference between the heated microchannel wall and the coolant. A combined microchannel heat sink with nanofluids had the potential as the next generation cooling devices for removing ultrahigh heat flux. Nguyen et al. designed a closed liquid circuit to investigate the heat transfer enhancement of a liquid cooling system by replacing the base fluid (distilled water) with a nanofluid composed of distilled water and Al2O3 nanoparticles at various concentrations.

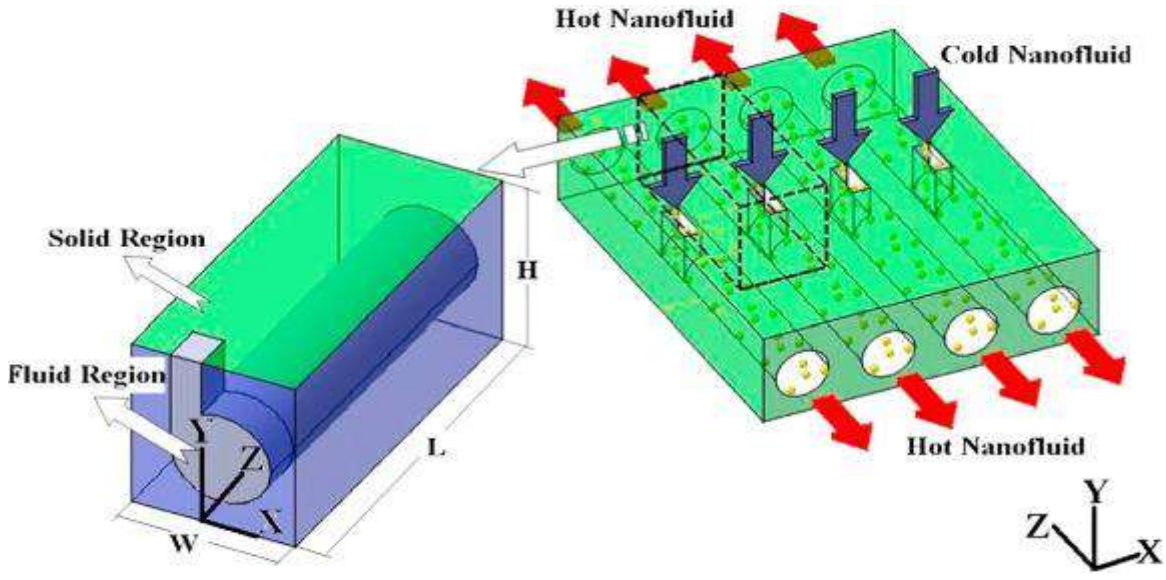


Figure II.9: Electronics cooling with nanofluids

Measured data have clearly shown that the inclusion of nanoparticles within the distilled water has produced a considerable enhancement in convective heat transfer coefficient of the cooling block. With particle loading 4.5 vol%, the enhancement is up to 23% with respect to that of the base fluid. It has also been observed that an augmentation of particle concentration has produced a clear decrease of the junction temperature between the heated component and the cooling block. Silicon microchannel heat sink performance using nanofluids containing Cu nanoparticles was analyzed. It was found that nanofluids could enhance the performance as compared with that using pure water as the coolant. The enhancement was due to the increase in thermal conductivity of coolant and the nanoparticle thermal dispersion effect. The other advantage was that there was no extra pressure drop, since the nanoparticle was small, and particle volume fraction was low.

II.9.6.3: Transportation:

Nanofluids have great potentials to improve automotive and heavy-duty engine cooling rates by increasing the efficiency, lowering the weight and reducing the complexity of thermal management systems. The improved cooling rates for automotive and truck engines can be used to remove more heat from higher horsepower engines with the same size of cooling system. Alternatively, it is beneficial to design more compact cooling system with smaller and lighter radiators. It is, in turn, beneficial the high performance and high fuel economy of car and truck. Ethylene glycol based nanofluids have attracted much attention in the application as engine coolant due to the low- pressure operation compared with a 50/50 mixture of ethylene glycol and water, which is the nearly universally used automotive coolant.

The nanofluids has a high boiling point, and it can be used to increase the normal coolant operating temperature and then reject more heat through the existing coolant system. Kole et al. prepared car engine coolant (Al2O3 nanofluid) using a standard car engine coolant (HP KOOLGARD) as the base fluid and studied the thermal conductivity and viscosity of the coolant. The prepared nanofluid, containing only 3.5% volume fraction of Al2O3 nanoparticles, displayed a fairly higher thermal conductivity than the base fluid, and a maximum enhancement of 10.41% was observed at room temperature. Tzeng et al. applied nanofluids to the cooling of automatic transmissions. The experimental platform was the transmission of a four-

wheel drive vehicle. The used nanofluids were prepared by dispersing CuO and Al2O3 nanoparticles into engine transmission oil. The results showed that CuO nanofluids produced the lower transmission temperatures both at high and low rotating speeds. From the thermal performance viewpoint, the use of nanofluid in the transmission has a clear advantage.

II.9.6.4: Industrial Cooling Applications:

The application of nanofluids in industrial cooling will result in great energy savings and emissions reductions. For US industry, the replacement of cooling and heating water with nanofluids has the potential to conserve 1 trillion Btu of energy. For the US electric power industry, using nanofluids in closed loop cooling cycles could save about 10–30 trillion Btu per year (equivalent to the annual energy consumption of about 50,000–150,000 households). The associated emissions reductions would be approximately 5.6 million metric tons of carbon dioxide, 8,600 metric tons of nitrogen oxides, and 21,000 metric tons of sulfur dioxide. Experiments were performed using a flow-loop apparatus to explore the performance of polyalphaolefin nanofluids containing exfoliated graphite nanoparticle fibers in cooling. It was observed that the specific heat of nanofluids was found to be 50% higher for nanofluids compared with polyalphaolefin, and it increased with temperature. The thermal diffusivity was found to be 4 times higher for nanofluids. The convective heat transfer was enhanced by 10% using nanofluids compared with using polyalphaolefin.

II.9.6.5: Heating Building and Reducing Pollution:

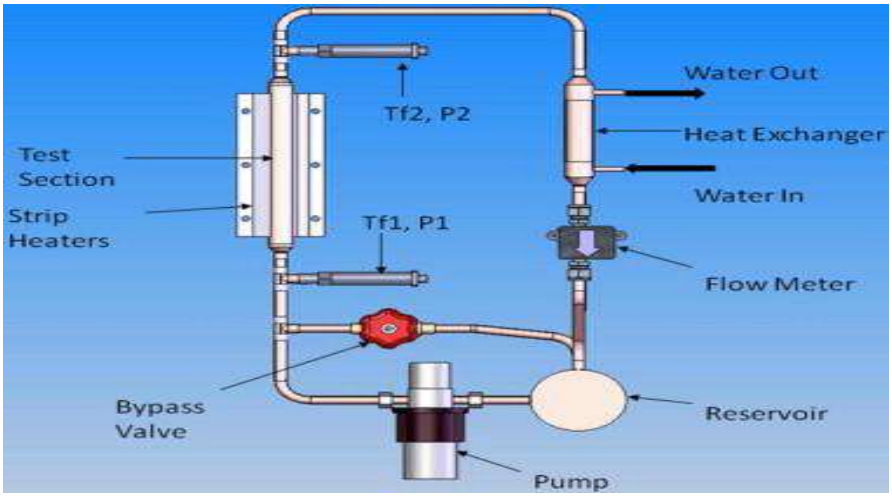


Figure II.10: Application of nanofluids in heating buildings and reducing pollution

Nanofluids can be applied in the building heating systems. Kulkarni et al. evaluated how they perform heating buildings in cold regions. In cold regions, it is a common practice to use ethylene or propylene glycol mixed with water in different proportions as a heat transfer fluid. So, 60: 40 ethylene glcol/water (by weight) was selected as the base fluid. The results showed that using nanofluids in heat exchangers could reduce volumetric and mass flow rates, resulting in an overall pumping power savings. Nanofluids necessitate smaller heating systems, which are capable of delivering the same amount of thermal energy as larger heating systems but are less expensive. This lowers the initial equipment cost excluding nanofluid cost. This will also reduce environmental pollutants, because smaller heating units use less power, and the heat transfer unit has less liquid and material waste to discard at the end of its life cycle.

II.9.6.6: Mass Transfer Enhancement:

Several researches have studied the mass transfer enhancement of nanofluids. Kim et al. initially examined the effect of nanoparticles on the bubble type absorption for NH3/H2O absorption system. The addition of nanoparticles enhances the absorption performance up to 3.21 times. Then, they visualized the bubble behavior during the NH3/H2O absorption process and studied the effect of nanoparticles and surfactants on the absorption characteristics. The results show that the addition of surfactants and nanoparticles improved the absorption performance up to 5.32 times. The addition of both surfactants and nanoparticles enhanced significantly the absorption performance during the ammonia bubble absorption process. The theoretical investigations of thermodiffusion and diffusionthermo on convective instabilities in binary nanofluids for absorption application were conducted. Mass diffusion is induced by thermal gradient. Diffusionthermo implies that heat transfer is induced by concentration gradient. Ma et al. studied the mass transfer process of absorption using CNTs-ammonia nanofluids as the working medium.

So far, the mechanism leading to mass transfer enhancement is still unclear. The existing research work on the mass transfer in nanofluids is not enough. Much experimental and simulation work should be carried out to clarify some important influencing factors.

II.9.6.7: Energy Applications:

For energy applications of nanofluids, two remarkable properties of nanofluids are utilized, one is the higher thermal conductivities of nanofluids, enhancing the heat transfer, another is the absorption properties of nanofluids.

II.9.6.7.1: Energy Storage:

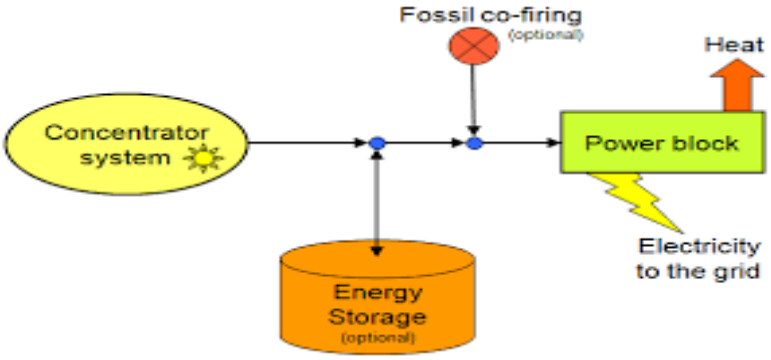


Figure II.11: Schematic diagram of Thermal energy storage

The difference of energy source and energy needs made necessary the development of storage system. The storage of thermal energy in the form of sensible and latent heat has become an important aspect of energy management with the emphasis on efficient use and conservation of the waste heat and solar energy in industry and buildings. Latent heat storage is one of the most efficient ways of storing thermal energy. Wu et al. evaluated the potential of Al2O3-H2O nanofluids as a new phase change material (PCM) for the thermal energy storage of cooling systems. The thermal response test showed the addition of Al2O3 nanoparticles remarkably decreased the supercooling degree of water, advanced the beginning freezing time, and reduced the total freezing time. Only adding 0.2 wt% Al2O3 nanoparticles, the total freezing time of Al2O3-H2O nanofluids could be reduced by 20.5%. Liu et al. prepared a new sort of nanofluid phase change materials (PCMs) by suspending small amount of TiO2 nanoparticles in saturated BaCl2 aqueous solution.

II.9.6.7.2: Solar Absorption:

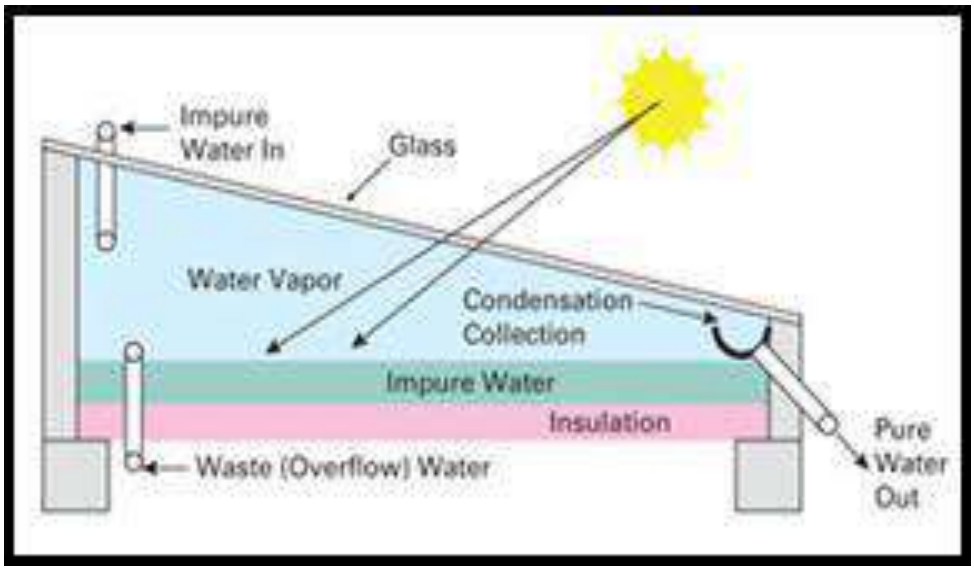


Figure II.12: Nanofluids based Solar Stills

Solar energy is one of the best sources of renewable energy with minimal environmental impact. The conventional direct absorption solar collector is a well established technology, and it has been proposed for a variety of applications such as water heating; however, the efficiency of these collectors is limited by the absorption properties of the working fluid, which is very poor for typical fluids used in solar collectors. Recently, this technology has been combined with the emerging technologies of nanofluids and liquid-nanoparticle suspensions to create a new class of nanofluid- based solar collectors. Otanicar et al. reported the experimental results on solar collectors based on nanofluids made from a variety of nanoparticles (CNTs, graphite, and silver). The efficiency improvement was up to 5% in solar thermal collectors by utilizing nanofluids as the absorption media. In addition, they compared the experimental data with a numerical model of a solar collector with direct absorption nanofluids. The experimental and numerical results demonstrated an initial rapid increase in efficiency with volume fraction, followed by a leveling off in efficiency as volume fraction continues to increase. Theoretical investigation on the feasibility of using a nonconcentrating direct absorption solar collector showed that the presence of nanoparticles increased the absorption of incident radiation by more than nine times over that of pure water. Under the similar operating conditions, the efficiency of an absorption solar collector using nanofluid as the working fluid was found to be up to 10% higher (on an absolute basis) than that of a flat plate collector.

II.9.6.8: Mechanical Applications;

Why nanofluids have great friction reduction properties? Nanoparticles in nanofluids form a protective film with low hardness and elastic modulus on the worn surface can be considered as the main reason that some nanofluids exhibit excellent lubricating properties. Magnetic fluids are kinds of special nanofluids. Magnetic liquid rotary seals operate with no maintenance and extremely low leakage in a very wide range of applications, and it utilizing the property magnetic properties of the magnetic nanoparticles in liquid.

II.9.6.8.1: Friction Reduction:

Advanced lubricants can improve productivity through energy saving and reliability of engineered systems. Tribological research heavily emphasizes reducing friction and wear. Nanoparticles have attracted much interest in recent years due to their excellent load-carrying capacity, good extreme pressure and friction reducing properties. Zhou et al. evaluated the tribological behavior of Cu nanoparticles in oil on a four-ball machine. The results showed that Cu nanoparticles as an oil additive had better friction-reduction and antiwear properties than zinc dithiophosphate, especially at high applied load. Meanwhile, the nanoparticles could also strikingly improve the load-carrying capacity of the base oil. Dispersion of solid particles was found to play an important role, especially when a slurry layer was formed.

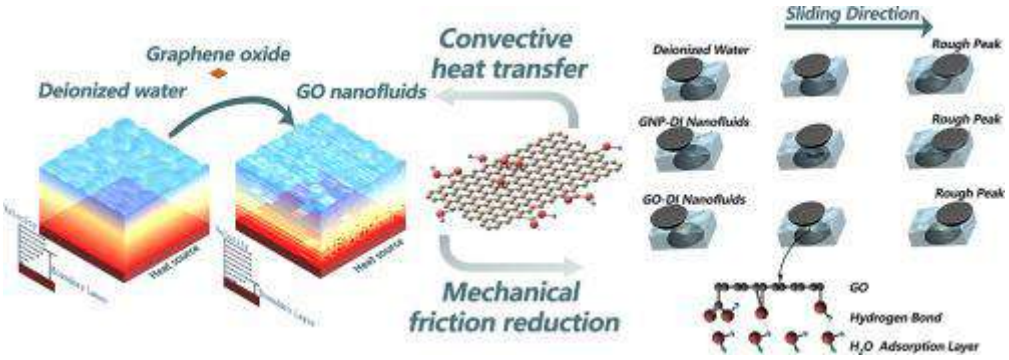


Figure II.13: Mechanical Friction Reduction and convective heat transfer relation

Water-based Al2O3 and diamond nanofluids were applied in the minimum quantity lubrication (MQL) grinding process of cast iron. During the nanofluid MQL grinding, a dense and hard slurry layer was formed on the wheel surface and could benefit the grinding performance. Nanofluids showed the benefits of reducing grinding forces, improving surface roughness, and preventing workpiece burning.

Compared to dry grinding, MQL grinding could significantly reduce the grinding temperature Wear and friction properties of surface modified Cu nanoparticles, as 50CC oil additive were studied.

The higher the oil temperature applied, the better the tribological properties of Cu nanoparticles were. It could be inferred that a thin copper protective film with lower elastic modulus and hardness was formed on the worn surface, which resulted in the good tribological performances of Cu nanoparticles, especially when the oil temperature was higher.

II.9.6.8.2: Magnetic Sealing:

Magnetic fluids (ferromagnetic fluid) are kinds of special nanofluids. They are stable colloidal suspensions of small magnetic particles such as magnetite (Fe3O4). The properties of the magnetic nanoparticles, the magnetic component of magnetic nanofluids, may be tailored by varying their size and adapting their surface coating in order to meet the requirements of colloidal stability of magnetic nanofluids with nonpolar and polar carrier liquids. Comparing with the mechanical sealing, magnetic sealing offers a cost-effective solution to environmental and hazardous gas sealing in a wide variety of industrial rotation equipment with high-speed capability, low-friction power losses, and long life and high reliability

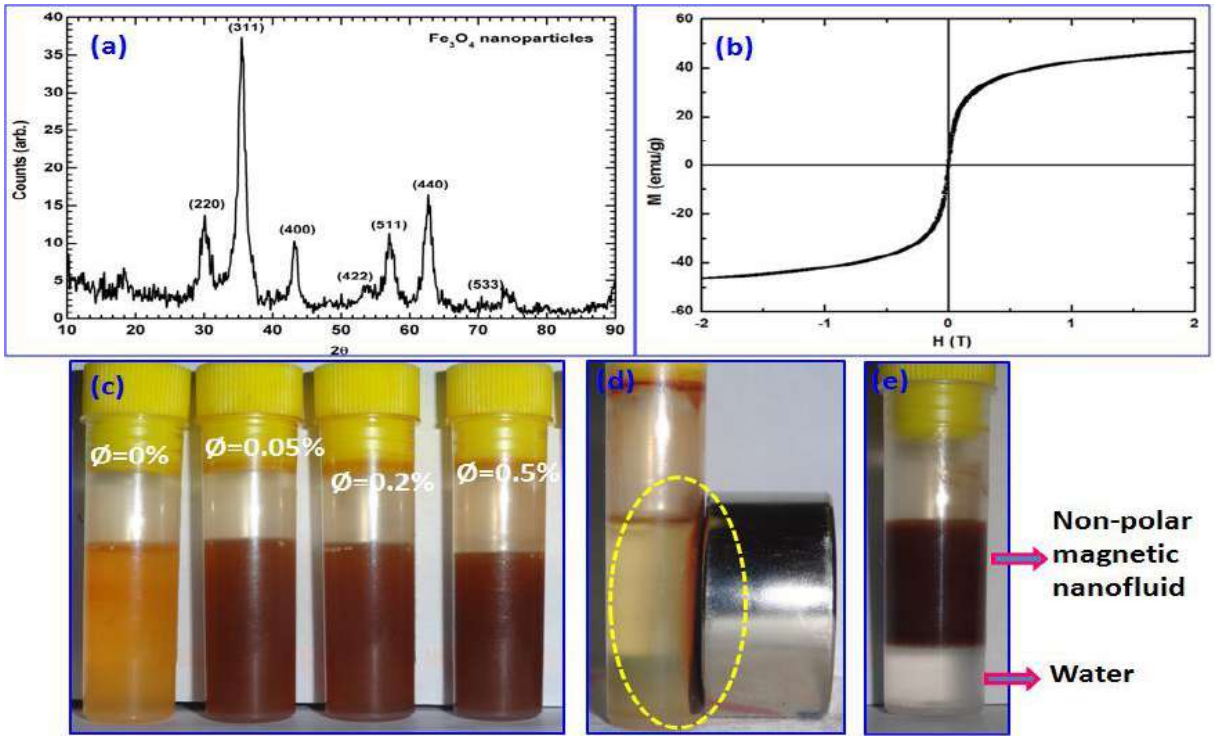


Figure II.14: Synthesized Fe3O4 nanoparticles: (a) XRD patterns, (b) M-H hysteresis, (c) VPO/Fe3O4 nanofluids samples, (d) nanoparticles showing its magnetic behavior even when they are dispersed in the base fluid, (e) magnetic nanofluid floating on water, indicating the magnetic nanofluid has non-polar behavior.

A ring magnet forms part of a magnetic circuit in which an intense magnetic field is established in the gaps between the teeth on a magnetically permeable shaft and the surface of an opposing pole block. Ferrofluid introduced into the gaps forms discrete liquid rings capable of supporting a pressure difference while maintaining zero leakage. The seals operate without wear as the shaft rotates, because the mechanical moving parts do not touch. With these unique characteristics, sealing liquids with magnetic fluids can be applied in many application areas. It is reported that an iron particle dispersed magnetic fluids was utilized in the sealing of a high rotation pump. The sealing holds pressure of 618 kPa with a 1800 r/min.

II.9.6.9: Biomedical Application:

For some special kinds of nanoparticles, they have antibacterial activities or drug-delivery properties, so the nanofluids containing these nanoparticles will exhibit some relevant properties.

II.9.6.9.1: Antibacterial Activity:

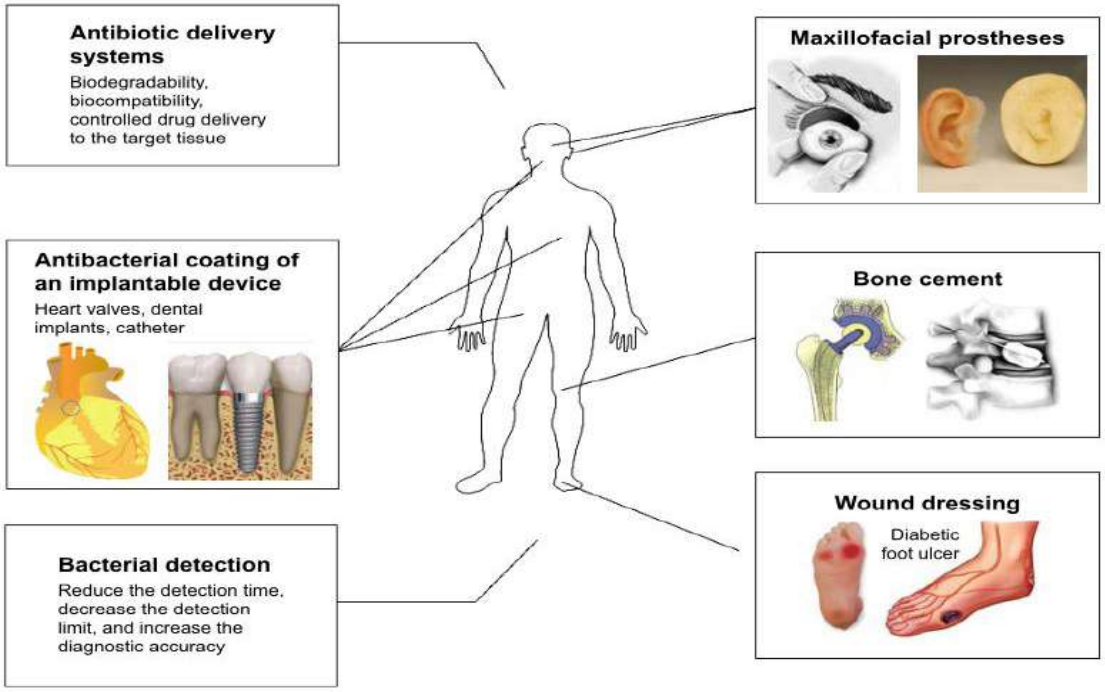


Figure II.15: The antibacterial application of nanoparticles

Organic antibacterial materials are often less stable particularly at high temperatures or pressures. As a consequence, inorganic materials such as metal and metal oxides have attracted lots of attention over the past decade due to their ability to withstand harsh process conditions. The antibacterial behavior of ZnO nanofluids shows that the ZnO nanofluids have bacteriostatic activity against. Electrochemical measurements suggest some direct interaction between ZnO nanoparticles and the bacteria membrane at high ZnO concentrations. Jalal et al. prepared ZnO nanoparticles via a green method. The antibacterial activity of suspensions of ZnO nanoparticles against Escherichia coli (E.coli) has been evaluated by estimating the reduction ratio of the bacteria treated with ZnO. Survival ratio of bacteria decreases with increasing the concentrations of ZnO nanofluids and time.

Further investigations have clearly demonstrated that ZnO nanoparticles have a wide range of antibacterial effects on a number of other microorganisms. The antibacterial activity of ZnO may be dependent on the size and the presence of normal visible light. Recent research showed that ZnO nanoparticles exhibited impressive antibacterial properties against an important foodborne pathogen, E. coli O157: H7 and the inhibitory effects increased as the concentrations of ZnO nanoparticles increased. ZnO nanoparticles changed the cell membrane components including lipids and proteins. ZnO nanoparticles could distort bacterial cell membrane, leading to loss of intracellular components, and ultimately the death of cells, considered as an effective antibacterial agent for protecting agricultural and food safety.

II.9.6.9.2: Nanodrug Delivery:

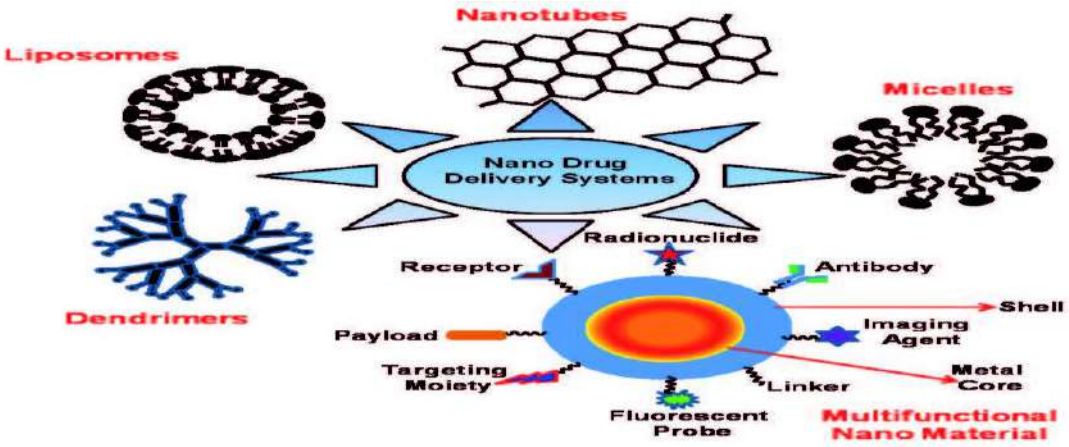


Figure II.16: Engineered nano-drug delivery systems.

Over the last few decades, colloidal drug delivery systems have been developed in order to improve the efficiency and the specificity of drug action. The small-size, customized surface improved solubility, and multifunctionality of nanoparticles opens many doors and creates new biomedical applications. The novel properties of nanoparticles offer the ability to interact with complex cellular functions in new ways. Gold nanoparticles provide nontoxic carriers for drug- and gene-delivery applications. With these systems, the gold core imparts stability to the assembly, while the monolayer allows tuning of surface properties such as charge and hydrophobicity.

Another attractive feature of gold nanoparticles is their interaction with thiols, providing an effective and selective means of controlled intracellular release. Nakano et al. proposed the drug-delivery system using nanomagnetic fluid, which targeted and concentrated drugs using a ferrofluid cluster composed of magnetic nanoparticles. The potential of magnetic nanoparticles stems from the intrinsic properties of their magnetic cores combined with their drug-loading capability and the biochemical properties that can be bestowed on them by means of a suitable coating. CNT has emerged as a new alternative and efficient tool for transporting and translocating therapeutic molecules. CNT can be functionalised with bioactive peptides, proteins, nucleic acids, and drugs and used to deliver their cargos to cells and organs. Because functionalised CNT display low toxicity and are not immunogenic, such systems hold great potential in the field of nanobiotechnology and nanomedicine. Pastorin et al. have developed a novel strategy for the functionalisation of CNTs with two different molecules using the 1, 3-dipolar cycloaddition of azomethine ylides.

The attachment of molecules that will target specific receptors on tumour cells will help improve the response to anticancer agents. Liu et al. have found that prefunctionalized CNTs can adsorb widely used aromatic molecules by simple mixing, forming forest-scrub‖-like assemblies on CNTs with PEG extending into water to impart solubility and aromatic molecules densely populating CNT sidewalls. The work establishes a novel, easy to make formulation of a SWNT-doxorubicin complex with extremely high drug loading efficiency.[14]

II.9.7: Challenges of Nanofluids and Future Direction:

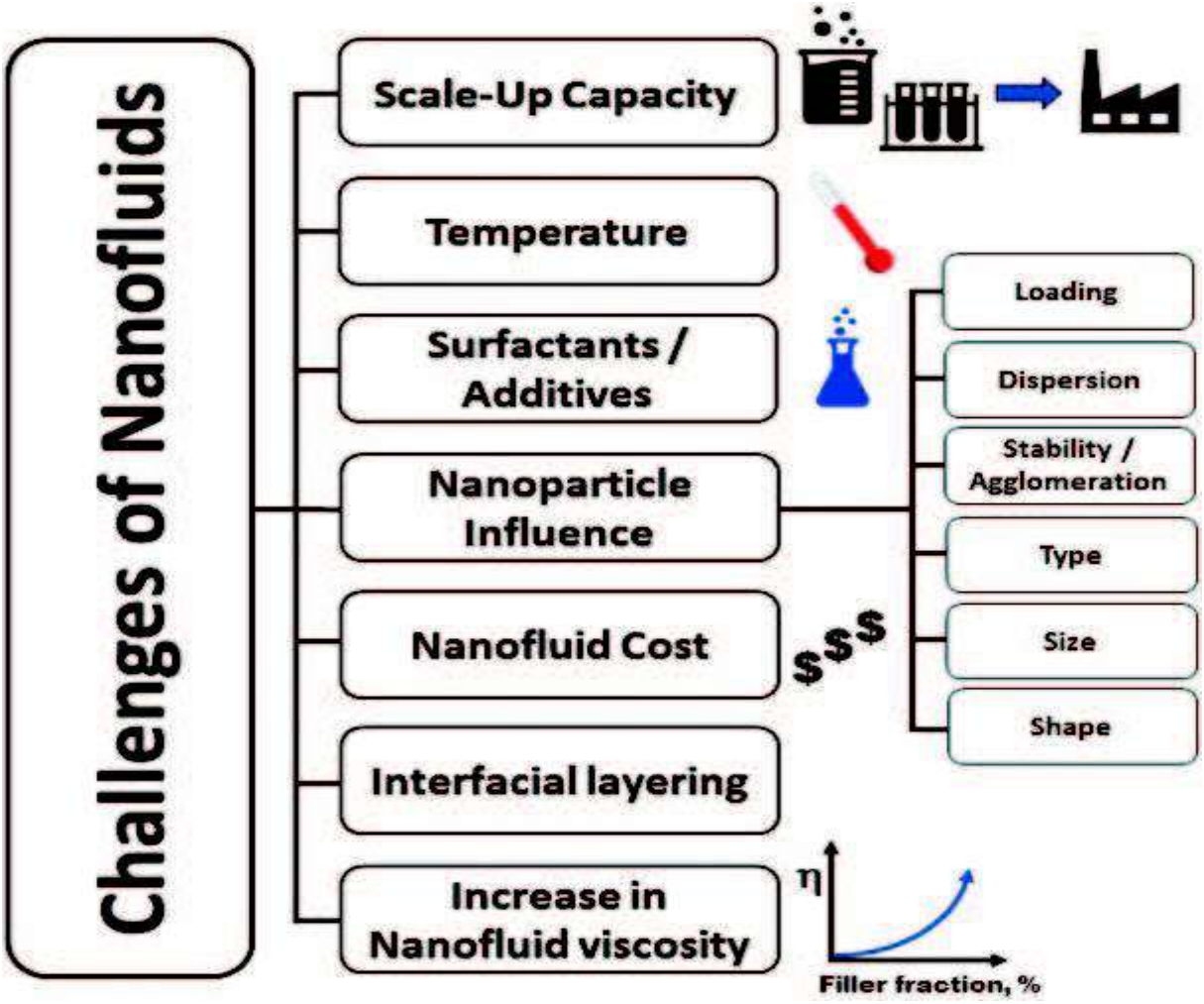


Figure II.17: Common challenges of nanofluid developments.

Nanofluids have been shown to be superior, as a HTF, to conventional known fluids available in the market. In order to commercialise such type of advanced fluids, some factors are required to be improved and better understood by researchers. Examples of these factors are listed below:

(i) Experimental investigations of nanofluids need to be optimised with respect to stability, preparation technique, temperature, particle size, particle shape, and particles type.

(ii) The right ratio of nanoparticles to basefluid should be found to obtain the highest effective thermal conductivity as well as the lowest possible effective viscosity from the fabricated nanofluid. This is important to meet the applications of heat transfer and overcome the pressure drop in the system.

(iii) Additional research inputs are needed to develop much precise correlations, which can predict the changes in nanofluids pH value caused by temperature, particle concentration, type of basefluid, and so forth, since this affects the stability and thermophysical properties of nanofluids.

(iv) Several studies have considered the fouling effect of nanofluids in a thermal aspect but, to the best of our knowledge, have ignored their influence on the dynamics of the fluid. Though, if fully deposited on the inner pipe surface, it can provide similar wettability properties as nanocoating.

The aforementioned challenges need to be focused on andtackled by researches so that commercialisation of nanofluids can be possible.[15]

II.10: CONCLUSION:

Modern nanotechnology provides great opportunities to process and produce materials with average crystallite sizes below 50 nm. Recognizing an opportunity to apply this emerging nanotechnology to established thermal energy engineering

Maxwell's concept of enhancing the thermal conductivity of fluids by dispersing solid particles is old, but the concept of nanofluids containing nanometer-sized particles that have become available to investigators only recently, is a new and innovative idea.

The envisioned benefits of nanofluids include improved heat transfer, improved suspension stability, decreased pumping power need, miniaturized systems, reduced heat transfer fluid inventories, minimal clogging in microchannels, and cost and energy savings.

III.1: Introduction:

Nanotechnology is being used or considered for use in many applications targeted to provide cleaner, more efficient energy supplies and uses. While many of these applications may not affect energy transmission directly, each has the potential to reduce the need for the electricity, petroleum distillate fuel, or natural gas that would otherwise be moved through energy transmission system. More efficient energy generation and use may decrease the amount of construction, maintenance, repair, and decommissioning activities.

Producing compact heating systems has become a basic and challenging purpose for obtaining higher efficiency in different industries. According to some previous studies, to increase the produced power in some power plants, or to some upgrading, there is an emergency need to increase the heat transfer capacity in existing systems

Along with achievements in heat transfer enhancement, researchers have been able to put into practice new heat transfer media to increase the heat exchange through channels, microchannels and micropipe.

Therefore, in novel equipment, the heat transfer issue has high importance among the researchers using this science. By combining some methods such as using nanofluids and microchannels with other methods, the researchers have improved the efficiency of heat transfer equipment. Behnampour et al

In the present study, the effect of triangular, rectangular, Elliptical and trapezoidal ribs on the laminar heat transfer of water and water-Ag nanofluid in a ribbed triangular channel under a constant heat flux was numerically studied using finite volume method. Height and width of ribs have been assumed to be fixed in order to study the effect of different rib forms. Modeling were performed for laminar flow (Re=1, 10, 50 and 100) and nanofluid volume fractions of 2% and 4%

III.2: Geometry:

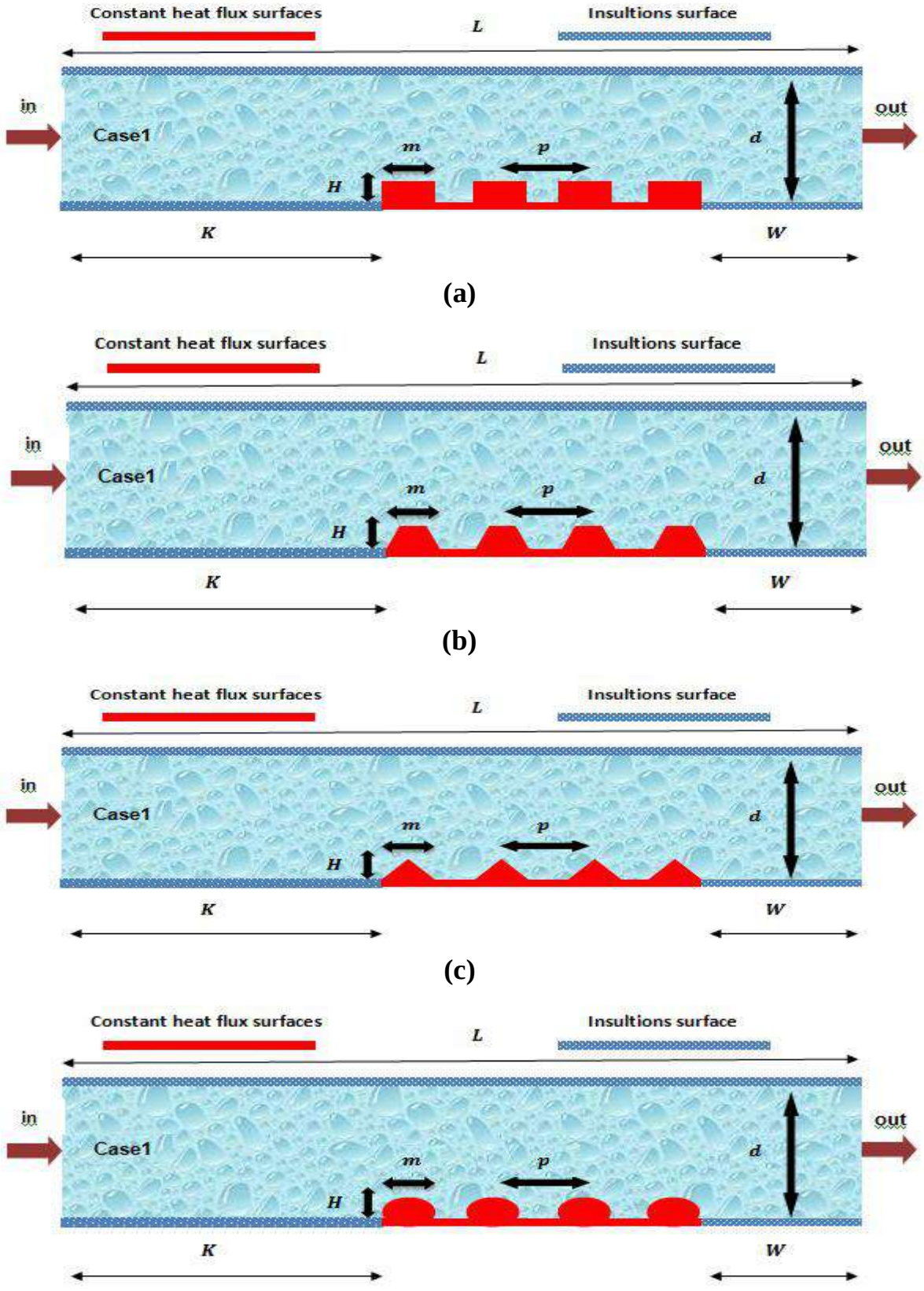


Figure.III.1: Schematic of the studied microchannels. a)rectangular, b) trapezoidal, c)triangular, d)Elliptical.

III.3: Mathematical Formulation:

III.3.1: Governing equations of the two-dimensional laminar flow [16]:

The governing equations of flow and the forced, two-dimensional, laminar, constant and single-phase heat transfer including consistency, momentum and energy equations are as follows:

$$\frac{\partial u}{\partial x}+\frac{\partial x}{\partial y}+\frac{\partial w}{\partial z}=0 \tag{3.1}$$

$$u\frac{\partial u}{\partial x}+v\frac{\partial u}{\partial y}=-\frac{1}{\rho_{\mathrm{nf}}}\frac{\partial p}{\partial x}+v_{\mathrm{nf}}\left(\frac{\partial}{\partial x}\left(\frac{\partial u}{\partial x}\right)+\frac{\partial}{\partial y}\left(\frac{\partial u}{\partial y}\right)\right) \tag{3.2}$$

$$u\frac{\partial v}{\partial x}+v\frac{\partial v}{\partial y}=-\frac{1}{\rho_{\mathrm{nf}}}\frac{\partial p}{\partial x}+v_{\mathrm{nf}}\left(\frac{\partial}{\partial x}\left(\frac{\partial v}{\partial x}\right)+\frac{\partial}{\partial y}\left(\frac{\partial v}{\partial y}\right)\right) \tag{3.3}$$

$$u\frac{\partial T}{\partial x}+v\frac{\partial T}{\partial y}=\alpha_{\mathrm{nf}}\left(\frac{\partial}{\partial x}\left(\frac{\partial T}{\partial x}\right)+\frac{\partial}{\partial y}\left(\frac{\partial T}{\partial y}\right)\right) \tag{3.4}$$

The equations related to the non-dimensioning of governing equations of laminar and forced nanofluid flow are described as follows:

$$\begin{aligned} &X=\frac{x}{H},Y=\frac{y}{H},U=\frac{u}{u_{\mathrm{c}}},V=\frac{v}{u_{\mathrm{c}}},P=\frac{\bar{P}}{\rho_{\mathrm{nf}}u_{\mathrm{c}}^{2}}\\ &\theta=\frac{T-T_{\mathrm{c}}}{\Delta T},Re=\frac{u_{\mathrm{c}}\times H}{v_{f}},\mathrm{Pr}=\frac{v_{\mathrm{f}}}{\alpha_{\mathrm{f}}},\Delta T=\frac{q''D_{\mathrm{h}}}{k_{\mathrm{f}}}\end{aligned} \tag{3.5}$$

By substituting the dimensionless Eq. [3.5] in Eqs ([3.1]–[3.4]), the consistency, momentum and energy equations in the dimensionless state can be written as follows:

$$\frac{\partial U}{\partial X}+\frac{\partial V}{\partial Y}=0 \tag{3.6}$$

$$U\frac{\partial U}{\partial X}+V\frac{\partial U}{\partial Y}=-\frac{\partial P}{\partial X}+\frac{\mu_{\mathrm{nf}}}{\rho_{\mathrm{nf}}v_{\mathrm{f}}}\frac{1}{Re}\left(\frac{\partial^{2}U}{\partial X^{2}}+\frac{\partial^{2}U}{\partial Y^{2}}\right) \tag{3.7}$$

$$U\frac{\partial V}{\partial X}+V\frac{\partial V}{\partial X}=-\frac{\partial P}{\partial Y}+\frac{\mu_{\mathrm{nf}}}{\rho_{\mathrm{nf}}v_{\mathrm{f}}}\frac{1}{Re}\left(\frac{\partial^{2}V}{\partial X^{2}}+\frac{\partial^{2}V}{\partial Y^{2}}\right) \tag{3.8}$$

$$U\frac{\partial\theta}{\partial X}+V\frac{\partial\theta}{\partial Y}=\frac{\alpha_{\mathrm{nf}}}{\alpha_{\mathrm{f}}}\frac{1}{\mathrm{RePr}}\left(\frac{\partial^2\theta}{\partial X^2}+\frac{\partial^2\theta}{\partial Y^2}\right) \quad (3.9)$$

The dimensionless boundary conditions for the studie geometrics of the present paper are defined as follows:

$$U=0,\ V=0 \text{ and } \theta=0 \text{ for } X=0 \text{ and } 0\le Y\le 1 \quad (3.10)$$

$$V=0 \text{ and } \frac{\partial U}{\partial X}=0 \text{ for } X=150 \text{ and } 0\le Y\le 1 \quad (3.11)$$

$$U=0,\ V=0 \text{ and } \frac{\partial\theta}{\partial Y}=0 \text{ for } Y=1 \text{ and } 0\le X\le 150 \quad (3.12)$$

$$U=0, V=0 \text{ and } \frac{\partial\theta}{\partial Y}=0 \text{ or } \frac{\partial\theta}{\partial Y}=-\frac{k_{\mathrm{f}}}{k_{\mathrm{nf}}} \text{ for } Y=0 \text{ and } 0\le X\le 15 \quad (3.13)$$

III.3.2: The equations related to the computation of nanofluid properties and flow parameters [16]:

Following equations are used for calculating the density and the specific heat capacity of nanofluid:

$$\rho_{\mathrm{nf}}=(l-\varphi)\rho_{\mathrm{f}}+\varphi\rho_{\mathrm{s}} \quad (3.14)$$

$$\left(\rho C_{\mathrm{p}}\right)_{\mathrm{nf}}=(l-\varphi)\left(\rho C_{\mathrm{p}}\right)_{\mathrm{f}}+\varphi\left(\rho C_{\mathrm{p}}\right)_{\mathrm{s}} \quad (3.15)$$

Chon equation has been used for computing the thermal conductivity of nanofluid.

$$\frac{k_{\mathrm{m}}}{k_{\mathrm{f}}}=1+64.7\phi^{0.746}\left(\frac{d_{\mathrm{f}}}{d_{\mathrm{np}}}\right)^{0.369}\left(\frac{k_{\mathrm{np}}}{k_{\mathrm{f}}}\right)^{0.7476}Pr^{0.9955}Re^{1.2321}$$

$$Re=\frac{\rho_{\mathrm{f}}k_{\mathrm{b}}T}{3\pi\mu^2 l_{\mathrm{f}}},\mathrm{Pr}=\frac{\mu_{\mathrm{f}}}{\rho_{\mathrm{f}}\alpha_{\mathrm{f}}},\mu=A\times 10^{\frac{B}{T-C}},C=140(\mathrm{K})$$

$$B=247(\mathrm{K}),A=2.414\times 10^{-5}(\mathrm{Pa.s}),T=T_{\mathrm{in}} \quad (3.16)$$

In the above equations, the indexes of ρ, k, φ and Cp are, respectively, the density, thermal conductivity coefficient, volume fraction of nanoparticle and the specific heat capacity and the subindexes of s, f and nf are, respectively, the solid nanoparticles, base fluid and nanofluid. For calculating the effective dynamic viscosity, Brinkman equation is used:

$$\mu_{\mathrm{nf}} = \frac{\mu_{\mathrm{f}}}{(l-\varphi)^{2.5}} \tag{3.17}$$

For calculating the local Nusselt number along the microchannel walls, following equation is used:

$$Nu(x) = \frac{h(x)\cdot H}{k_{\mathrm{f}}} \tag{3.18}$$

For calculating Fanning friction factor, following equation is used:

$$C_{\mathrm{f}} = \frac{\tau_{\mathrm{w}}}{\frac{1}{2}\times\rho\times u_{\mathrm{in}}^2} \tag{3.19}$$

The performance evaluation criterion and the pressure drop between the inlet and outlet sections are calculated by following equations:

$$\mathrm{PEC} = \frac{\left(\frac{Nu_{\mathrm{ave}}}{Nu_{\mathrm{ave},\varphi=0}}\right)}{\left(\frac{f}{f_{\varphi=0}}\right)^{(1/3)}} \tag{3.20}$$

$$\Delta P = \bar{P}_{\mathrm{out}} - \bar{P}_{\mathrm{in}} \tag{3.21}$$

III.4: border conditions:

Figure.III.1**:** shows the investigated geometry. This study aims to simulate heat transfer and nanofluid flow in 2-D microchannels with rectangular, trapezoidal, triangular and Elliptical rib shapes. The length and hydraulic diameter of the microchannel are $5\ mm$ and $100\ \mu m$, respectively. Top wall of the microchannel is insulated but the mid section of the bottom wall where the ribs are located, there is under a constant thermal flux equal to$q''= 1000\ W/m2$. The inlet and outlet insulated length of the bottom wall are equal to $2.5\ mm$ and $1\ mm$, respectively. Pitch, height and length of the ribs are considered equal to 300, 20 and$100\ \mu m$. The inlet temperature of working fluid is $Tc = 290\ K$. It is also assumed that water and the silver nanoparticles are in thermal balance; while nanoparticles are spherical. The flow along the microchannel is laminar, Newtonian and incompressible and the effect of radiation is negligible under a no-slip boundary condition in the walls. The thermophysical properties of distilled water (base fluid), nanoparticles and nanofluid in different volume fractions for average temperature of $298\ K$ are depicted in Table IV.1. In this study, numerical analysis and a calculation of fluid flow and heat transfer parameters have been conducted in Reynold numbers 1, 10, 50 and 100 and nanoparticle volume fractions of 0.00, 0.02 and 0.04.

Table.III.1: Thermophysical properties of base fluid, nanoparticles and nanofluids

	Distilled water	Ag	Nanofluid $\varphi = 0.02$	Nanofluid $\varphi = 0.04$
$Cp/Jkg^{-1}k^{-1}$	4179	235	3481.3	2976.2
ρ/kgm^{-3}	997	10,500	1187.2	1377.2
$k/Wm^{-1}k^{-1}$	0.613	429	1.0052	1.4137
$\mu/Pa\ s$	8.91×10^{-4}	_	9.37×10^{-4}	9.86×10^{-4}

III.5: Simulation software:

ANSYS Workbench is a new generation solution from ANSYS that provides powerful methods for interacting with the ANSYS solver functionality. This environment provides a unique integration with CAD systems, and your design process, enabling the best CAE results.

III.5.1: Introduction:

ANSYS Workbench is a project management tool. It can be considered as the top level interface linking all our software tools.

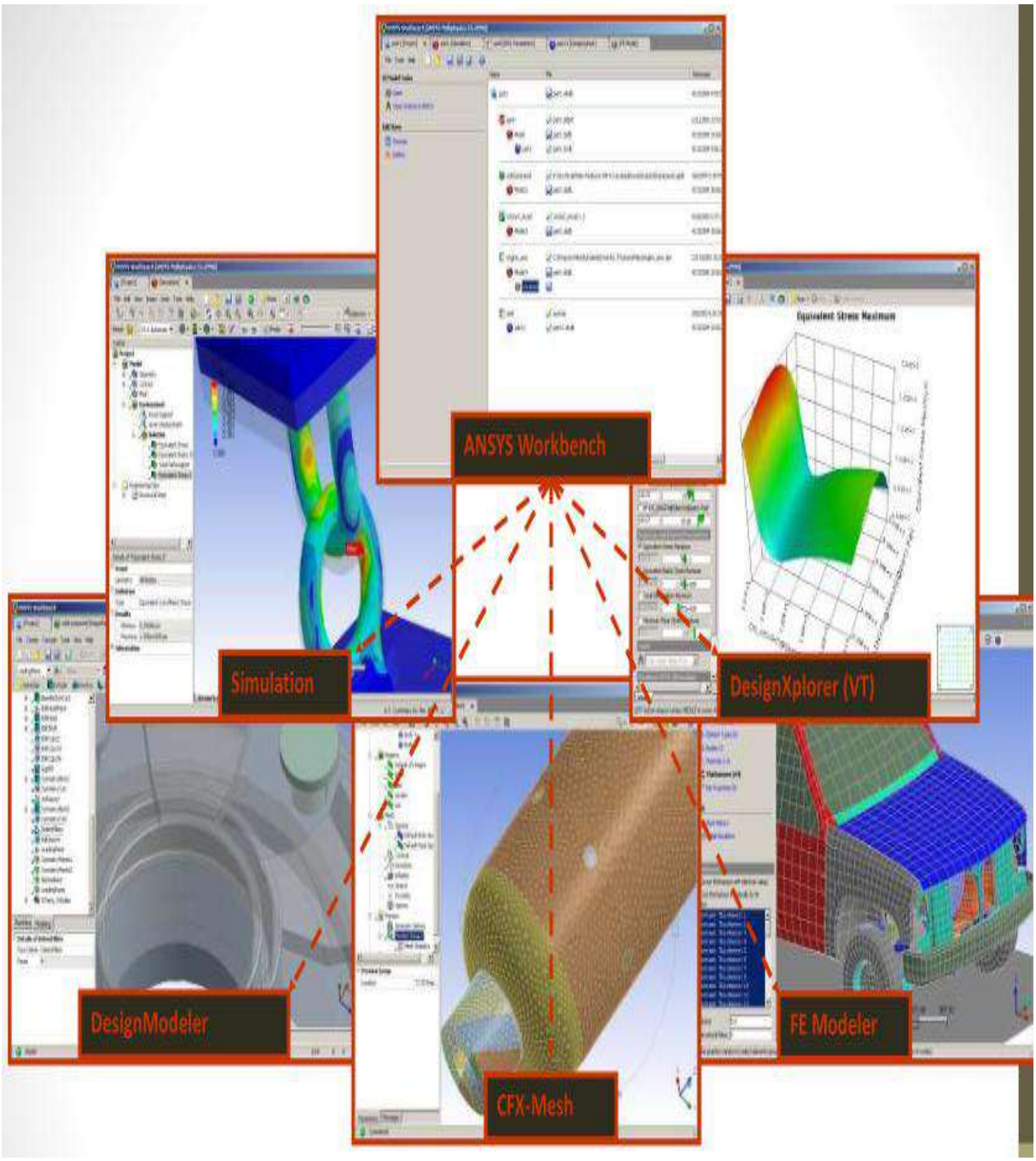
Workbench handles the passing of data between ANSYS Geometry / Mesh / Solver / Postprocessing tools.

This greatly helps project management. You do not need worry about the individual files on disk (geometry, mesh etc). Graphically, you can see at a glance how a project has been built because Workbench can manage the individual applications AND pass data between them; it is easy to automatically perform design studies (parametric analyses) for design optimisation.[17]



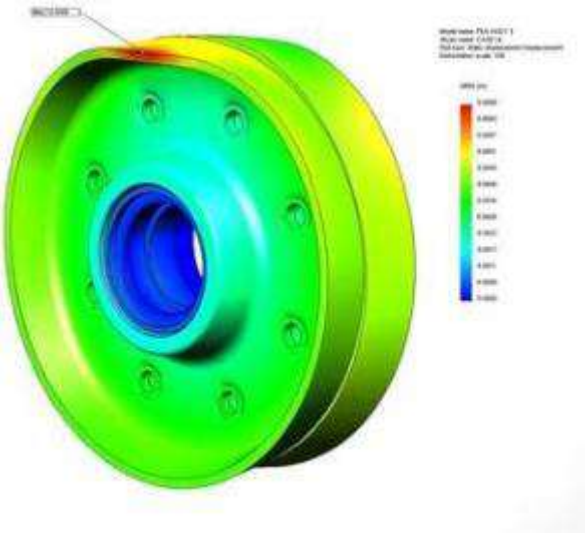
III.5.2: Analysis types in Workbench:

Analysis types available in Simulation:



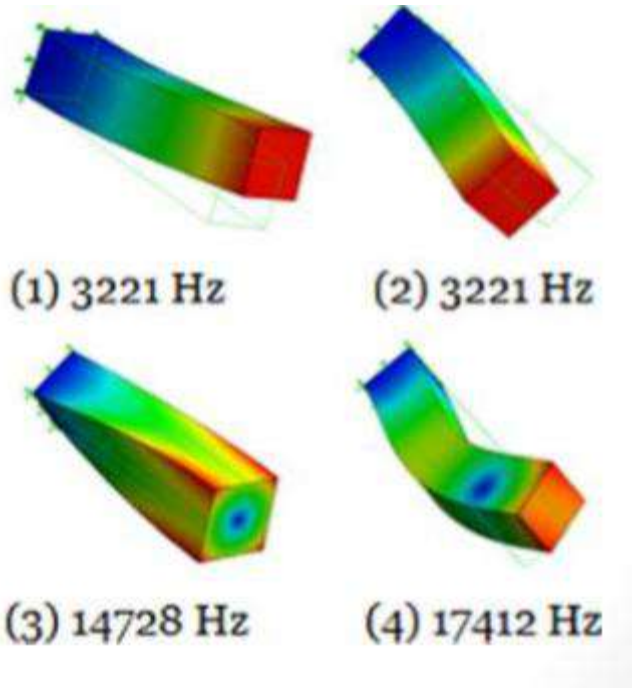
- **Linear Stress:**

Determines deflections, stresses, factors of safety, etc. based on standard strength of materials concepts under static loading



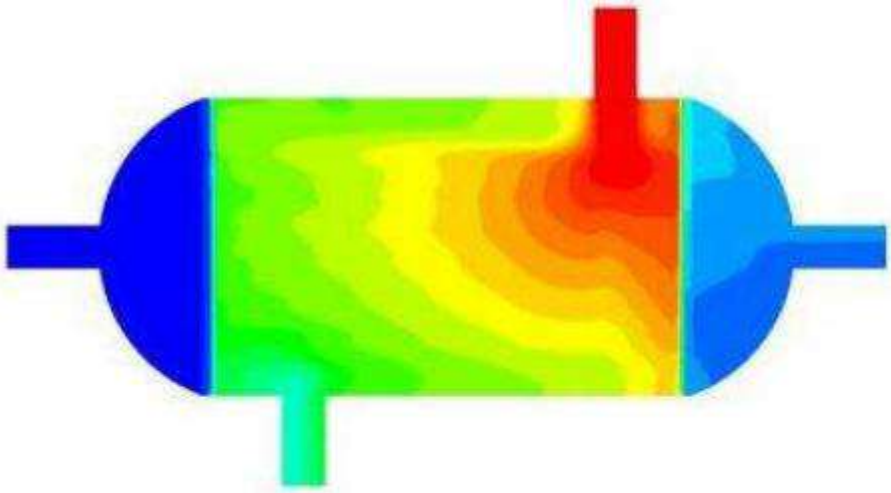
- **Modal:**

Determines natural frequencies of a system (free vibration), including the effects of loading on a pre-stressed structure.



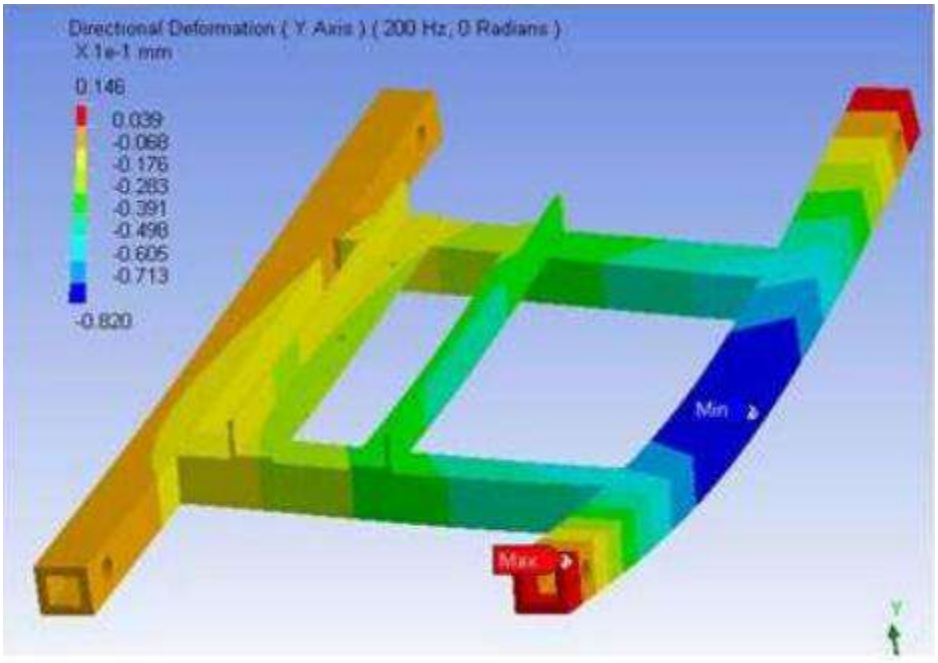
- **Heat Transfer:**

Steady state thermal analyses to solve for temperature field and heat flux. Temperature dependent conductivity and convection allowed. Thermal-stress analysis supported as well.



- **Harmonic:**

Determines structural response of system under sinusoidal excitation as a function of frequency.



- **Linear Buckling:**

Determines failure load or safety factor for buckling and its buckling mode shapes.

- **Shape Optimization:**

Indicates areas of possible volume reduction based on load paths through the part using Topological Optimization technology.

- **Nonlinear Structural:**

Calculates deflections and stresses of system under static loading, accounting for large deflection effects, plasticity, and contact nonlinearities.

III.5.3: Types of licenses:

Types of licenses available for Simulation:

• ANSYS DesignSpace Entra: All DesignSpace capabilities but for parts only.

• ANSYS DesignSpace: Structural capabilities are linear static, modal, and buckling analyses of assemblies. Thermal and shape optimization included.

• ANSYS Professional: Linear structural (including harmonic) and thermal analyses

• ANSYS Structural: All structural capabilities, including linear and nonlinear

• ANSYS Mechanical (including ANSYS Multiphysics): All structural and thermal capabilities

• (Other ANSYS licenses are supported for meshing only). [18]

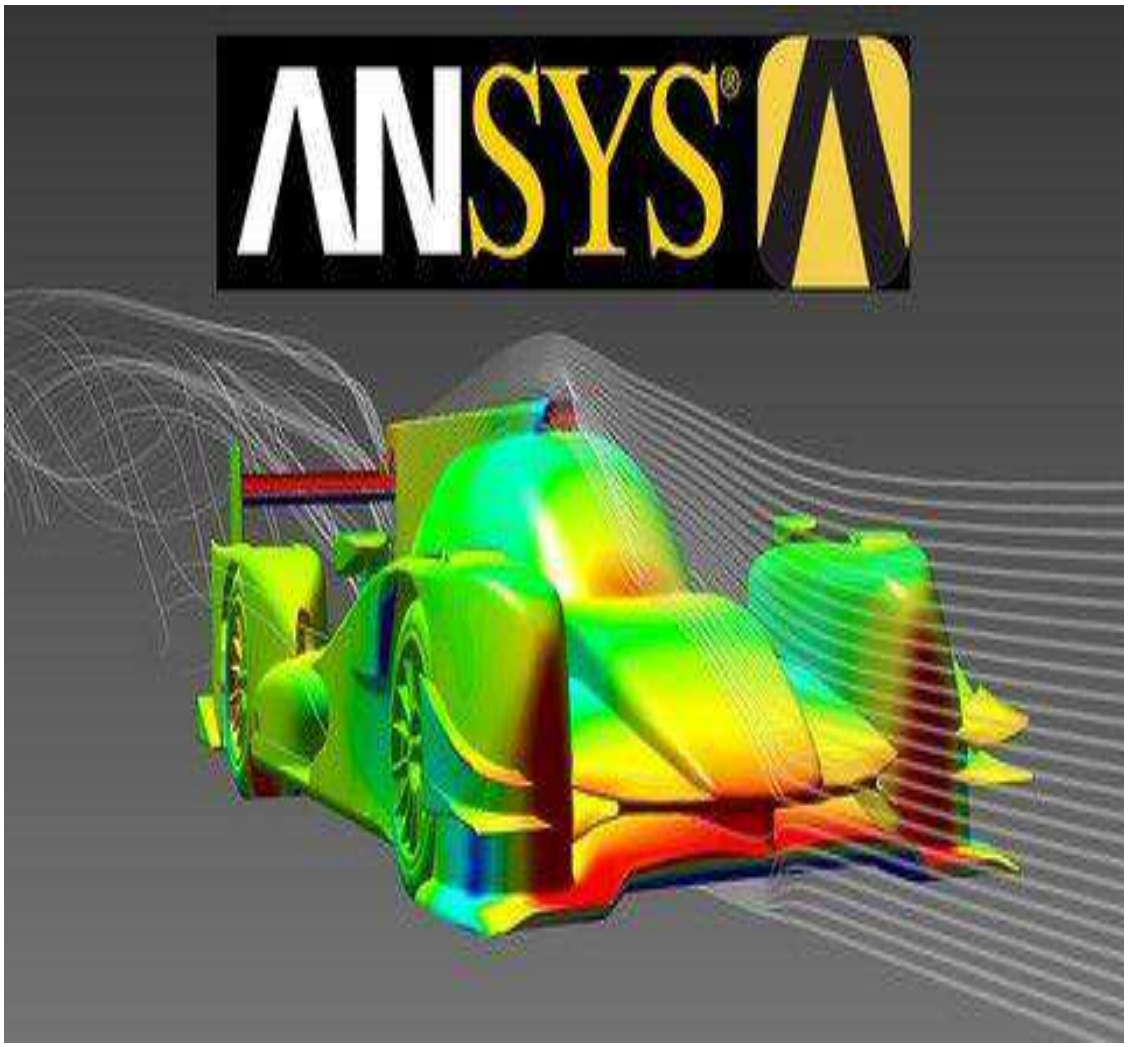
III.5.4: conclusion:

ANSYS Workbench is a convenient way of managing your simulation projects.

Workbench is used to launch the individual software components, and used to transfer data between them.

It is easy to see at a glace how a model has been built, and determine which files were used for a particular simulation (pairing geometry files to solver runs)

Workbench also makes it straightforward to perform parametric analyses (without the user needing to manually launch each application in turn), and makes it easy to simulate multi-physics scenarios like fluid-structure interaction.

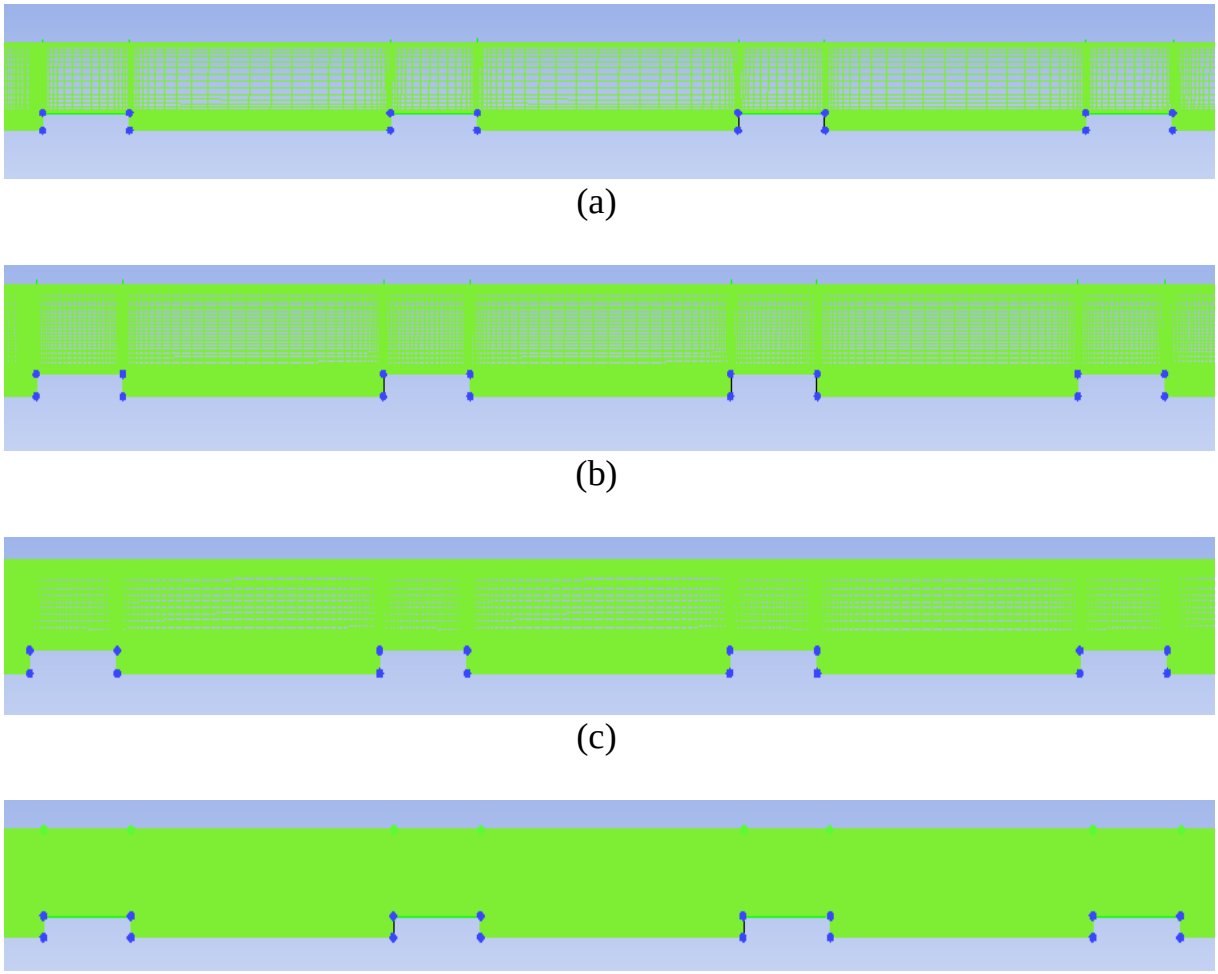


IV.1: Introduction:

In this paper, to simulate the flow and heat transfer of water and nanofluid, the finite volume method was used. Ansys Workbrench was utilized to discrete continuity, momentum and energy equations. To control the numerical error and ensure of iteration numbers.

IV.2: Meshing:

To study the mesh sensitivity, Nusselt number was studied on the hot wall of microchannel for rectangular shape ribs (Table IV.1) shows the results for various numbers of meshes. Based on these results, (c) mesh was chosen for all the modeling. The obtained results from this number of meshes have an acceptable error with an optimum CPU usage time and number of iterations



(a)

(b)

(c)

(d)

Figure.IV.1: different meshings of rectangular microchannel

Table.IV.1: The study of grid independency for state of Re = 50 and u = 0.0% of nanoparticles.

	(a)	(b)	(c)	(d)
Nu	425.192	39.8868	3.99115	39.8554
Grid number	26734	31044	51254	79414

IV.3: Simulation 1:

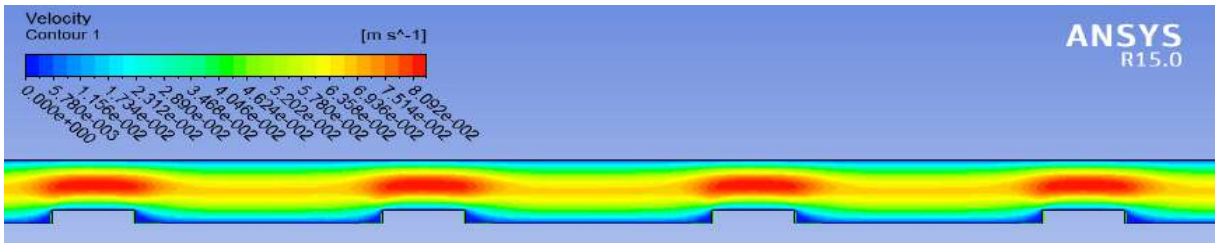
Fluid used **(Water).**

Simulation of different Reynolds number (1, 10, 50 and 100) for rectangular ribs.

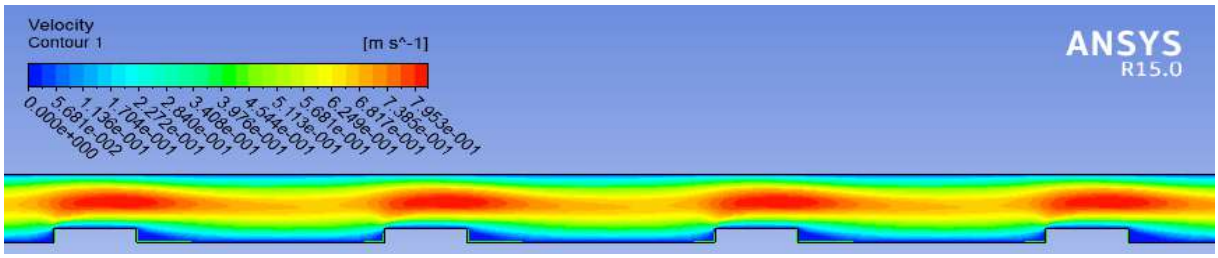
IV.3.1: Contours:

Figure.IV.2 and **Figure.IV.3** shows dimensionless axial velocity and temperature contours in Reynold number of (1, 10, 50 and 100) for rectangular ribs. Velocity in and temperature decreases the most we rise Reynold number.

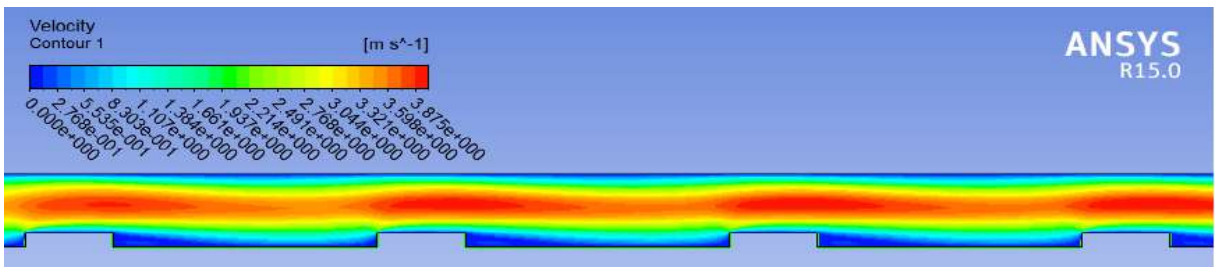
●Velocity contours:



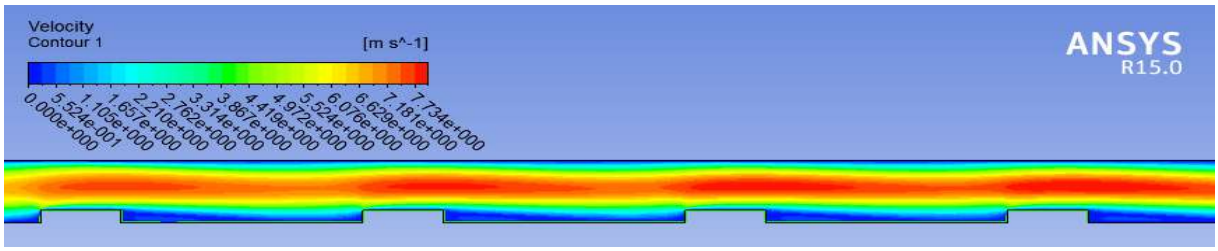
Re=1



Re=10



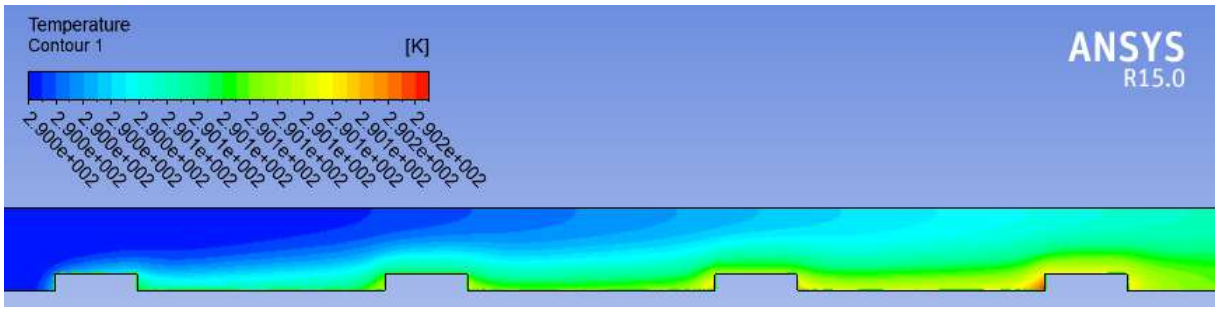
Re=50



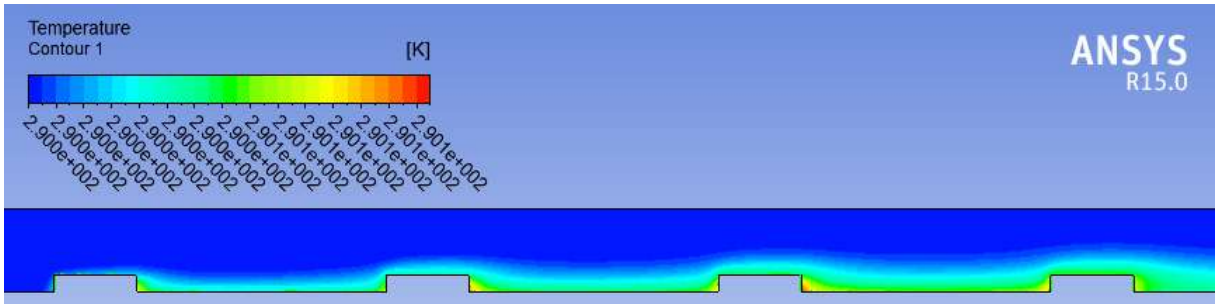
Re=100

Figure.IV.2: dimensionless velocity contours

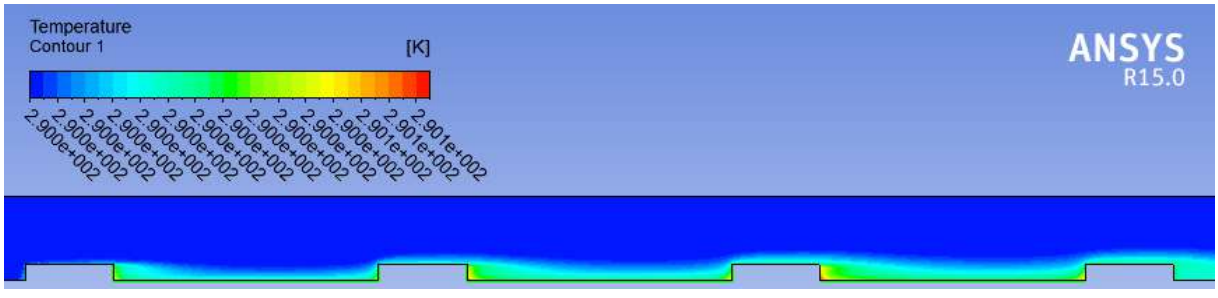
- **Temperature contours:**



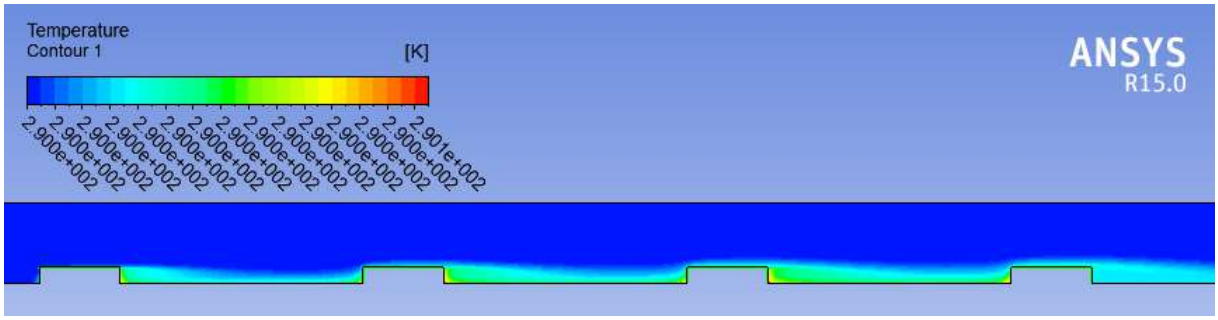
Re=1



Re=10



Re=50



Re=100

Figure.IV.3: dimensionless temperature contours.

IV.3.2: graphs and discussion:

Before Data plotting we draw five virtual lines (Table IV.2) before, between and after the ribs on the microchannel so we could calculate velocity, temperature and friction in different places in the microchannel and theirs evolution.

Table.IV.2: coordinates of the virtual lines on the microchannel.

	X1	X2	X3	X4	X5
X[mm]	2.65	2.95	3.25	3.55	3.85

Figure.IV.4 and **Figure.IV.5** shows velocity and temperature graphs in Reynold number of (1, 10, 50 and 100) for rectangular ribs in five virtual lines. Both velocity and temperature decreases the most we rise Reynold number we can see this clearly in the fifth line x5 of Re=50 and Re=100

Figure.IV.6 and **Figure.IV.7** shows velocity and temperature graphs in Reynold number of (1, 10, 50 and 100) for rectangular ribs in five virtual lines but this time we did the similar lines in the same graph. So in all the lines velocity and temperature decreases for high Reynold numbers

Figure.IV.8 demonstrates the amounts of friction and average friction factor in different Reynolds numbers of (1, 10, 50 and 100). In all cases, by increasing the Reynolds number, the friction coefficient is reduced.

Based on this results we choose the higher Reynolds number Re=10 for the next simulation

- graphs of the same Reynolds number for different lines:

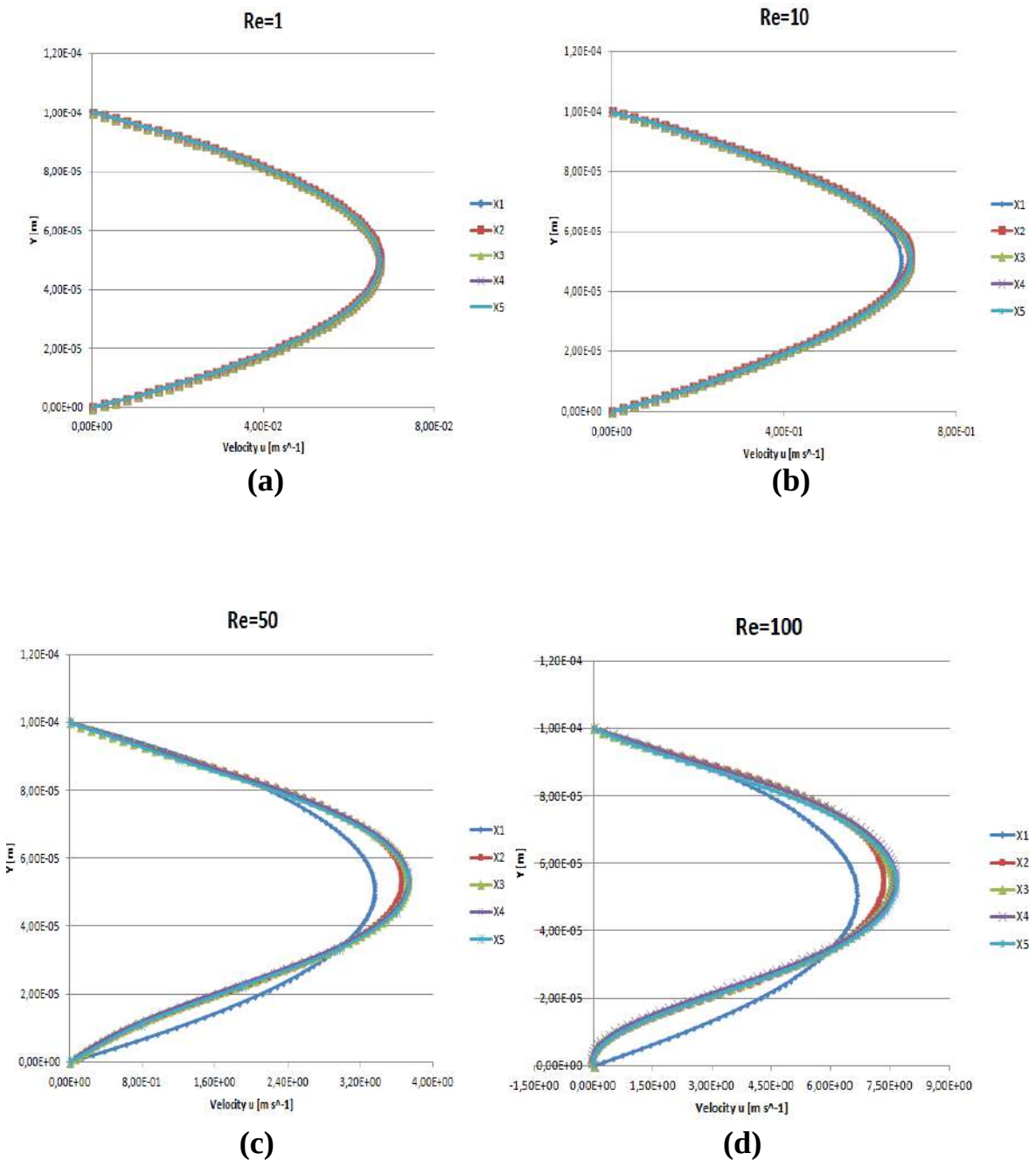


Figure.IV.4: $y = f(velocity)$ for different lines.

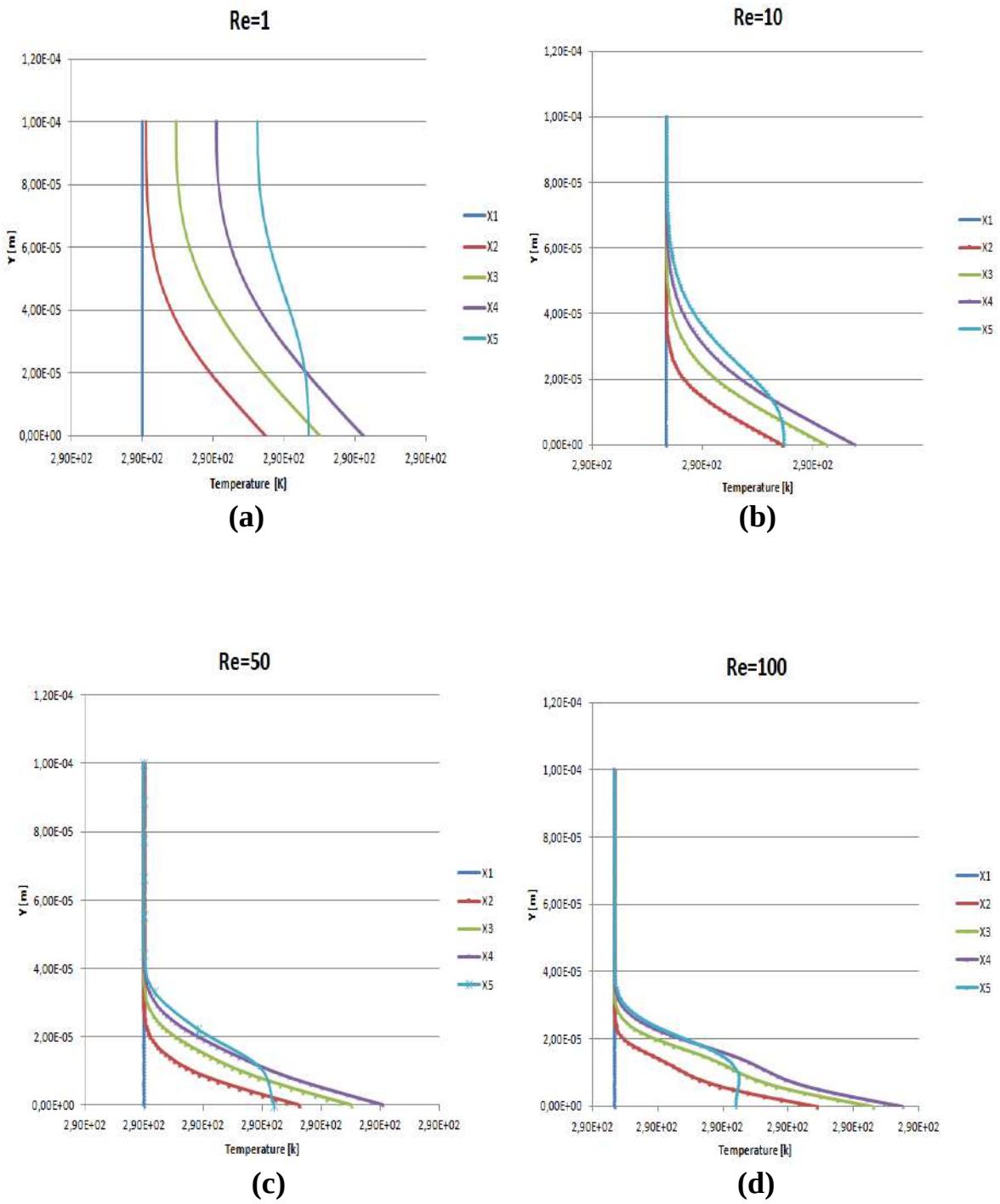


Figure.IV.5: $y = f\ (temperature)$ for different lines.

.

- graphs of the same lines for different Reynolds number:

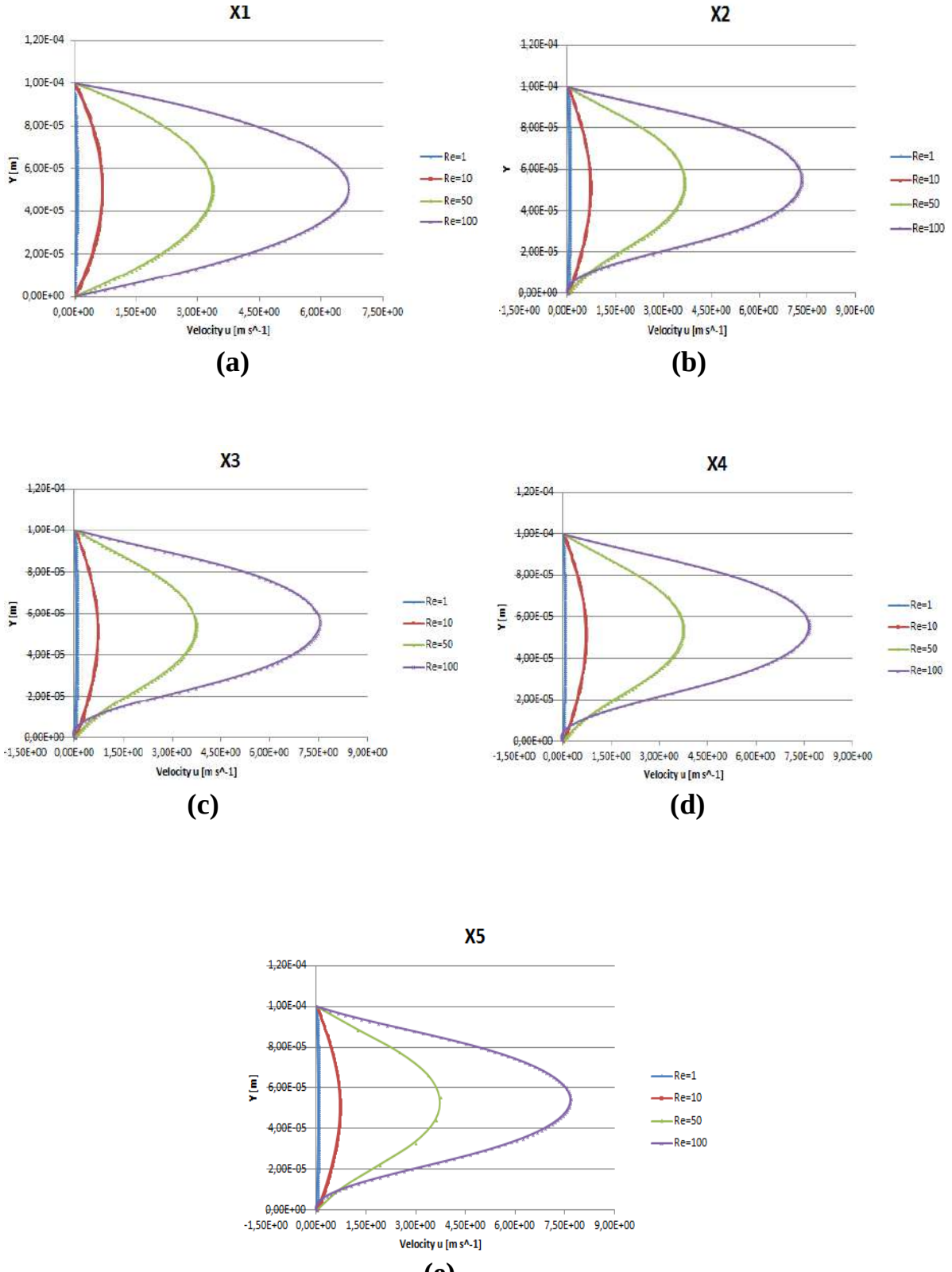


Figure.IV.6: $y = f\ (velocity)$ for different Re.

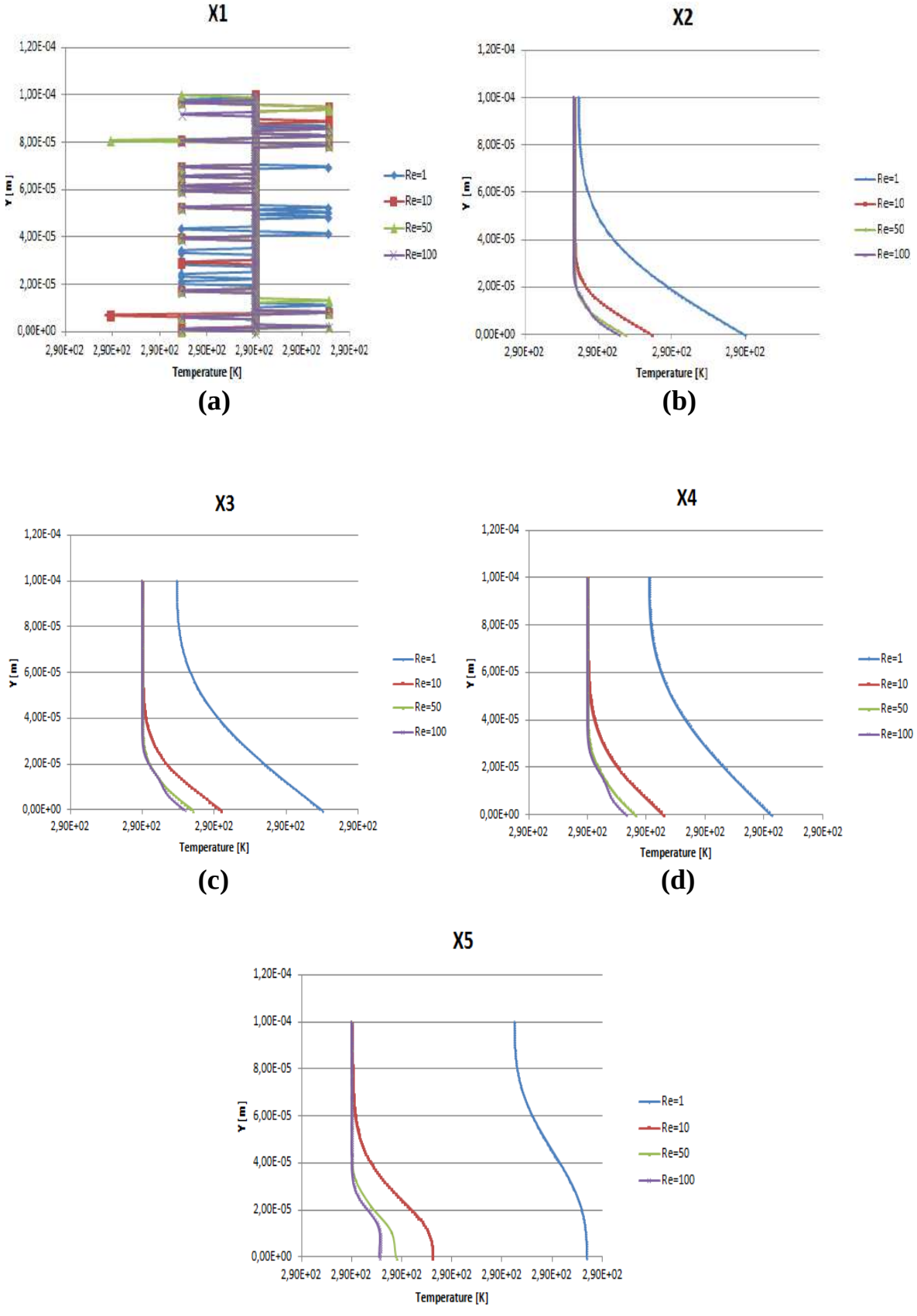
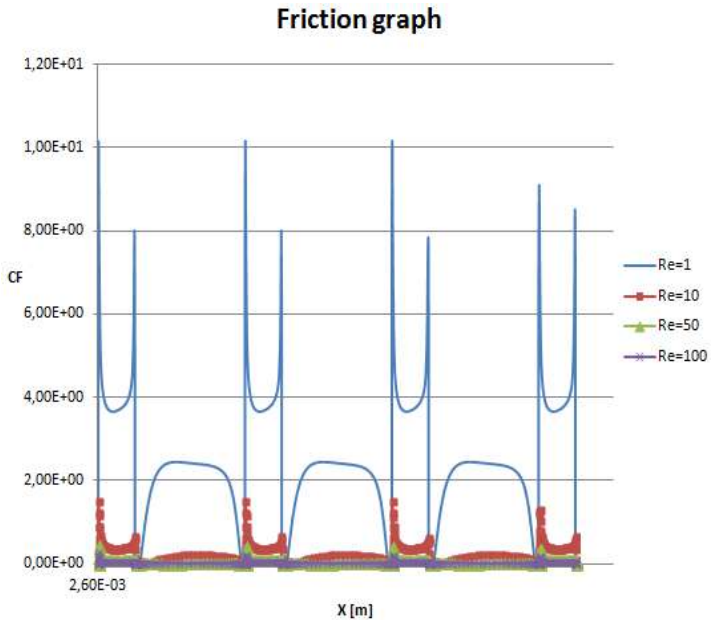
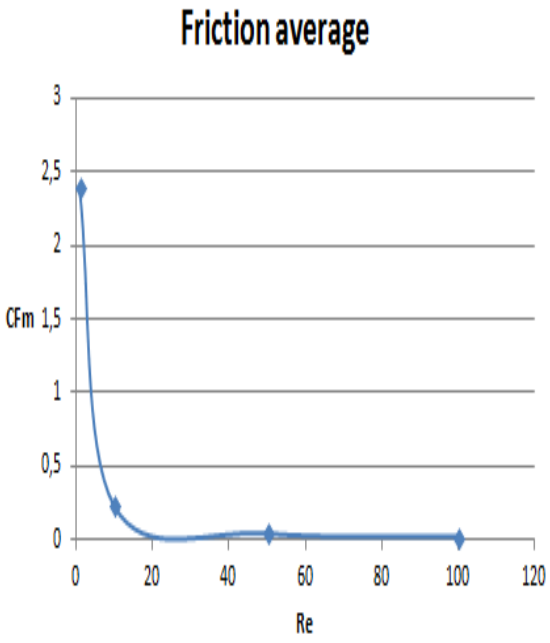


Figure.IV.7: $y = f\ (temperature)$ for different Re.



(a)



(b)

Figure.IV.8: $Friction = f\ (x)$ for different Re. (a) friction graph. (b) average friction graph.

IV.4: Simulation 2:

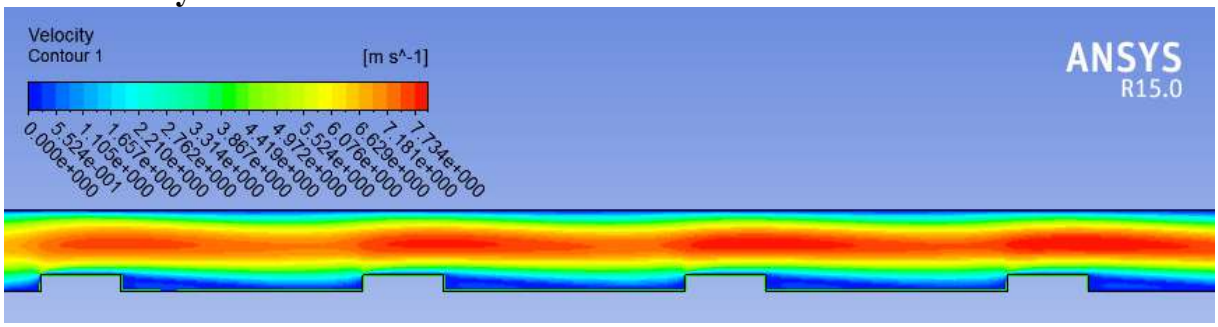
Fluid used **(Water).**

Simulation of different ribs shapes (rectangular, trapezoidal, triangular and Elliptical) for fixed Reynolds number Re=100.

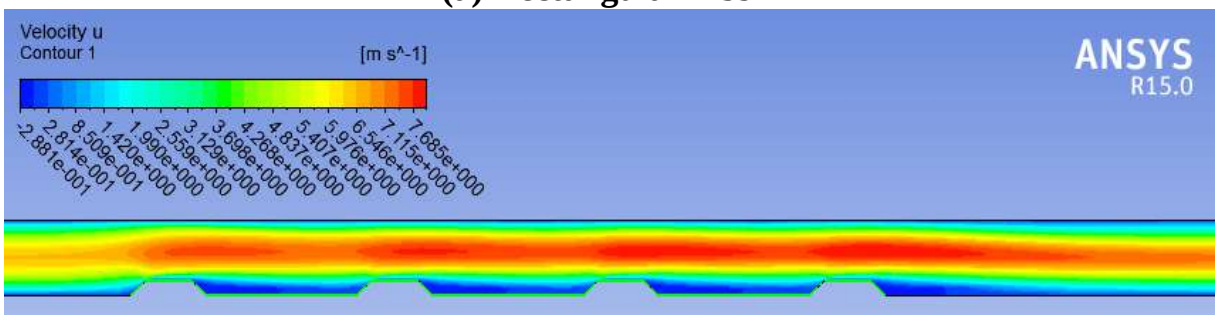
IV.4.1: Contours:

Figure.IV.9 and **Figure.IV.10** shows dimensionless axial velocity and temperature contours in Reynold numbers of 100 for rectangular, trapezoidal, triangular and elliptical ribs.

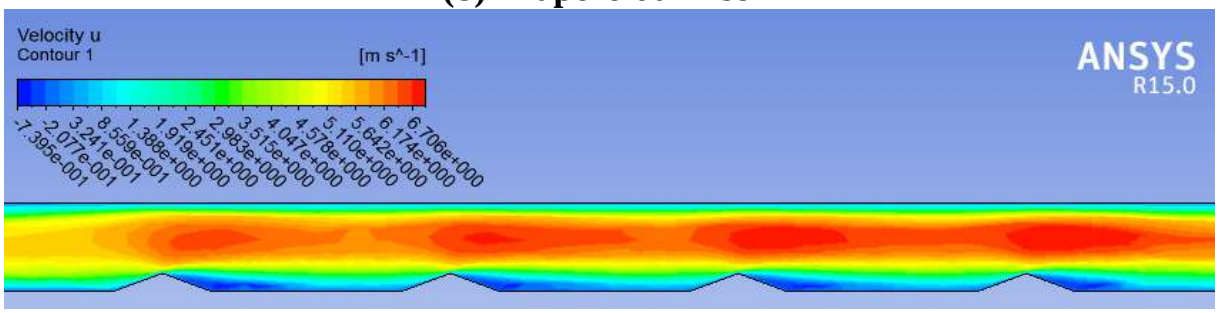
●Velocity contours:



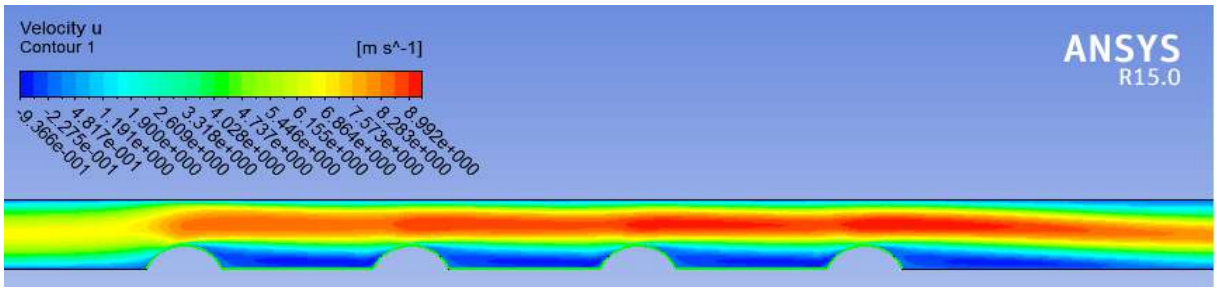
(a) Rectangular ribs



(b) Trapezoidal ribs



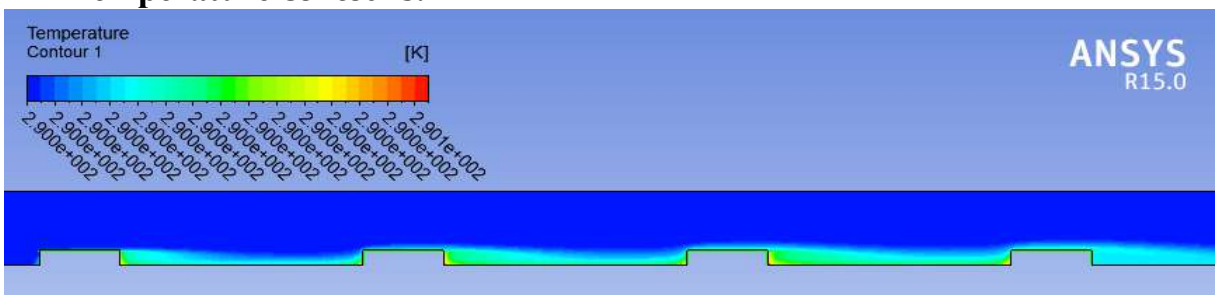
(c) Triangular ribs



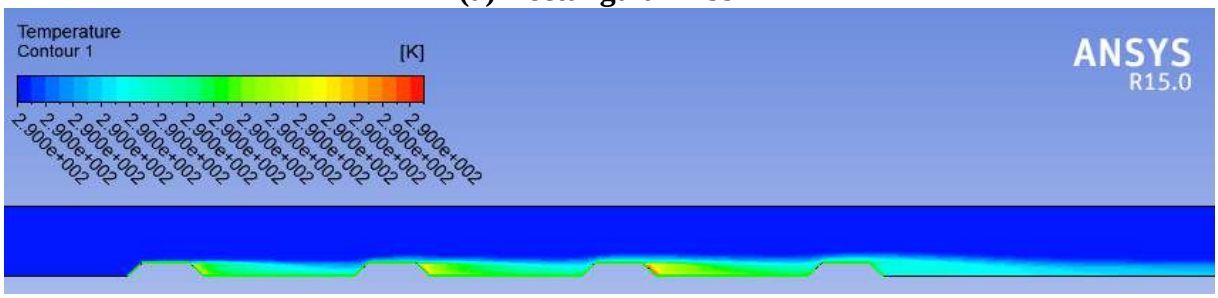
(d) Elliptical ribs

Figure.IV.9: dimensionless velocity contours for all shapes.

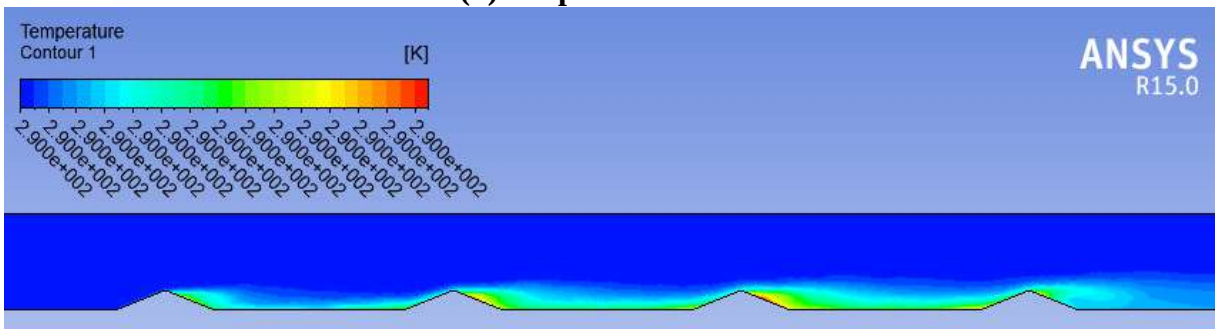
- **Temperature contours:**



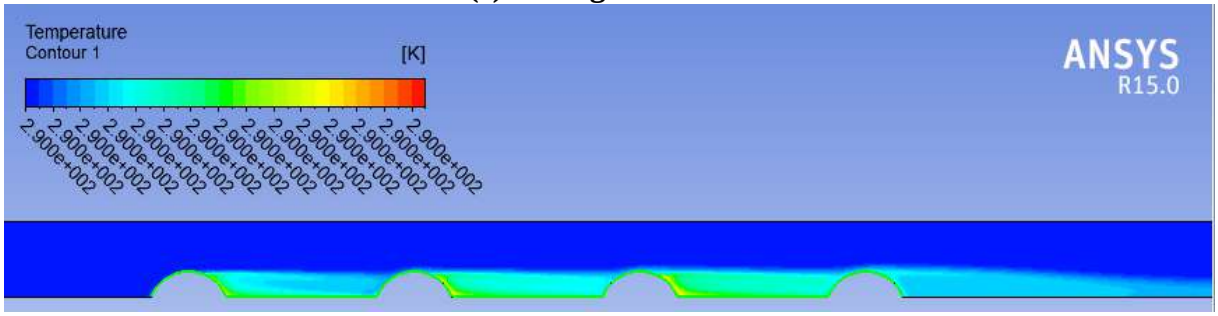
(a) Rectangular ribs



(b) Trapezoidal ribs



(c) Triangular ribs



(d) Elliptical ribs

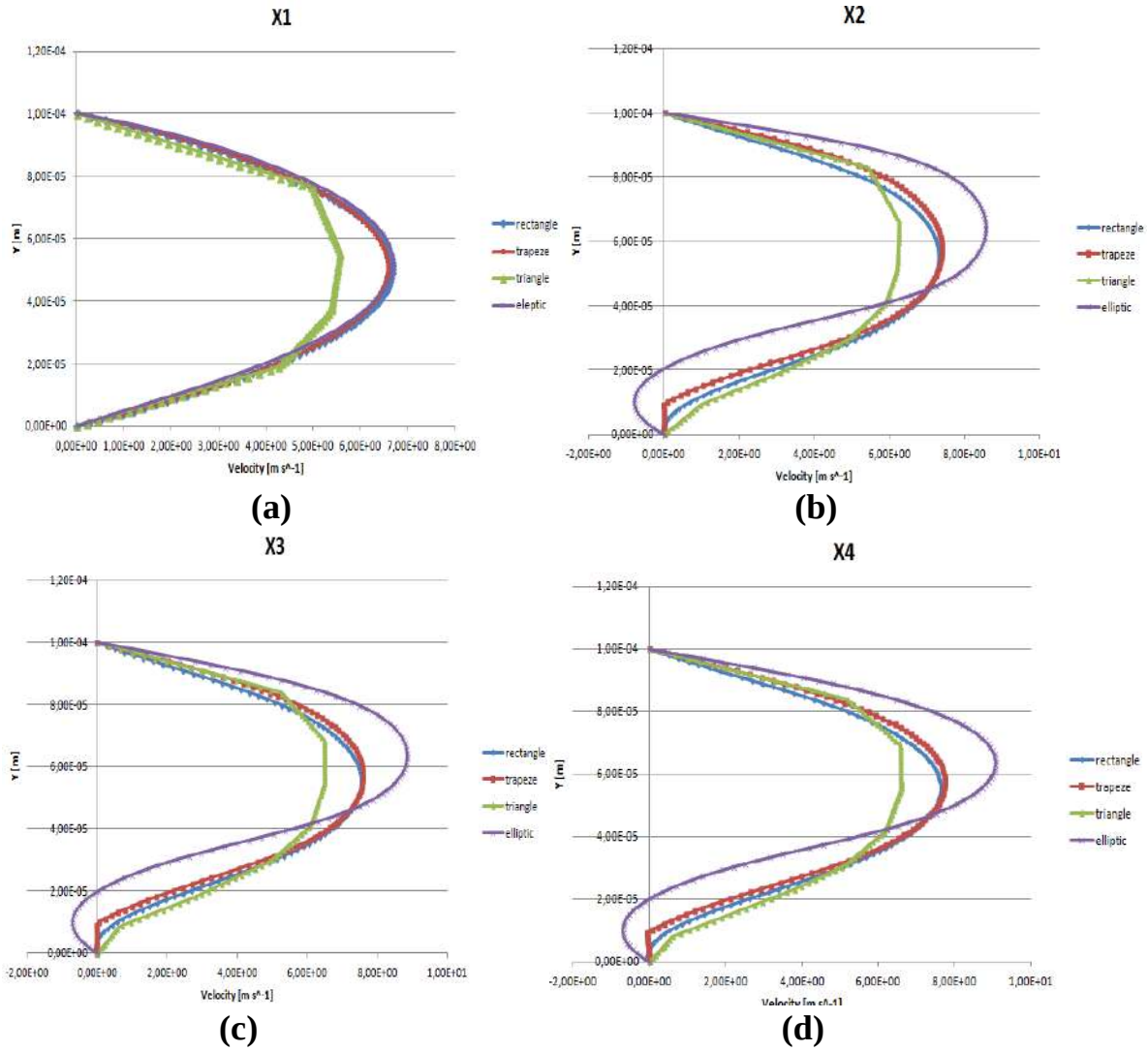
Figure.IV.10: dimensionless temperature contours for all shapes.

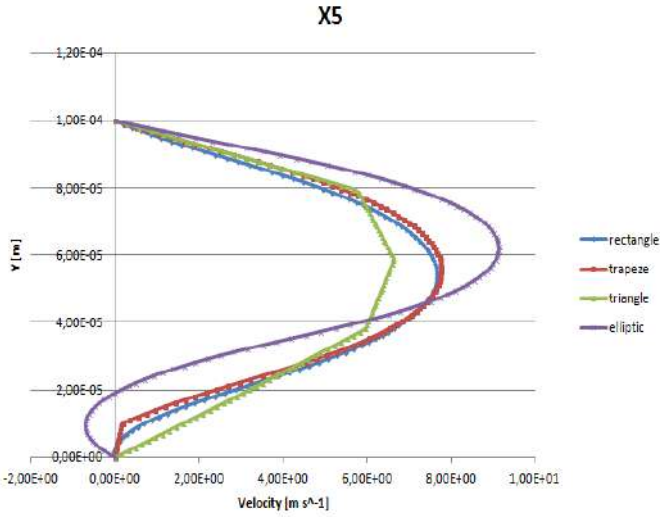
IV.4.2: graphs and discussion:

Figure.IV.11 and **Figure.IV.12** shows the evaluation of velocity and temperature in Reynold numbers of 100 for rectangular, trapezoidal, triangular and elliptical ribs. Among all of the investigated rib forms, the triangular form has the best thermal performance evaluation criteria values and the best fluid velocity in all the lines.

Figure.IV.13 shows the friction coefficient for different types of ribs in Reynolds numbers of 100. Such that in the Trapezoidal ribs form, coefficient of friction is topmost, than the rectangular form. That's because the rectangular ribs made the most changes in the streamlines, than elliptical, than triangular is the lessmost between all the shapes. Trapezoidal ribs are recommended in high Reynold numbers as we used in this experience.

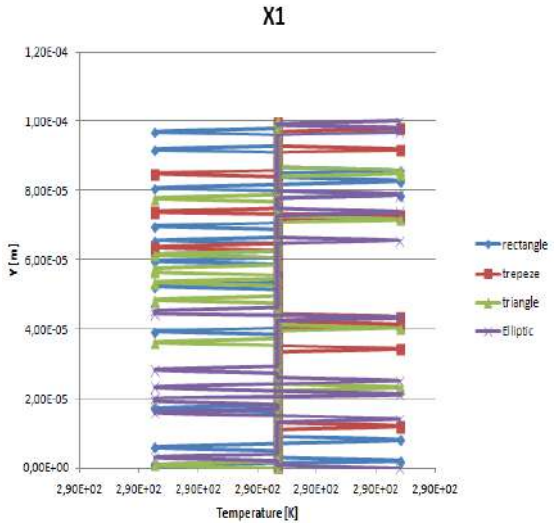
- graphs of the same Reynolds number for different shapes:



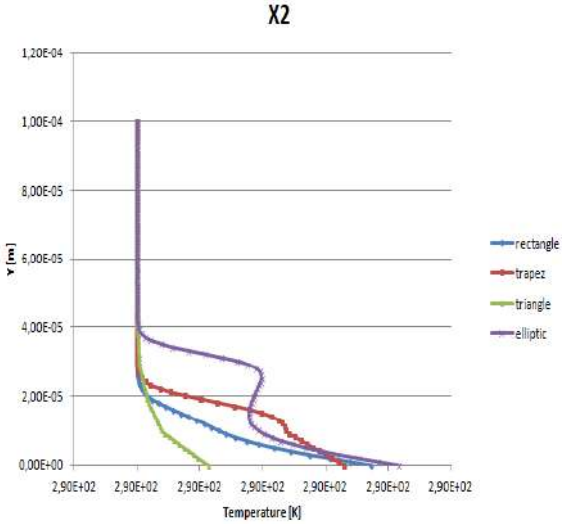


(e)

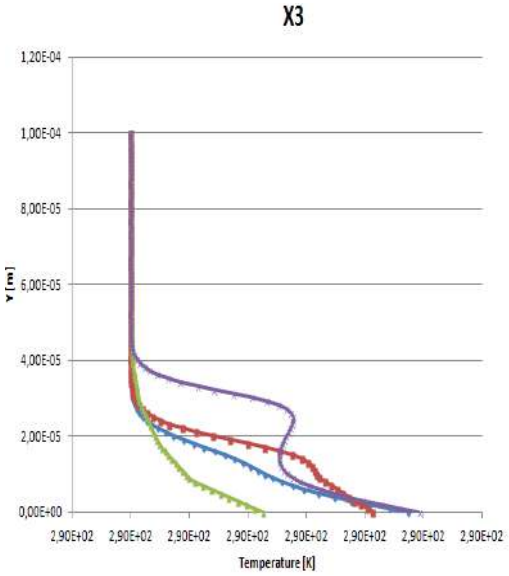
Figure.IV.11: $y = f\ (velocity)$ for different shapes.



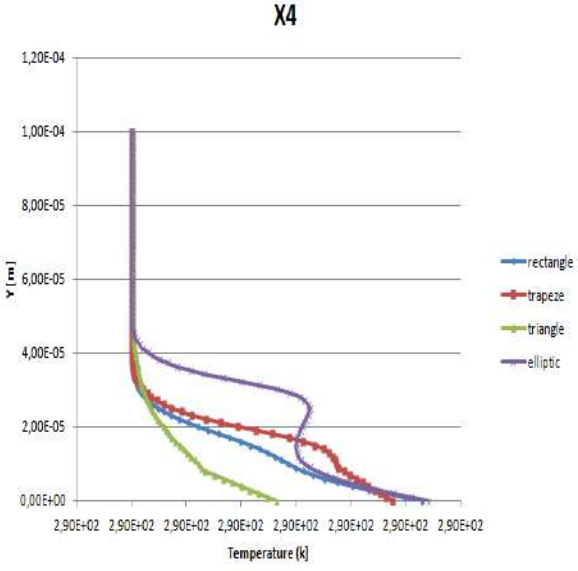
(a)



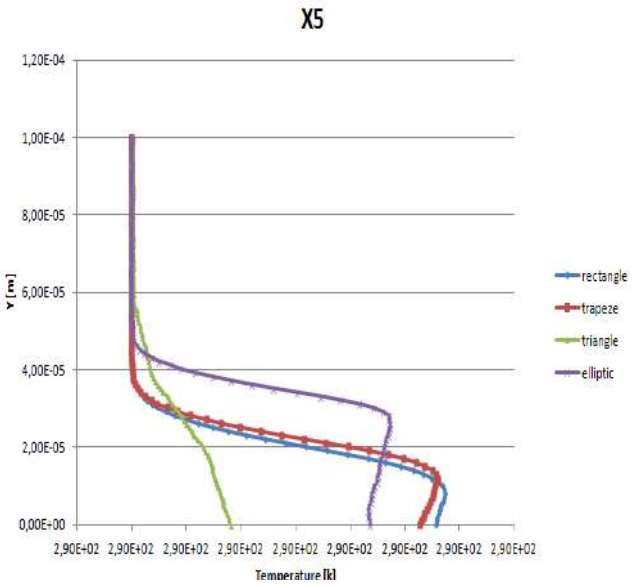
(b)



(c)



(d)



(e)

Figure.IV.12: $y = f\ (temperature)$ for different shapes.

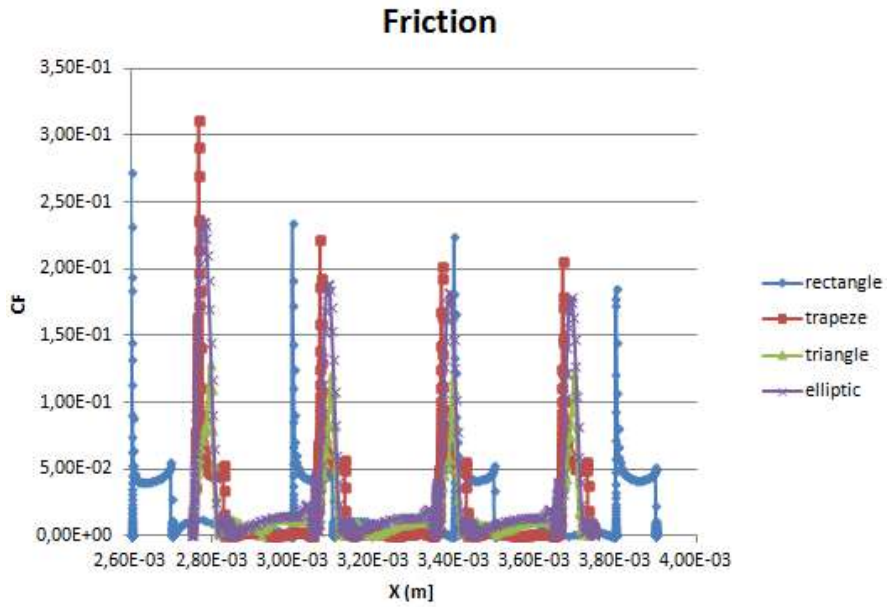


Figure.IV.13: $Friction = f\ (x)$ for different shapes.

IV.5: Simulation 3:

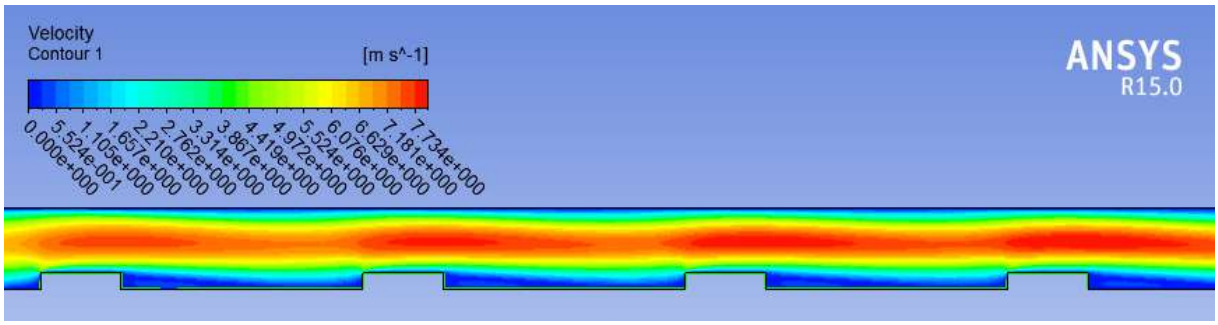
Fluid used **(Water)** & **(Water-Ag nanofluid).**

Simulation of water 0% and different nanofluid volume fractions of 2% and 4% and fixed Reynolds number Re=100 and different nanofluid volume fractions for rectangular ribs.

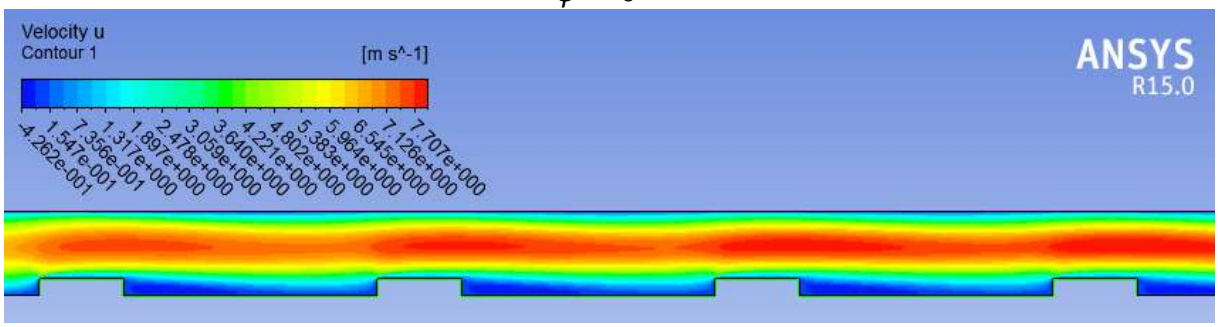
IV.5.1: Contours:

Figure.IV.14 and **Figure.IV.15** shows dimensionless axial velocity and temperature contours in Reynold numbers of 100 and for rectangular ribs shape.

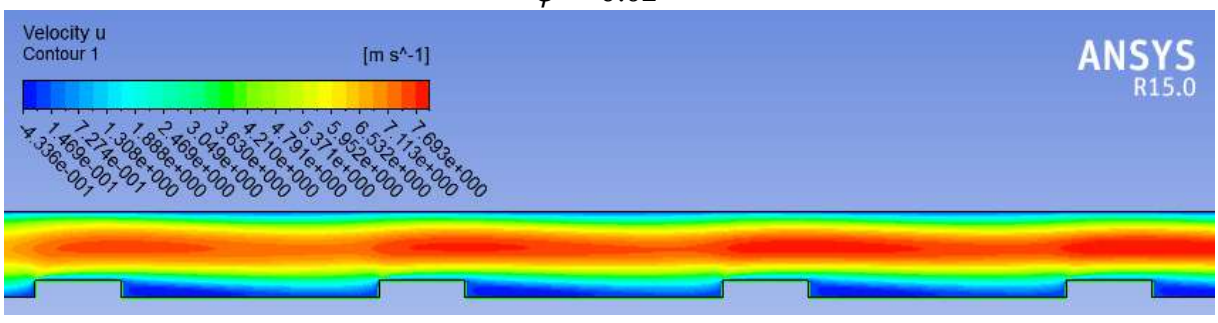
●Velocity contours:



$\varphi = 0$



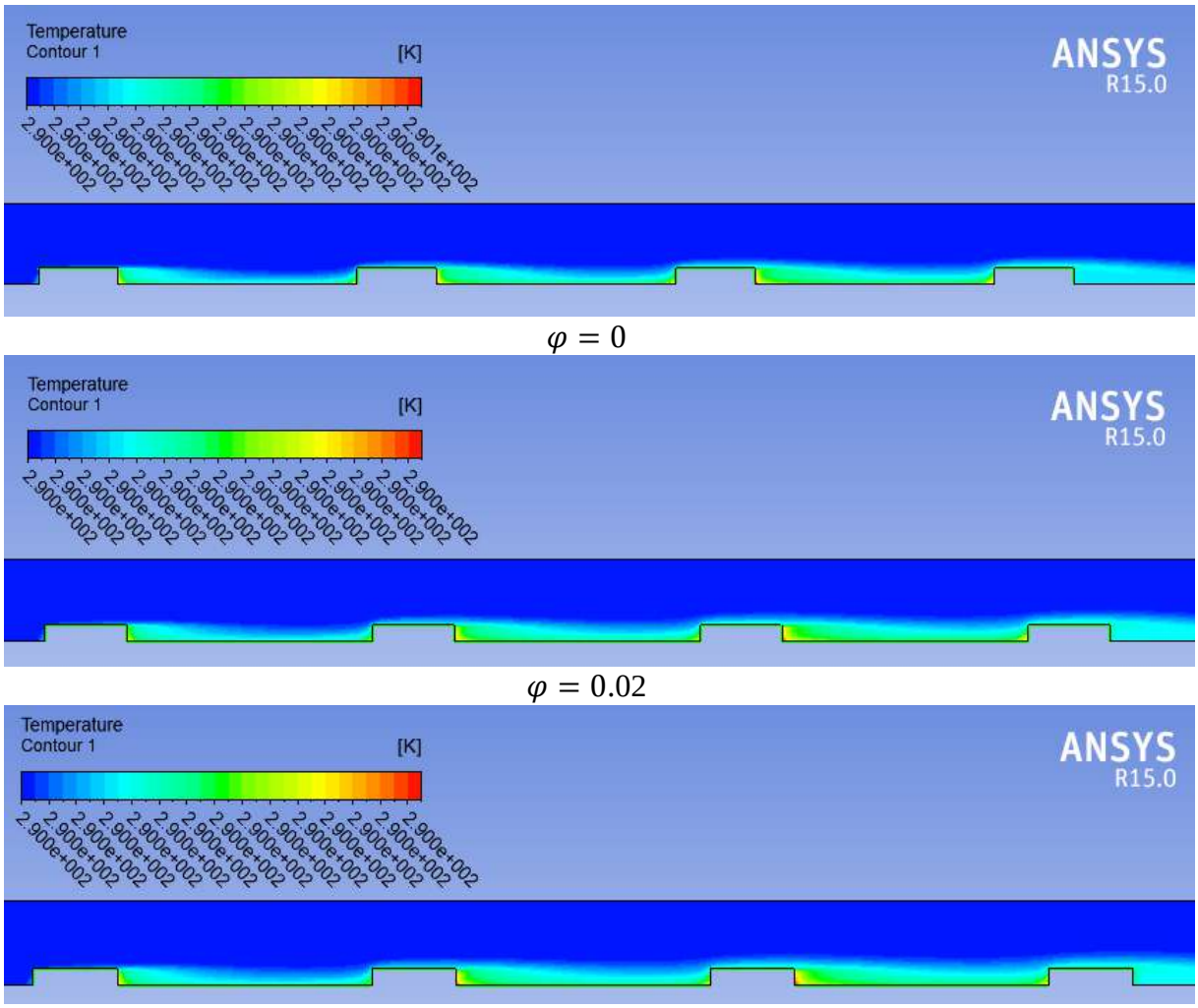
$\varphi = 0.02$



$\varphi = 0.04$

Figure.IV.14: dimensionless velocity contours for different nanofluid volume fractions.

●Temperature contours:



$\varphi = 0$

$\varphi = 0.02$

$\varphi = 0.04$

Figure.IV.15: dimensionless temperature contours for different nanofluid volume fractions.

IV.5.2: graphs and discussion:

Figure.IV.16, Figure.IV.17 and Figure.IV.18 shows the evaluation of velocity and temperature in Reynold numbers of 100 for rectangular ribs. It can be observed that the enhancement of volume fraction of nanoparticles in the base fluid causes the decreases of temperature and friction with no change of velocity.

●graphs of the same Reynolds number and different nanofluid volume fractions for rectangular ribs shape:

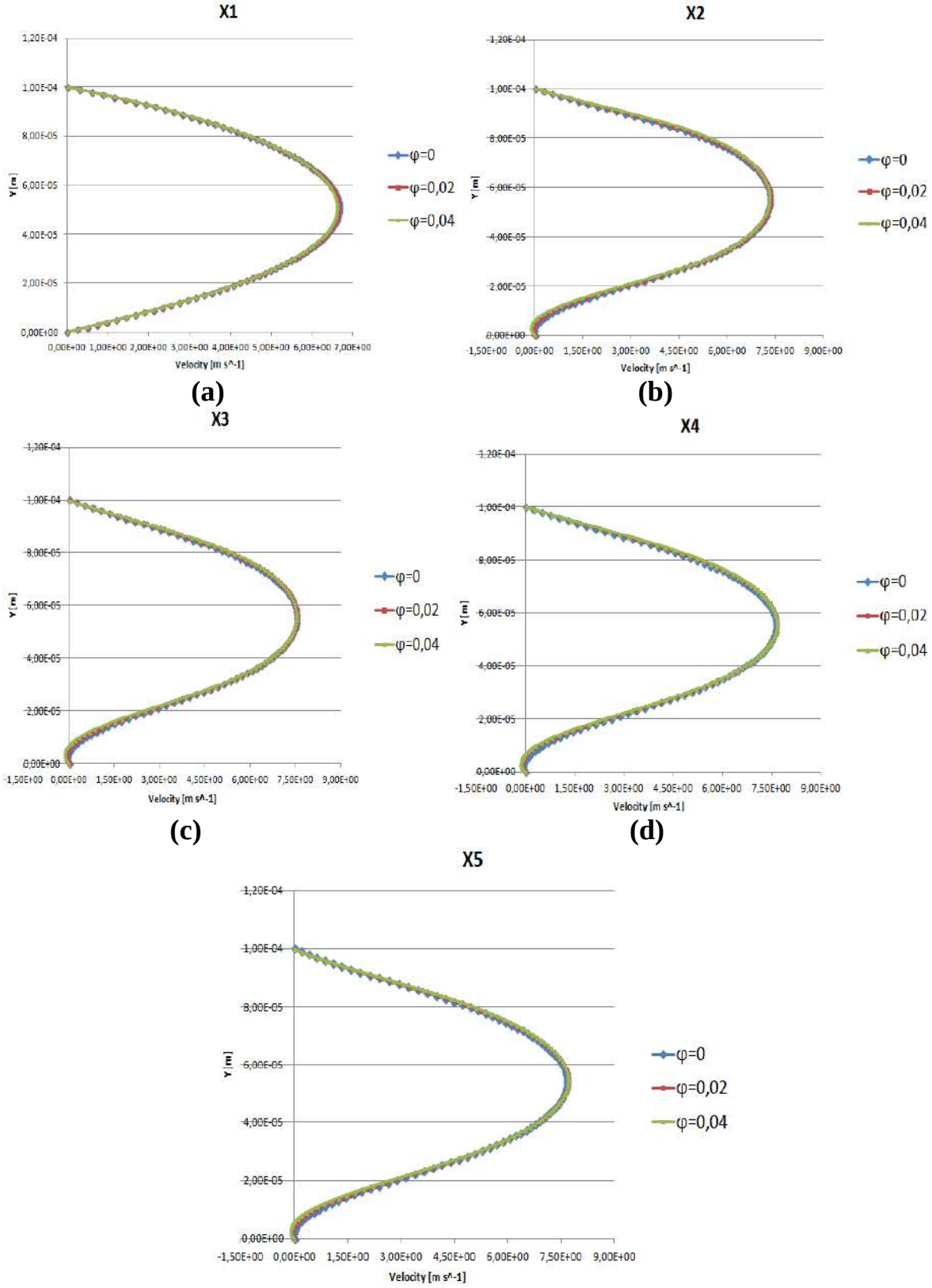


Figure.IV.16: $y = f\ (velocity)$ for different nanofluid volume fractions.

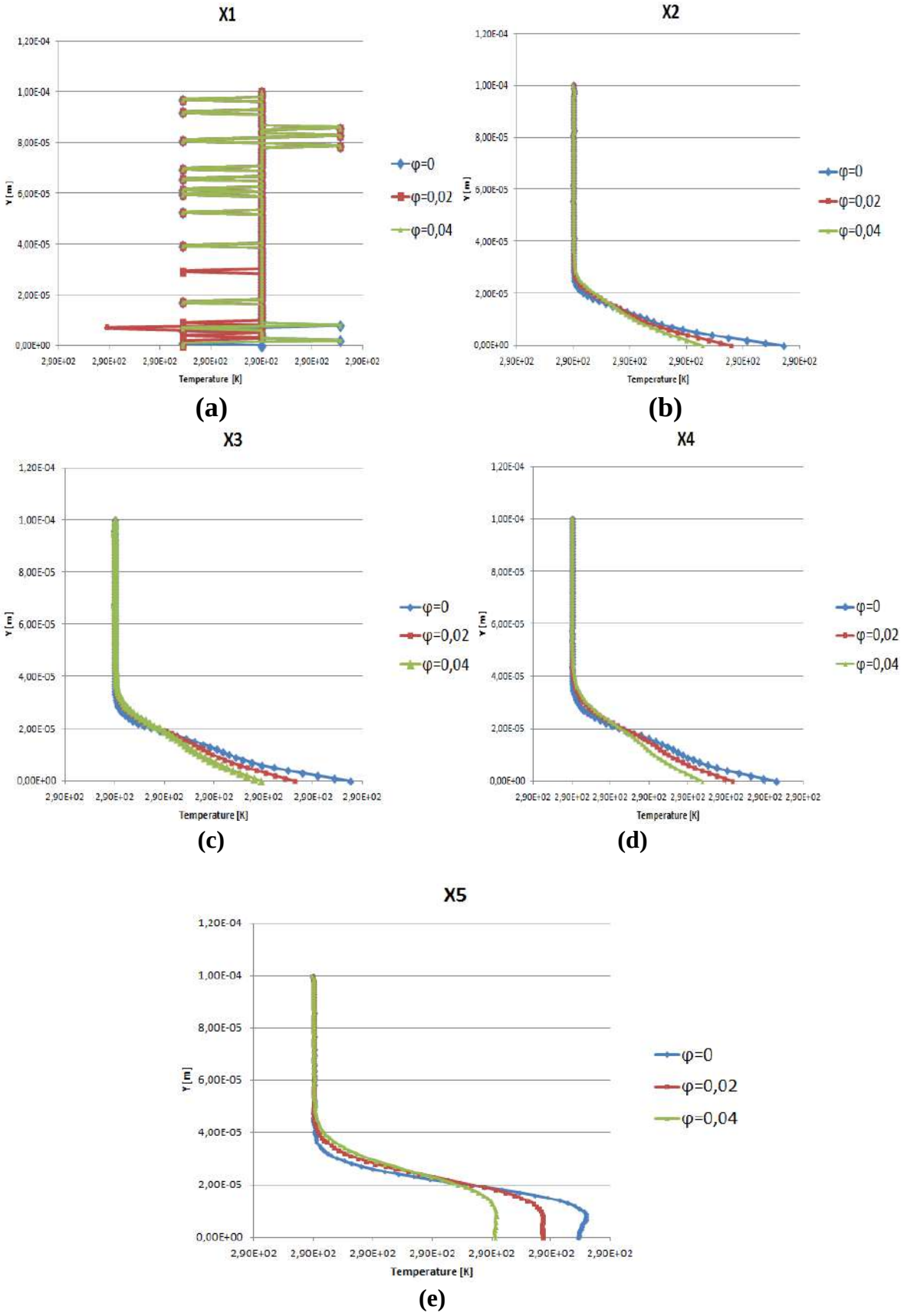


Figure.IV.17: $y = f\ (temperature)$ for different nanofluid volume fractions.

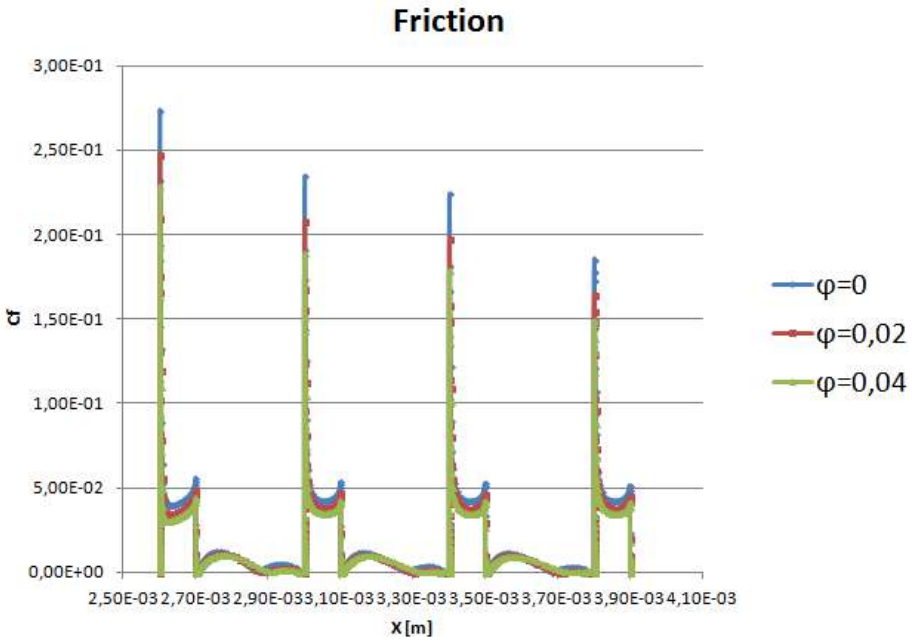


Figure.IV.18: $Friction = f\ (x)$ for different nanofluid volume fractions.

Conclusion:

In the present study, heat transfer and hydrodynamic behavior of the laminar water/silver nanofluid studied in a two-dimensional rectangular microchannel with rectangular, triangular, trapezoidal and elliptical ribs. The results of this research have been compared with each other in Reynolds numbers of 1, 10, 50 and 100 and different volume fractions of solid nanoparticles 0%, 2% and 4%, the findings indicated that for rectangular rib form, increasing Reynolds number input velocity, temperature and fraction decrease significantly due to better mixing of the cooling fluid. Among different studied rib shapes, in Reynolds numbers of 100, the best conformity of friction factor has been obtained in the trapezoidal, rectangular, elliptical and triangular rib shapes, respectively. Also the triangular rib forms have the highest thermal performance evaluation; the temperature behavior of trapezoidal ribs almost resembles the rectangular ones. An increase in nanoparticles volume fraction from 0% to 2% than 4% leads to higher temperature and friction loss, that is what we wanted to achieve in this study.

Generally speaking, according to the importance of heat transfer Enhanced methods, expected results Research and other research in the field, Applicable and useful in today's industry, for example Electronics, power stations, aerospace and automotive manufacturing.

[1] SCHAUM'S OUTLINE OFTHEORY AND PROBLEMSOFHEAT TRANSFER Second Edition DONALD R. PITTS, Ph.D.& LEIGHTON E, SISSOM, Ph.D., P.E.

[2] Nonlinear Systems in Heat Transfer Mathematical Modeling and Analytical Methods 2018, Pages 35-104.

[3] Theoretical Foundations of Conduction and Convection Heat Transfer Michael Wendl.

[4] Eckert, E. R. G. and Drake, R. M., Heat and Mass Transfer, McGraw Hill Book Company, 1959.

[5] Eckert, E. R. G. and Drake, R. M., Analysis of Heat and Mass Transfer, Hemisphere Pub. Corp 1987.

[6] Incropera, F. P. and Dewitt, D. P., Fundamentals of Heat and Mass Transfer, Wiley, 1990.

[7] Lienhard, J. H., A Heat Transfer Textbook, Prentice-Hall, 1987.

[8] Mills, A. F., Heat Transfer, Irwin, 1992.

[9] Ian Papautsky, Tim Ameel , A. Bruno Frazier A Review Of Laminar Single-Phase Flow In Microchannels.

[10] What is Laminar Flow in Microchannels & Reynolds Number? By Serhat Sevli on October 20, 2020

[11] George M. Whitesides, The origins and the future of microfluidics

[12] Muhammad Shafiq Bin Hasnan, Summary Of Nanofluid

[13] Prof. Pushparaj Singh, Jay Prakash Pandey, A Review on Heat Transfer Enhancement Using Nanofluids

[14] A.R. Prasad, Sumer Singh, Harish Nagar**,** A Review on Nanofluids: Properties and Applications

[15] Naser Ali, Joao A. Teixeira, and Abdulmajid Addali, A Review on Nanofluids: Fabrication, Stability, and Thermophysical Properties

[16] Mohammad Reza Gholami , Omid Ali Akbari, Ali Marzban , The effect of rib shape on the behavior of laminar flow of oil/MWCNT nanofluid in a rectangular microchannel.

[17] Introduction to ANSYS Workbench, ansys.com.

[18] Prof. N. S. Surner, ANSYS Workbench.